PROPERTY RANGES AND CORRELATIONS IN INTERMETALLIC COMPOUNDS

A Thesis submitted

in partial fulfillment of the requirement

for the Degree of

## Master of Technology

By

U. D. Sai Baba
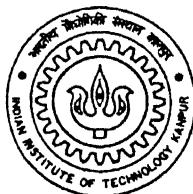
MATERIALS SCIENCE PROGRAMME

INDIAN INSTITUTE OF TECHNOLOGY, KANPUR

APRIL 2000
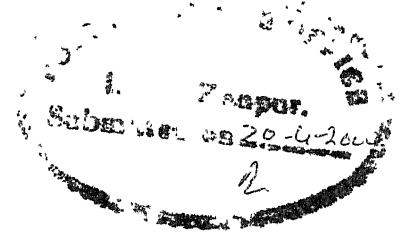
CERTIFICATE

It is certified that the work contained in this thesis entitled *"Property Ranges and Correlations in Intermetallic Compounds"*, by **U.D.Saibaba** has been carried out under my supervision and this work has not been submitted elsewhere for a degree.

(Om Prakash)
Assistant Professor
Dept. of Mechanical Engineering
Indian Institute of Technology
Kanpur (UP)-208016

APRIL 2000

Acknowledgements

*"The more a man thinks, the better adapted he becomes
to thinking, and education is nothing if it is not the
methodical creation of the habit of thinking"*

- *Ernest Dimet*

It is a pleasure to acknowledge my gratefulness to my thesis supervisor, Dr. Om Prakash, who has suggested me the problem and guided me throughout for a satisfactory completion of my work outlined in this thesis. Discussions with him have aided a lot in structuring and cohering the thoughts to give a good shape to this work.

I am sincerely thankful to Prof. D.C.Agrawal, Prof. Jitendra Kumar and Prof. K.N.Rai for their valuable teachings during my course work. Their classes are indeed a new experience to me in grasping fundamental concepts and letting me to interact with the new concepts of materials science courses.

I express my deep indebtedness to Prof. A.K..Kapoor, Dr. P.K.Panigrahi and Dr. Seshu Bai and some other faculty in Department of Physics, University of Hyderabad for their valuable suggestions and moral encouragement in completing my M.Tech. degree. Without their inspiration I would have not achieved my goals. I feel it is nostalgic to remember them in my first acknowledgements.

I am sincerely thankful to Dr. Asima Pradhan for her valuable suggestions during my stay at I.I.T.Kanpur.

I express my deep gratitude to Mr. S. Srikanth, for his moral support, patience, friendly approach and helping nature throughout my M.Tech. course. I learned both spiritually and intellectually a lot from his friendship. He made my life easy in kanpur. I could not forget his care and he stood by me in getting my placement in the campus. To him I owe more than what I can mention..... I take this opportunity to wish him a very bright future.

I would like to extend my sincere thanks to Ms. Sudha Siva Rani, my junior in Materials Science Programme as well as in M.Sc (Physics), for her timely help in the calculation part of my thesis. Without her assistantship, I would have not completed my thesis in time. My best wishes will be always there with her.

I would like to express my deep gratitude to Ms. Jayanthi.S, my co-scholar at University of Hyderabad during my six months research work under guidance of Prof. A.K.Kapoor. Her approach towards the research problem inspired me a lot in solving my M.Tech. thesis problem. My heartful wishes for her bright research career.

Financial assistantship from the authorities of Council of Scientific and Industrial Research (CSIR), India, in award of junior research fellowship (JRF) is gratefully acknowledged. My special regards

Abstract

Intermetallic compounds are formed with two or more metals or metalloid elements producing a new phase with specific composition, crystal structure and properties. These are an important class of materials with potential high temperature application and currently extensive work is being carried out to understand their structure and properties and to develop new intermetallic compounds with improved properties.

Properties play an important role in materials selection for design. It is necessary to have properties database for intermetallic compounds. However, all property data for all intermetallic compounds is not available. Therefore, it is often necessary to estimate missing property data using related information. Accordingly, this work has the following objectives

    (a) Compilation of property data for intermetallic compounds
    (b) Develop correlations which may help in estimating unknown property data

For the latter, it has been shown elsewhere, that an idea about respective property ranges is very useful.

Results are presented on property ranges and correlations for various classes of intermetallic compounds. Two types of correlations are presented (a) those between various physical properties, and (b) correlations between physical properties and average Mendeleev number of intermetallic compounds.

Contents

Chapter 1

Introduction

Chapter 2

Property Ranges in Intermetallic Compounds

Chapter 3

Correlations in Intermetallic Compounds

Chapter 4

Correlations based on Mendeleev Number

Chapter 5

Conclusions and Objectives of Future work

List of Figures

List of Tables

Chapter 1

Introduction

1.1 Definition

Intermetallic compounds are compounds formed with two or more metals, or metalloid elements producing a new phase with specific composition, crystal structure and properties.

The stoichiometric of intermetallic compounds was first noticed in the beginning of the nineteenth century, when the first systematic studies of alloy systems were being made. A number of investigators noted behaviour at certain alloy compositions strikingly like that of ordinary chemical compounds and began to speculate as to whether compounds might exist between metals. It appears that the first true observation of an intermetallic was that of the German chemist Karl Karsten, who in 1839 noticed that a discontinuity occurred in the action of acids on alloys of copper and zinc at the equiatomic composition and suggested the formation of compound [1]. The compound Karsten claimed does exist and is the now familiar beta brass β-CuZn.

During the second half of the century, similar discontinuities in other properties-electrical, mechanical, and magnetic, as well as chemical were detected in other alloy systems and led to the suggested formulation of still other intermetallic compounds. Today the number of intermetallic compounds known is very large.

From application point of view, intermetallic compounds are currently not used widely on their own because of their brittleness. However, they provide excellent dispersion strengthening in alloy systems [2]. When the solubility of a material is exceeded by adding too much of an alloying element, a second phase forms and a two-phase alloy is produced. The boundary between two phases is a surface at which the atomic arrangement is not perfect. As a result, this boundary interferes with the slip of dislocations and strengthens the material. Regarding emerging trends, intensive effort is directed at developing high temperature applications based on intermetallic compounds. This is in view of their high melting point, stiffness, and resistance to oxidation and creep. A variety of new materials based on intermetallic compounds are being developed, particularly for aircraft and engine components. These new materials maintain their strength and even can develop usable ductility at elevated temperatures. These materials may be classified based on their primary constituent into categories such as

- Aluminides
- Berylides
- Silicides
- Miscellaneous intermetallic compounds

The list the current/intended applications of some of the more important intermetallic compounds are listed in the following section. Recent trends regarding materials property data is discussed in Section 1.3.

1.2 Examples, Uses and Applications

1.2.1 Structural Applications

Aluminides

The aluminides are of interest because of their strength and their oxidation resistance. Nickel aluminides have been investigated more extensively than any other aluminides.

Ni_3Al and its alloys

Ni_3Al based alloys can be prepared by the melting and casting techniques available for nickel based super alloys. Test bars and turbine blades with single-crystal or directionally solidified structures were produced by the same industrial processes as used for nickel-based super alloys [3]. Various applications of Ni_3Al include [4]:

1. Automotive turbochargers: Turbocharger rotors in diesel trucks are the near-term application of Ni_3Al alloys

2. High temperature dies and molds: High temperature oxidation resistance together with excellent strength during deformation at high strain rates make Ni_3Al alloy attractive as die materials for glass processing.
3. Cutting tools: Nickel aluminide bonded tungsten carbide composites have better low- and high- temperature strength and cutting properties than cobalt bonded tungsten carbide materials.
4. Pistons and valves for automobile diesel engines: Ni_3Al alloys are suitable for piston and valve applications because of their good wear resistance.
5. Turbine blades and valves for jet engines: Directionally solidified Ni_3Al alloy with the composition Ni-16.3Al-8.2Mo-0.26B (at%) has superior strength and creep resistance at temperatures above 1000 °C in oxidising environments. Hence, this alloy has the potential to be used for turbine blades for jet engines.

NiAl and its alloys

NiAl has been studied extensively as a potential structural material in the aerospace industry. The attractive attributes of NiAl include a high melting temperatures, low density, good environmental resistance, high thermal conductivity, attractive modulus, metal like properties above a modest ductile-to-brittle transition temperature and low raw materials cost [3].

γ-TiAl and its alloys

TiAl based materials are pursued mainly because of the desire to raise the thrust to weight ratio of high performance aircraft engines. To increase the specific thrust, one would have to develop light weight materials such as those based on γ-TiAl [3].

Zr_3Al

Zr_3Al satisfies the needs of nuclear engineering, more specifically, the special requirements of the CANDU (Canadian Deuterium Uranium) power reactor. This system uses natural uranium as fuel and heavy water as both moderator and coolant and it distributes the coolant amongst large thin-walled, small diameter pressure tubes. The CANDU reactor thus requires structural elements which not only resist oxidation, corrosion and creep deformation but which are also relatively transparent to thermal neutrons. The last requirement is particularly important and accounts largely for the current use of the zirconium based alloys [3].

FeAl and Fe_3Al alloys

Iron aluminides based on Fe_3Al and FeAl are ordered intermetallic alloys that offer good oxidation resistance, and potentially lower cost than many high temperature structural materials. Iron aluminides have been shown to have potential for elevated-temperature applications [3].

Silicides

Silicides are an important group of intermetallic materials with diverse applications. These are used as a high temperature structural material for advanced aerospace applications, heating elements and protective high-temperature coatings particularly for refractory materials. In microelectric devices, thin silicides layers are used as contacts and connections because they have lower electrical resistivity than polycrystalline silicon and are compatible with silicon substrate. When metal thin films are brought in contact with silicon substrates, the interaction results in the formation of silicides at the interface at low temperatures.

The high melting points and the good oxidation resistance of semiconducting disilicides are desirable properties for thermoelectric generators converting solar into electrical energy. In terms of magnetic properties, silicides of the first long period transition metals are all paramagnetic with susceptibilities similar to those of the elementary transition metals, whereas silicides of the heavier transition elements are diamagnetic, with zirconium disilicide possessing a particularly large diamagnetism. Fe_3Si and Fe_5Si_3 have been confirmed to be ferromagnetic. $MoSi_2$ is used as the furnace element [3].

Beryllides

The beryllides are a class of refractory materials in which interest exist because of observed high strengths, strength retention at elevated temperatures, thermal shock resistance and oxidation resistance. Beryllides of tantalum, niobium and zirconium are considered to have potential for structural application at elevated temperatures. Beryllium intermetallic compounds have the values of high elastic stiffness, low density and relatively high temperature. The most important beryllides are $Be_{17}Nb_2$, $Be_{13}Zr$, $Be_{12}Nb$ and $Be_{12}Ti$. These are having good oxidation resistance [5].

1.2.2 Electromagnetic Applications

Intermetallics for Optical Applications

LED: GaP, GaAs, InP, ZnSe, PbSe, PbTe

There are two types of LEDs: Surface emitting type and edge emitting type, which emit the light in the direction perpendicular to or parallel to the interfaces of the films. The surface emitting type is more widely used in practical applications.
Laser diodes: The first laser diode successfully worked in the visible region was InGaP laser diode. Its wavelength region is 0-6 μm
InSb Hall devices: InSb n type shows the highest mobility among the III − V group semiconductors. This device exhibits high sensitivity and has a low power consumption. It is thus capable of application as a magnetic head for audio signals.

Much more electromagnetic applications of intermetallic compounds are found in [3]. These are magnetic, semiconductor, superconductor, magneto-optical, thermoelectric and electrical applications. The detailed discussion of these applications is given in [3]

1.2.3 Chemical and Metallurgical Applications

Most of these applications have been described in [3]. These are high temperature coatings for gas turbines, electrochemical applications and process metallurgy applications.

1.3 Trends in Advanced Materials Data

Although there is a lot of effort in developing and studying various aspects of intermetallic compounds, from design point of view, it is desirable to have some idea about properties of these intermetallic compounds as a family of materials. Specifically it would be useful to determine property ranges and develop correlations between various properties for these compounds.

The first difficulty is in regard to the number of intermetallic compounds. The search for new materials that have new or greatly improved properties is an intrinsic part of materials science. Given the elements of the periodic table, there are countless combinations that will result in materials with new or required properties. Table 1.1 shows experimentally known systems, relative to the estimated maximum number of compounds that are grouped by elemental composition. It is taken that the starting number of elements is 100.

Table 1.1: Estimation of material combinations [6]

Compounds	Experimentally Known systems	Maximum number
Unaries	100	100
Binaries	4000 (81%)	4,950
Ternaries	8000 (5%)	1,61,700
Quaternaries	1000 (<0.1%)	39,21,225

In calculating the number of compounds for intermetallics, if one start up with 89 elements and assumes 2 compounds per system (e.g., high temperature, high-pressure phases), the result is 198 unaries, 7823 binaries, 227128 ternaries and 4.8×10^6 quaternaries. Fig. 1.1 shows the distribution of the number of these compounds for which there are crystallographic data: 19597 (48.1%) unaries, 18586 (45.6%) binaries, 19597 (48.1%) ternaries and 1928 (4.7%) quaternaries. These numbers, relative to the estimated maximum number of compounds for each group, shows that binaries are fully investigated, while only 8% of the ternaries have been studied, and research in quaternary field has only just started.

6
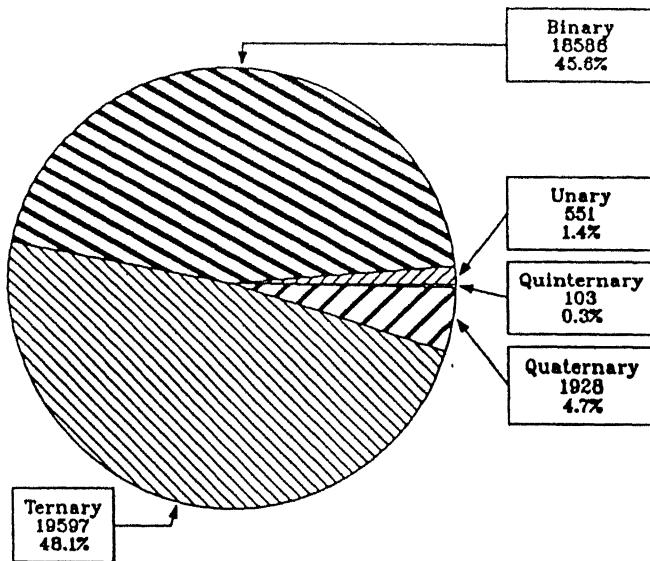
Fig. 1.1: Distribution of experimentally known intermetallic compounds by elemental composition

1.3.1 Properties and Correlations

Material properties of solids lie in a wide range and are characteristic of the class for a given structure and bond-type. Beyond this correlations exist between the values of mechanical, thermal, electrical and other properties based on the nature of bonding and arrangement of the atoms in the material. Some of these correlations can be expressed as dimensionless groups with much narrower value ranges. This allows one to check the consistency on property values and certain properties can be estimated when values for others are known. Others, which are empirical, can be found by an appropriate search routine. They too can be used to estimate the missing properties, and to assign a reliability range to the estimates [7].

The arrangement of atoms or molecules in space (structure) and the nature of bonding between them determine the properties of solids. Similarities in the properties can be seen in materials with similar structure and bonding. Their values lie within defined ranges, characteristic of the class and are, to varying degrees, interrelated.

$$C_L < P_i < C_H$$

Based on the classification of materials, individual properties of a material class have certain characteristic ranges of values. Certain properties, which originate from the nature of atomic bonding exhibit strongest correlations and those that are derived from the dependency on defects have less strong correlations. The examples in former case are

correlation between modulus and melting point and in later case are strength and toughness. There exist weak correlations when interaction with the environment is involved as in corrosion and wear. There are good reasons for these correlations, which can often be expressed as limits for the values of physically based dimensionless property groups.

The dimensionless property groups take the form

$$C_L < P_1 P_2^n < C_H$$

$$C_L < P_1 P_2^n P_3^m < C_H$$

Where P_1, P_2 and P_3 are material properties, n and m are simple powers and C_L and C_H are dimensionless constants represents lower and upper limits between which the property group lies. When such correlations exist they permit checks and estimates which are more discriminating and precise than do the range checks [7].

1.3.2 Structure Mapping

The crystal structures of tens of thousands of binary, ternary and quaternary compounds have been determined since the advent of X-ray crystallography in 1910. To date more than two thousand different types of structure have been identified. The purpose of structure maps is to order this vast empirical data base within two-dimensional or three dimensional plots, so that all compounds with a given structure type are located in well-defined domains which are separated from the domains containing other structure types. The structure maps can then be used for predicting other possible compounds are alloys with a given desired crystal structure. These maps were constructed by choosing coordinates based on those physical factors which felt to be important in controlling structural stability. For example Villars [8-10] has recently plotted three-dimensional maps (ΔX, ΔR, e/a) for binary compounds with the AB, AB_2, AB_3 and A_3B_5 stoichiometries. The three coordinates reflect the importance of the electronegativity difference ΔX, the atomic size difference ΔR and the average number of valence electrons per atom e/a in determination of structural stability [11,12]. These three dimensional plots suffer several drawbacks. These fairly related to the neglect of the angular dependence of the valence orbitals, since whether the electrons have s-, p- or d-like quantum character is not reflected in the choice of classical coordinates (ΔX, ΔR, e/a).

The alternative approach to the construction of structure maps has been proposed by D.G. Pettifor [13-15], rather than trying to find a set of microscopic coordinates which will produce a separation. The structural types within same n dimensional space, he look instead for a single phenomenological coordinate which would lead to good structural separation of empirical data on binary systems within two dimensions [16].

This was achieved by running a one-dimensional string through the two-dimensional periodic table [11] as shown in Fig. 1.2. Pulling the ends of the string apart orders all the elements along a one dimensional axis, their sequential order being termed the Mendeleev number M. This simple procedure is found to provide excellent structural

separation of all binary compounds with a given stoichiometry A_mB_m within a single two-dimensional plot (M_A, M_B). For example AB and also AB_2 structure map is shown in Figs. 1.3 and 1.4. For other structure maps like AB_3, AB_4, AB_5 etc. can be found in Ref. [17]. The values of Mendeleev number and their structure are shown in Table 1.2.
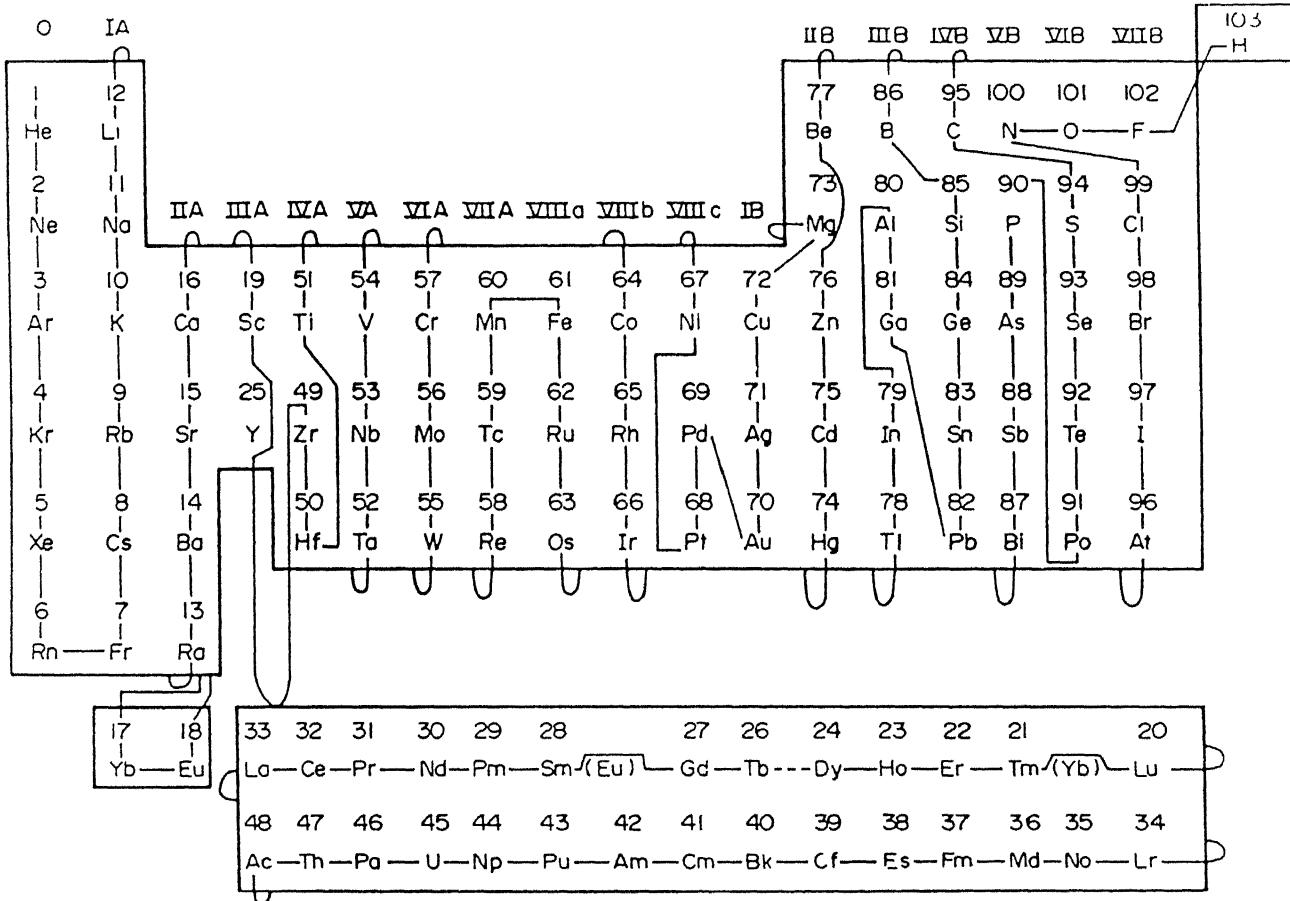
Fig. 1.2: Periodic table showing the achievement of Mendeleev number

1.4 Motivation and Objective of the present work

In view of the preceding discussion, it is clear that intermetallic compounds are an important class of emerging compounds. From a design point of view there is a need to organize property data so that it may either be used directly in design calculation or may be used to estimate unknown data through the use of correlations. Accordingly, in this work we
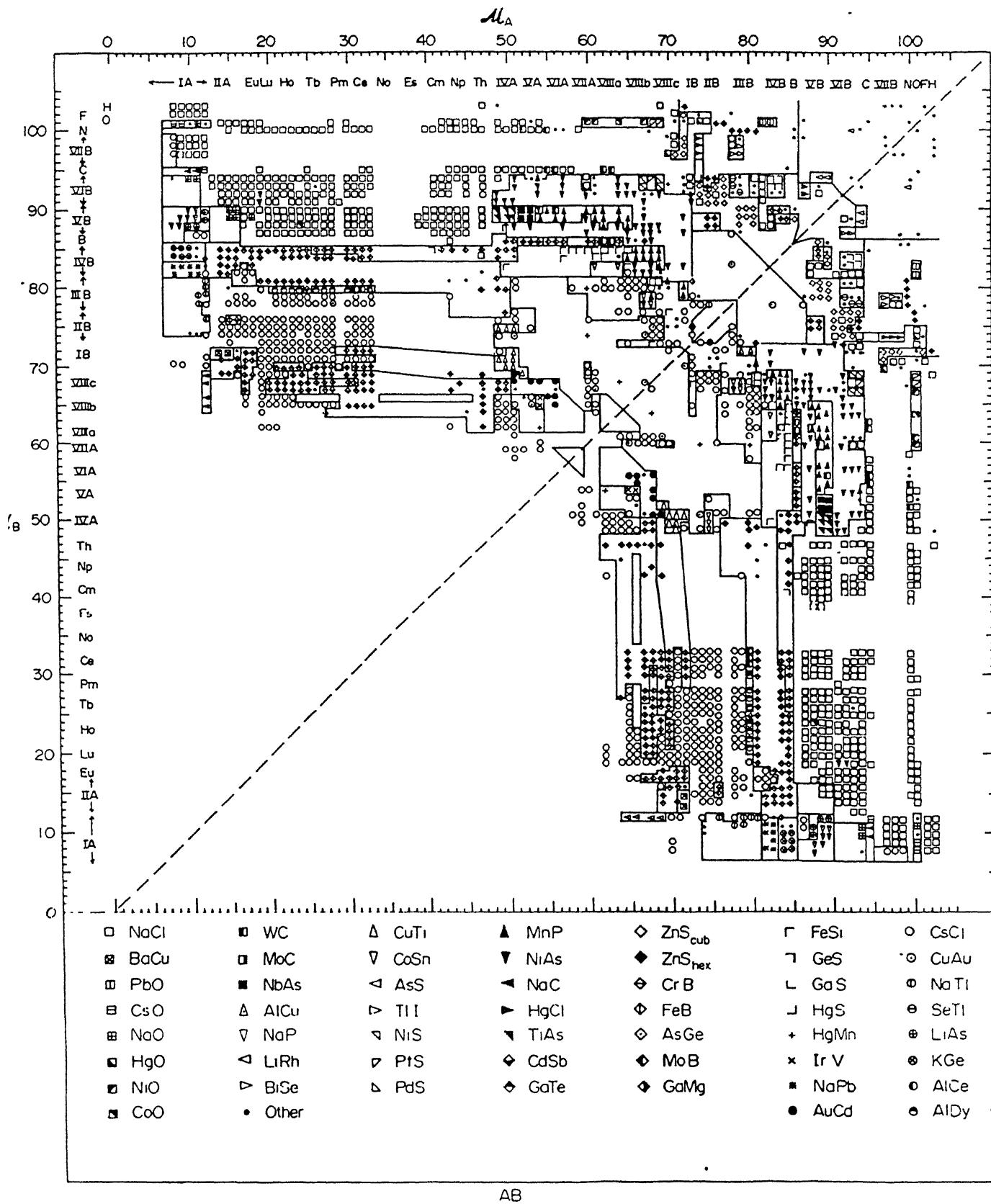
Fig. 1.3: Structure map for AB type compounds
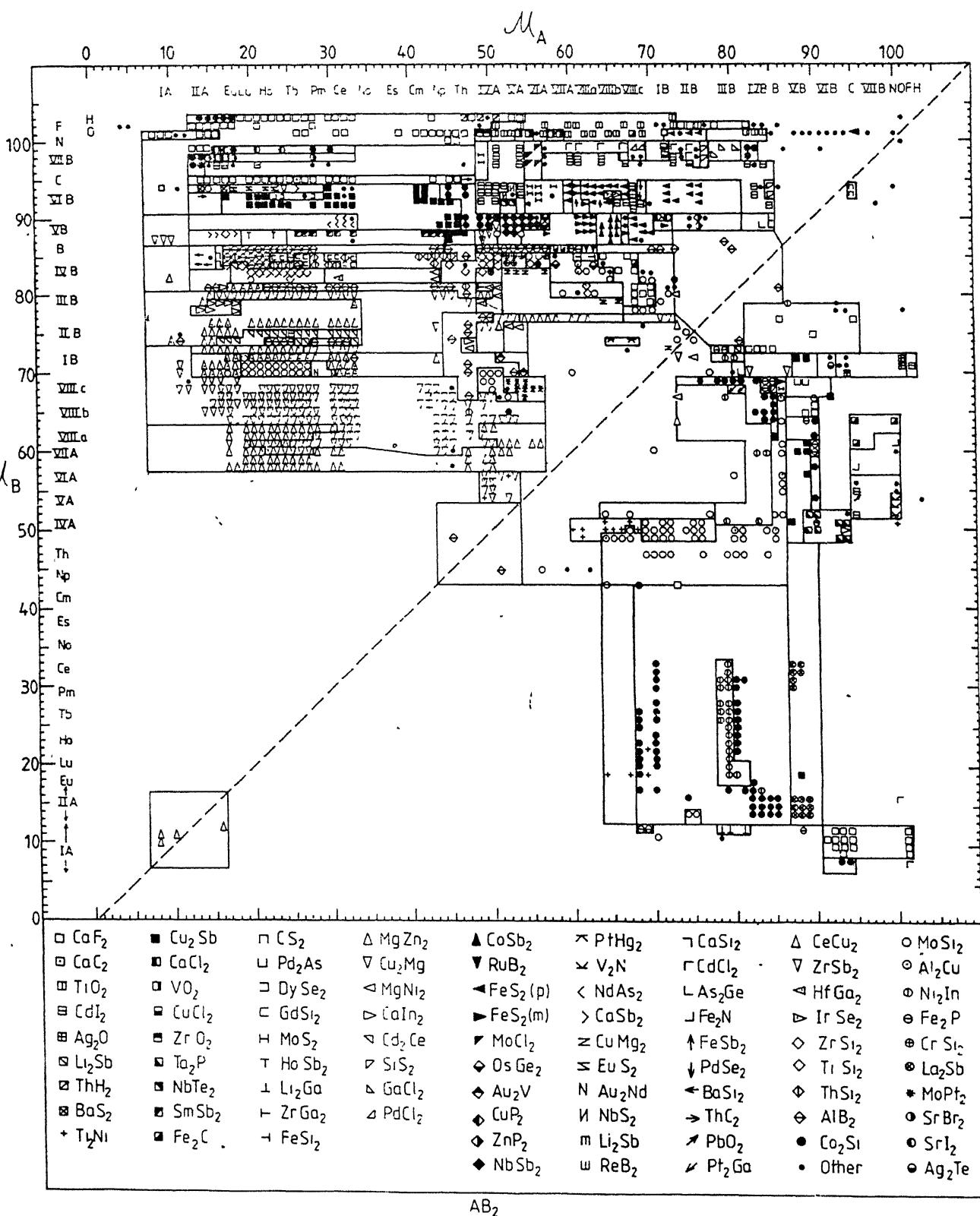
Fig. 1.4 Structure map for AB₂ type compounds

Table 1.2: Mendeleev numbers for the elements in the periodic table with their crystal structure [17]

Mendeleev no M	Element	Structure	Mendeleev no M	Element	Structure
1	Ho	hcp	53	Nb	bcc
2	Ne	fcc	54	V	bcc
3	Ar	fcc	55	W	bcc
4	Kr	fcc	56	Mo	bcc
5	Xe	fcc	57	Cr	bcc
6	Rn		58	Re	hcp
7	Fr		59	Tc	hcp
8	Cs	bcc	60	Mn	compl
9	Rb	bcc	61	Fe	bcc
10	K	bcc	62	Ru	hcp
11	Na	hcp	63	Os	hcp
12	Li	cp	64	Co	hcp
13	Ra		65	Rh	fcc
14	Ba	bcc	66	Ir	fcc
15	Sr	fcc	67	Ni	fcc
16	Ca	fcc	68	Pt	fcc
17	Yb	hcp	69	Pd	fcc
18	Eu	bcc	70	Au	fcc
19	Sc	hcp	71	Ag	fcc
20	Lu	hcp	72	Cu	fcc
21	Tm	hcp	73	Mg	hcp
22	Er	hcp	74	Hg	rhom
23	Ho	hcp	75	Cd	hcp
24	Dy	hcp	76	Zn	hcp
25	Y	hcp	77	Be	hcp
26	Tb	hcp	78	Tl	hcp
27	Gd	hcp	79	In	tetr
28	Sm	cp	80	Al	fcc
29	Pm	dhcp	81	Ga	compl
30	Nd	dhcp	82	Pb	fcc
31	Pr	dhcp	83	Sn	dia
32	Ce	fcc	84	Ge	dia
33	La	dhcp	85	Si	dia
34	Lr		86	B	compl
35	No		87	Bi	lay
36	Md		88	Sb	lay
37	Fm		89	As	lay
38	Es		90	P	compl
39	Cf	dhcp	91	Po	sc
40	Bk	dhcp	92	Te	chain
41	Cm	dhcp	93	Se	chain
42	Am	dhcp	94	S	ring
43	Pu	compl	95	C	gra
44	Np	orth	96	At	dim
45	U	orth	97	I	dim
46	Pa	tetr	98	Br	dim
47	Th	fcc	99	Cl	dim
48	Ac	fcc	100	N	dim
49	Zr	hcp	101	O	dim
50	Hf	hcp	102	F	dim
51	Ti	hcp	103	H	dim
52	Ta	bcc			

sc simple cubic, bcc body centred cubic, fcc face centred cubic, hcp hexagonal close packed, cp close packed, tetr tetragonal, orth orthorhombic, rhom rhombohedral, compl complex, dia daimond, gra graphite, lay, chain, ring and dim are structure types built up from puckered layers, helical chains, rings and dimers respectively.

- Develop a intermetallic compound database
- Determine various property ranges and this has been described in chapter 2
- Investigate correlation between various physical properties as well as correlations between properties and structure maps. The later is based on the presume that properties are function of the structure.

Chapter 2

Property Ranges in Intermetallic Compounds

2.1 Introduction

The conventional classification of engineering materials is generally given by

- Metals and alloys
- Polymers
- Ceramics and Glasses
- Composites

In addition to the above classification, intermetallic compounds may be treated as a separate category of materials. This is so because they are stoichiometric compounds of metallic and metalloid elements and are similar to metallic materials in regard to some properties but similar to ceramics in regard to other properties. For example, the brittleness of many intermetallics on account of highly directional bonding has

similarities with ceramic materials. In contrast their thermal conductivity is comparable to that of metallic materials.

Metals have relatively high moduli. Their strength can be increased by alloying or by mechanical and heat treatment. These remain ductile and can be used in deformation processes. The general characteristics of these materials are good electrical and thermal conductivity, relatively high strength, high stiffness, ductility or formability and shock resistance. These are particularly useful for structural and load bearing applications. Although pure metals are occasionally used, combination of metals (alloys) is normally designed to provide improvement in a particular desirable property.

Polymers have low moduli and strength. They can take large elastic deflections. They creep, even at room temperature. Their properties depend on temperature and their maximum service temperature is about 200 °C. They are easy to shape. The large elastic deflections allow the design of polymer components which snap together, making assembly fast and cheap. Polymers are corrosion resistant and they have low coefficient of friction.

Polymers include rubber, plastics and many adhesives. They are produced by creating large molecular structures from organic molecules in a process known as polymerization. Thermoplastic polymers in which, long molecular chains are not rigidly connected, have good ductility and formability. Thermosetting polymers are stronger but more brittle because molecular chains are highly lined.

Ceramics and Glasses have high moduli but are brittle when compared with metals. Their brittle compression strength is fifteen times larger than the brittle fracture strength. Their brittleness shows a wide scatter in the strength, depends on the volume of material under load as well as time for which it is applied. They have attractive features as being stiff, hard and abrasion–resistant. They retain their strength at high temperatures and they are corrosion resistant.

The examples of ceramics are brick, glass, tableware, refractories and abrasives, have low electrical and thermal conductivity and consequently are often used as insulators. They have good optical properties also. So they are used in fibre optic system and a variety of devices. They are also used in integrated circuits.

Composite materials combine attractive properties of the constituent materials. They are light, stiff and strong and they can be tough. Most of the composite materials at present available to the engineer have a polymer matrix. Epoxy or polyester, usually reinforced by fibres of glass, carbon or kelvar. Composite components are extensive and they are relatively difficult to form and join. With composites we can produce lightweight, strong, ductile, high temperature resistant materials, shock resistant cutting tools. Advanced aircraft and aerospace engines rely heavily on composites such as carbon– fibre-reinforced polymers.

Intermetallics are emerging materials with potential high – temperature applications. Their melting point can be as high as 3000 °C. In addition, their strength and stiffness suggest that they may find use in various engine applications. Because of their high

melting points, many non-constitutional techniques are used for processing of intermetallic compounds. A comparative listing of processing techniques used for various classes of materials is given in Table 2.1.

2.2 Structure - Property Relationships

We can consider the properties of a material mainly in two categories

- Mechanical
- Physical

Mechanical properties describe how a material responds to an applied force. The most common mechanical properties are strength, ductility and stiffness (modulus of elasticity). However, we are often interested in how a material behaves when it is exposed to a sudden, intense blow (impact), continually cycled through an alternating force (fatigue), exposed to high temperatures (creep), or subjected to abrasive conditions (wear). Mechanical properties also determine the ease with which a material can be deformed into a useful shape.

Physical properties, which include electrical, magnetic, optical, thermal, elastic and chemical behaviour, depend on structure and processing of a material. Even small changes in composition cause profound changes in the electrical conductivity of many semiconducting materials.

The properties of a material depend on its structure. So for example, glassy polyethylene is transparent, whereas crystalline polyethylene is translucent. Imperfections in either type of atomic arrangement may be controlled to produce profound changes in properties.

A grain structure is found in most metals, semiconductors, ceramics and occasionally in polymers. The size and shape of the grain play a key role. In some cases, as with silicon chips for integrated circuits or metals for jet engine parts, we wish to produce a material containing only one grain, or a single crystal.

Finally, in most materials, more than one phase is present, with each phase having its unique atomic arrangement and properties. Control of the type, size, distributions and amount of these phases within the main body of the material provides an additional way to control properties.

Table 2.1: Materials processing techniques

Category and Technique	Process
Metals and alloys	
Casting	Sand, die casting, permanent mould, investment, continuous casting.
Forming	Forging, wire drawing, deep drawing, bending, rolling.
Rolling	Gas welding, resistance welding, brazing, arc welding, soldiering, friction welding.
Machining	Turning, drilling, milling, cutting
Powder metallurgy	Compaction of metal powders
Ceramics	
Casting	Slip casting
Compaction	Extrusion , pressing, isostatic pressing
Sintering	Compaction and followed by heating at high temperatures.
Polymers	
Moulding	Injection moulding, transfer moulding.
Forming	Spinning, extrusion, vacuum forming.
Composites	
Casting	
Forming	
Joining	Adhesive bonding, explosive bonding, diffusion bonding.
Compaction and sintering	Powder pressing and heating to cause the powder to join.
Intermetallics	
Extrusion	To compact powder and provide a wrought product in one step.
Rolling: Hot pack rolling	Maintaining high temperature in the intermetallic preform during transfer from furnace to rolls.
Joining: Fusion welding, Friction welding	Several pieces are joined together at high temperature.
Forging	Thermomechanical process
Electro deposition	The deposition ions from an electrolyte onto the cathode in an electrolytic cell under the influence of an applied potential e.g., Nb-Ge intermetallics
CVD	Thermally induced decomposition of gaseous species on or near a substrate eg., refractory metal silicides.

PVD	Condensation of deposition of gaseous species may be thermal vaporization from a liquid, sublimation from a solid or sputtering from a solid e.g., Pt-Ga.
Ion Implantation and Ion Beam Induced Mixing	An ion beam of the chemical species desired is accelerated at a target whose composition is to be modified. Accelerating voltages, in the range of hundreds to millions eV, ensure that the ions penetrate and become part of the near-surface region of the target material e.g., Ni-Si system.
Combustion synthesis/CS Reactive synthesis/RS Reactive Hot Isostatic (HIP) pressing	The rapid non-isothermal reaction of mixed elemental powders to from compounds is called CS/RS. If external pressure is applied during the reaction then the process may be designated as reactive hot pressing or reactive hot isostatic pressing.

2.3 Classification of Properties according to Crystal Structure

Based on their dependence on properties of a material may be classified as:

- Structure-sensitive
- Structure-insensitive

The structure insensitive properties are well defined properties of a phase and do not strongly depend on processing history and resultant microstructure whereas structure sensitive properties are dependent not only on the composition and crystal structure of the material but also on structural details that depend upon the previous history of the sample. Thus structure-sensitive properties are properties of a particular sample of a material, while the structure insensitive properties relate to the material. Different samples of the same material have essentially identical structure-insensitive properties, but structure-sensitive properties are identical only when the previous treatment has been equivalent. Some of the structure sensitive and structure insensitive properties are shown in Table 2.2.

Mechanical Properties

The application of a stress to a material may cause many changes.
Elastic deformation, in which strain appears and disappears simultaneously with the application and removal of the stress.
Anelastic deformation, in which strain reaches its maximum value after the stress has reached its maximum value, and, in which strain disappears after the removal of stress.
Plastic deformation, in which strain occurs simultaneously with the application of the stress, but does not vanish if the strain is removed.
Creep, in which non recoverable strain occurs, while the stress is held at a fixed value.
Fracture, in which separation takes place.

Of these properties, only first (elastic behaviour) is structure-insensitive. Anelasticity and creep would not be expected to occur in a perfect crystal and plastic deformation and fracture would occur in a perfect crystal at much higher stresses and strains than are normally found experimentally. These four properties are therefore, structure- sensitive and must be considered in relation to crystals that are imperfect.

Elastic modulus is defined as the slope of the linear elastic part of the stress-strain curve. In reality, moduli measured as slope of stresses are inaccurate, because of the contribution of anelasticity and other factors. Accurate moduli are measured by exciting the natural vibrations of a beam or wire, or by measuring the velocity of waves in the material.

Table 2.2: Classification of properties according to structure [28]

Property	Structure-Insensitive	Structure-Sensitive
Mechanical	Elastic moduli	Fracture strength Plasticity Fracture toughness Creep strength
Physical Thermal Electrical Magnetic Optical Nuclear	Density Thermal expansion Melting point Thermal conductivity Specific heat Emissivity Resistivity (metallic) Electrochemical potential Thermo electric properties Paramagnetic and Diamagnetic properties Reflectivity Absorption of radiation	 Diffusion Resistivity (Semiconductor and at low temperature) Ferromagnetic properties

Physical properties

Density of a crystal can be calculated from the mass of the atoms and geometry of the crystal. The latter one is described by the volume of unit cell of the structure and number of atoms per unit cell. These two parameters inturn depend on the type of the structure and ionic radius appropriate to the structure.

Melting temperature is the most useful structure-insensitive property because
- Its relative magnitude is a reasonable first approximation to the stiffness of a material, since the elastic moduli have a strong correlation with melting temperature.
- In all models of strengthening, values of flow stress increases with the magnitude of the elastic constants which inturn increase with T_m.
- Expansion coefficients are also vary inversely with T_m.
- It gives some idea about the maximum service temperature of a material.

2.4 Property Ranges for various Category of Materials

A general idea about property ranges of materials is useful in mechanical design. For example, ceramics are hard and brittle, metals are ductile and conduct well, polymers are light and have large expansion coefficients. Chemical engineers strive to survive materials in corrosive condition. Automobile engineers desire lightweight and durable materials. Aerospace engineering demand lightweight materials that perform well both at high temperatures and in the cold vacuum of outer space. The property ranges for various categories of materials are shown in Table 2.3. Such information has been found very, useful for materials selection in design. For example, Fig. 2.1 presents the materials selection map based on elastic modulus and density of various materials [22]. When this information is presented in terms of property ranges, different classes of materials occupy different regions on the plot. The material which offers the best combination of properties can then be located on such maps using the materials selection approach outlined in [22].

Fig. 2.1 gives the idea of materials selection for light and stiff compounds. The guide lines in this figure indicates

- $E/\rho = C$ (minimum weight design of stiff ties; minimum deflection in centrifugal loading, etc.)
- $E^{1/2}/\rho = C$ (minimum weight design of stiff beams, shafts and columns)
- $E^{1/3}/\rho = C$ (minimum weight design of stiff plates)

The property ranges are also useful in property checking of the new data. When creating a database and to tabulate the new data, property ranges are useful in checking whether each new data lies within the given property range. All properties have well defined ranges and any new data should generally lie in its proper band. Any discrepancy may then easily be checked again so as to avoid any gross errors from occuring in the compilation.
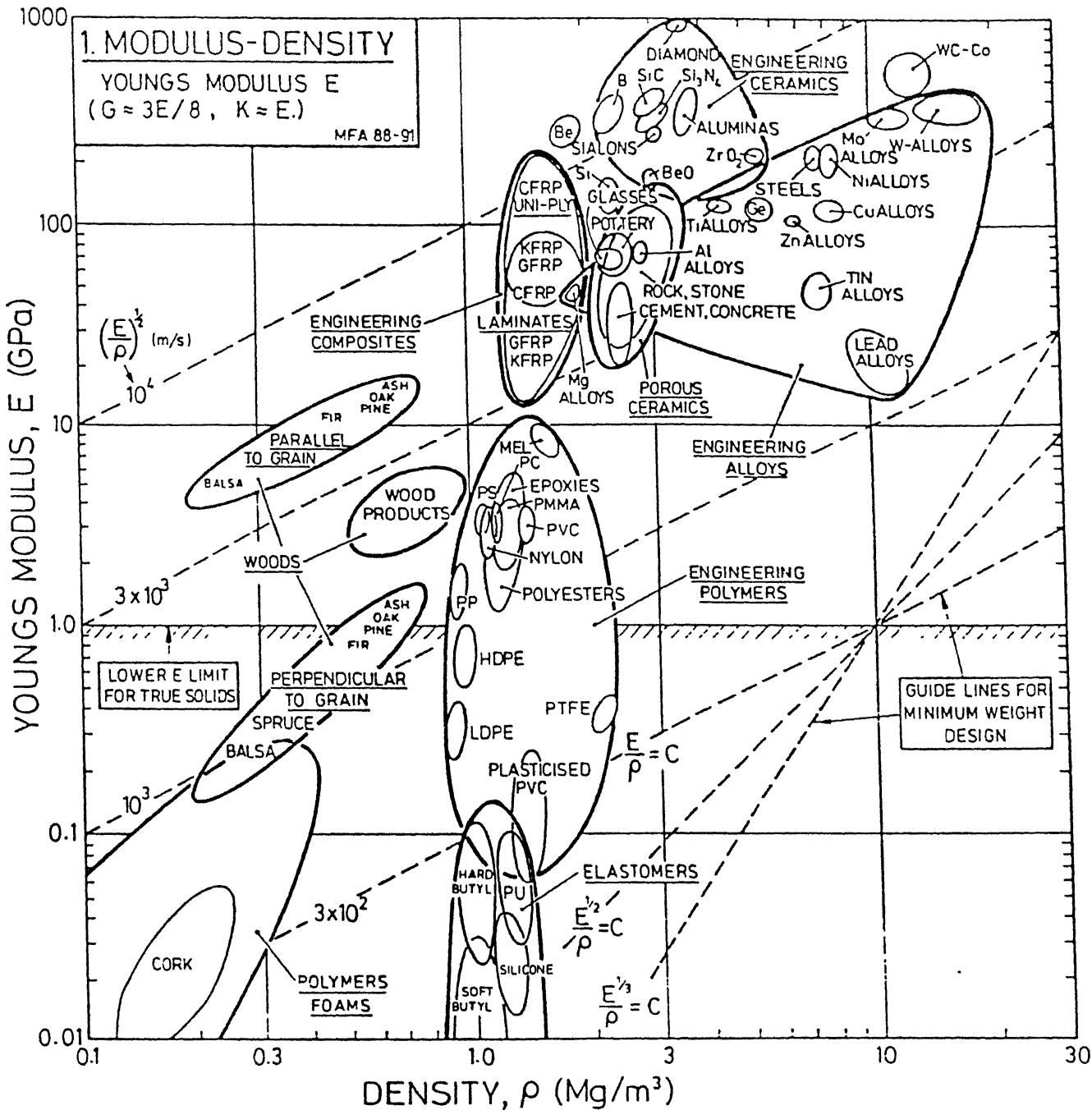
Fig. 2.1: Materials selection chart between young's modulus E and density ρ

2.5 Property Ranges for Intermetallic Compounds

Property range data for metals, polymers, ceramics and composites have been reported by [22]. In this section we present data on property ranges for intermetallic compounds based on a data compilation developed by us [19]. The property ranges for various categories of materials are shown in Table 2.3. The database has data for about 100 intermetallic compounds Representative properties are shown in Table 2.4. The structure of data is as follows and typical data sheet is shown for MoSi$_2$.

<div align="center">MoSi$_2$</div>

Crystallographic Data[*]	Space group	I4/mmm	[29,30]
	Crystal system	Tetragonal	[29,30]
	Strukturbericht type	C11$_b$	[29,30]
	Lattice constants	a= b=3.203Å	[29,30]
		c= 7.885 Å	[29,30]
	Pearson symbol	tI6	[29,30]
Thermal data	Melting Temperature, T$_m$ ($^{\circ}$C)	2032	[3]
	Heat of formation, -ΔH_f (k.cal/mole)	31.5	[25]
Physical data	Density, ρ (kg/m^3)	6120	[3]
	Electrical resistivity (Ω-m)	10^{-6}	[31]
Mechanical data	Hardness	13.2 –15.5(vickers)	[31]
	Elastic modulus, E (GPa)	4.397	[26]
	Shear modulus, G (GPa)	1.911	[26]
	Bulk modulus, K (GPa)	2.097	[26]
	Poisson's ratio, ν	0.151	[26]
Elastic constants	C$_{11}$, C$_{22}$, C$_{33}$, C$_{44}$, C$_{55}$, C$_{66}$,	4.17, 4.17, 5.15, 2.04,	[26]
	C$_{12}$, C$_{13}$, C$_{23}$	2.04, 1.94, 1, 0.84, 0.84	[26]

[*] Various nomenclatures of crystal structures of intermetallic compounds are shown in Appendix.

The results are presented in Figs. 2.2 – 2.10. Data for conventional materials is also included to enable comparisons to be made and generalisations to be drawn. Figs. 2.2 – 2.10 shows the schematic representation of property ranges for various properties for different categories of materials including intermetallic compounds. Fig. 2.11 summarizes all property ranges of intermetallic compounds. Narrower ranges are obtained if we consider various categories of intermetallic compounds such as aluminides, silicides and beryllides [19].

Table 2.2: *Property (Physical) ranges for various categories of materials*

Property	Material				
	Metals	**Ceramics**	**Polymers**	**Composites**	**Intermetallics**
Physical properties					
Density, gm/cc	$0.5 - 23$	$1 - 15$	$0.75 - 5$	$0.3 - 15$	$2 - 20$
Melting point, K	$234 - 3700$	$140 - 4000$	$200 - 800$	$250 - 1750$	$500 - 3000$
Electrical conductivity, $\Omega^{-1}cm^{-1}$	$10^5 - 10^9$	$10^{-19} - 10^{-5}$	$10^{-16} - 10^{-9}$	-	$10^3 - 10^9$
Thermal conductivity, W/m/K	$5 - 500$	$1 - 500$	$0.01 - 10$	$0.1 - 2$	$0.2 - 75$ (at 300K) $0.2 - 350$ ($75 - 2500$ K)
Coefficient of linear thermal expansion, K^{-1} ($X10^{-6}$)	$5 - 50$	$1 - 20$	$20 - 300$	$2 - 50$	$1.15 - 184.3$ ($293 - 1785$ K)
Heat of formation, k.cal/mole	-	-	-	-	$1 - 200$

Table 2.2: Property (Mechanical) ranges for various categories of materials (continued)

Property	Material				
	Metals	Ceramics	Polymers	Composites	Intermetallics
stic modulus, GPa	1.7 – 600	7 – 1000	10^{-3} – 20	0.5 – 700	50 – 500
ar modulus, GPa	1 – 250	-	-	-	20 – 250
k modulus, GPa	25 – 400	-	-	-	50 – 300
sson's ratio	0.1 – 0.5	-	-	-	0.1 – 0.5
cture toughness, MPa m$^{1/2}$	5 – 200	0.1 – 10	0.5 – 5	1 – 60	1 – 50
ep temperature, °C	5 – 200	-20 – 2000	0 – 200	0 – 2000	200 – 1500
ep resistance, MPa	-	-	-	-	1 – 150
longation	-	-	-	-	0 – 50
stic constant (C_{11}), GPa	-	-	-	-	50 – 500
ld strength, MPa	10 – 2000	3000 – 50000	0.2 – 400	2.5 – 1000	100 – 1500
sile strength, MPa	50 – 2000	1 – 800	5 – 100	100 – 1000	200 – 1500
rohardness, GPa	-	-	-	-	1 – 20

Table 2.4: Representative properties of intermetallic compounds

Property	Defining characteristics
Creep Strength	Melting temperature Nature of bonding
Oxidation Resistance	High activity of oxide – forming element Crystal structure
Ductility (DBTT)	Crystal structure Stoichiometry
Thermal Exapnsion	Melting temperature Nature of bonding Crystal structure
Elastic modulus	Crystal structure Nature of bonding
Alloying potential	Width of the phase field
Density	Principal element Crystal structure
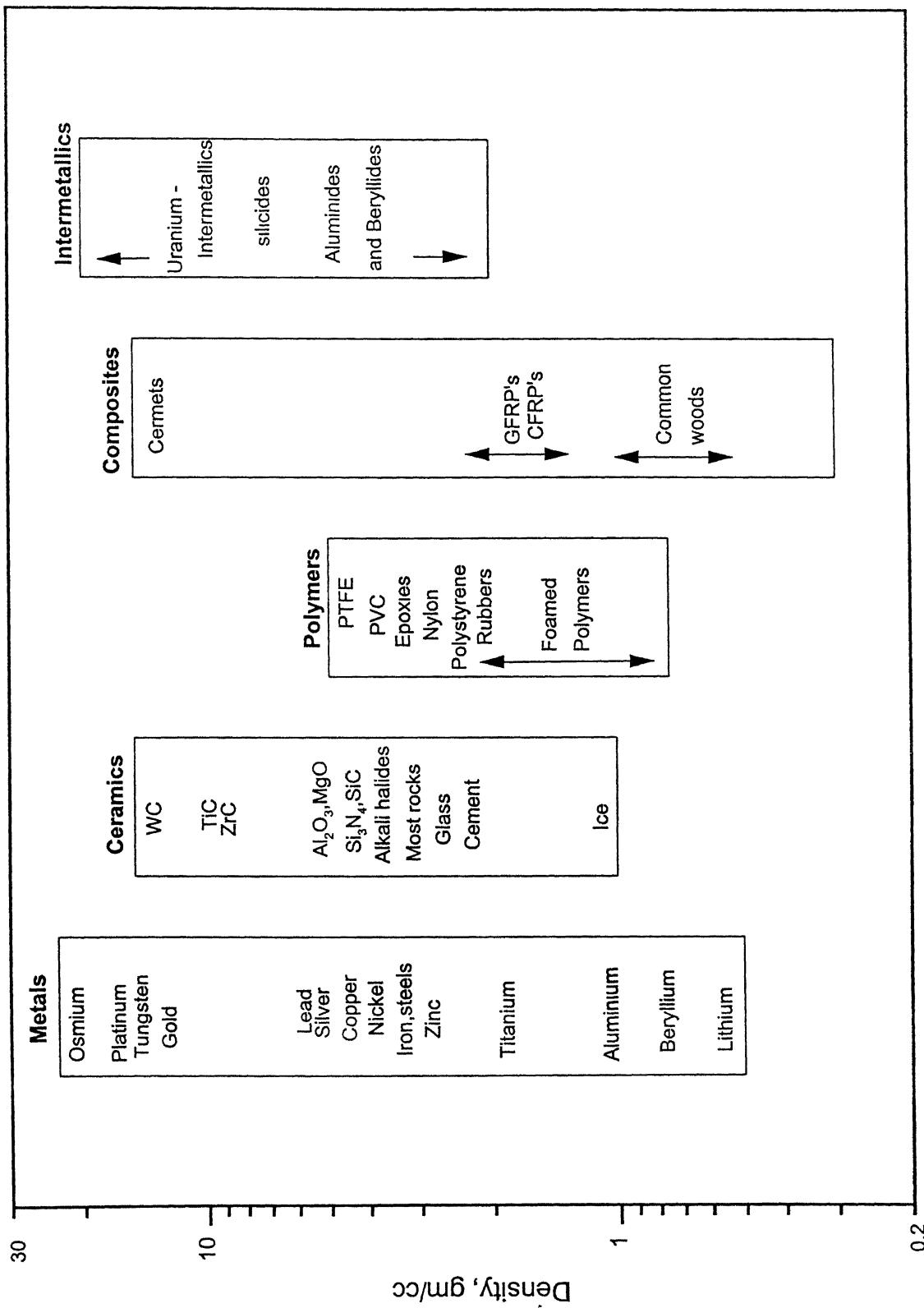
Fig. 2.2: Propety ranges for Density (ρ) for various category of materials
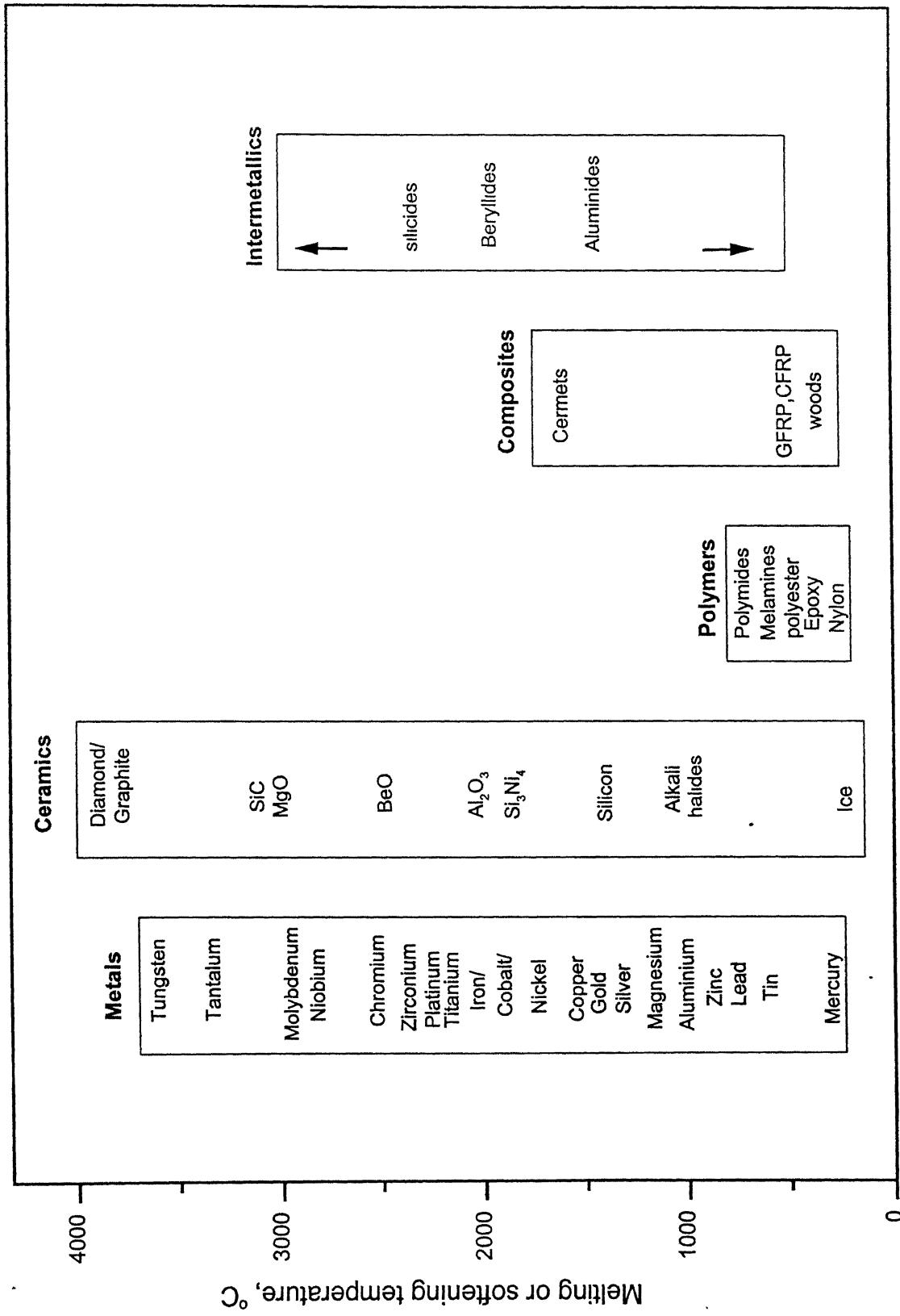
Fig. 2.3: Propety ranges for Melting or Softening Temperature (T_m) for various category of materials

Metals

Copper
Steel
Iron
Tin

Intermetallics

AlCu$_3$
NbSl$_2$
Si$_2$U$_3$

←
→

Ceramics

Silica brick

SiO$_2$ Crystals
Al$_2$O$_3$

Diamond

SiO$_2$ glass

Polymers

Nylon,rubber
Teflon
Polyethylene

10^{10}
10^{0}
10^{-10}
10^{-20}

Electrical conductivity σ, ohm^{-1}m^{-1}
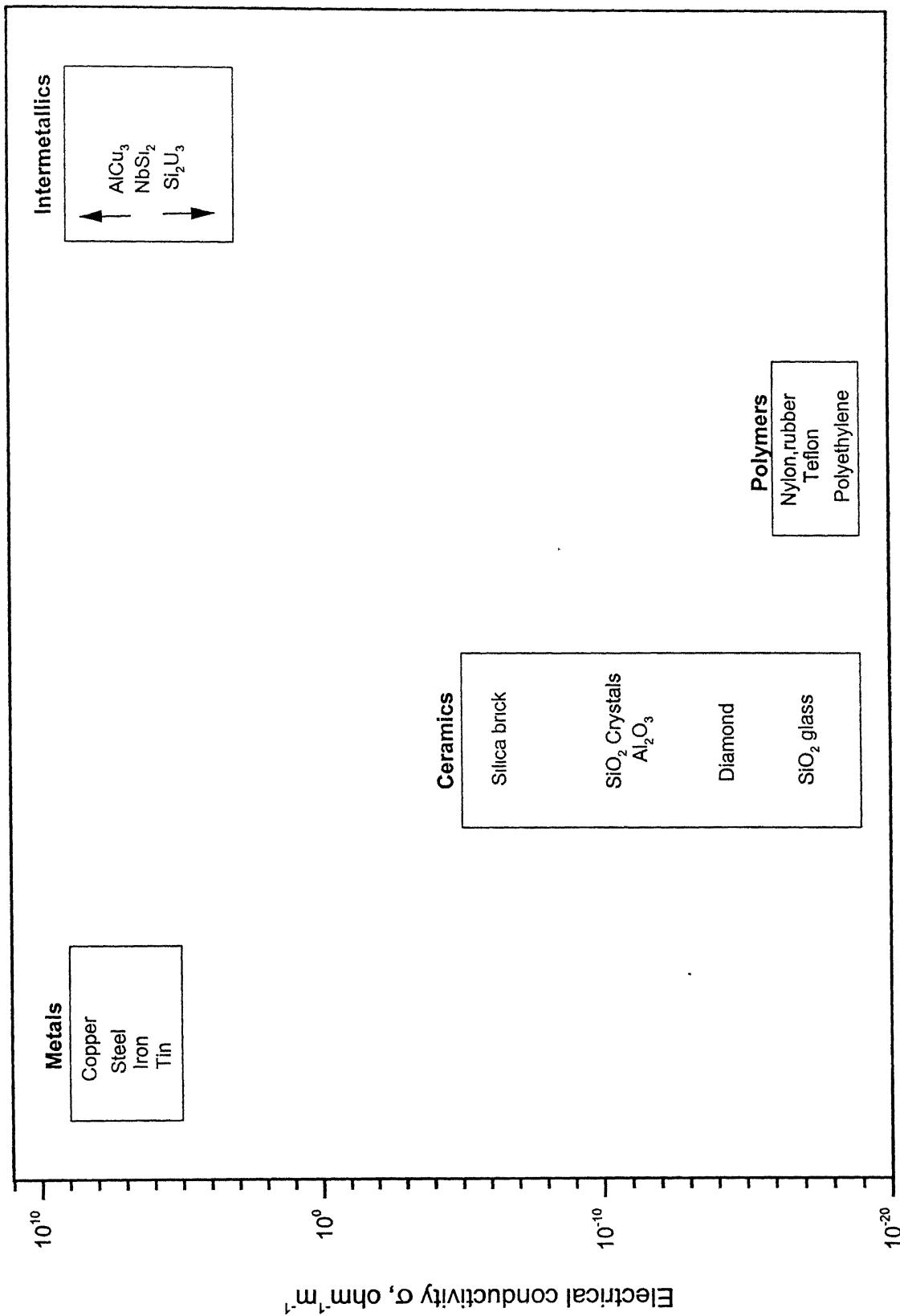
Fig. 2.4: Propety ranges for electrical conductivity (σ) for various category of materials
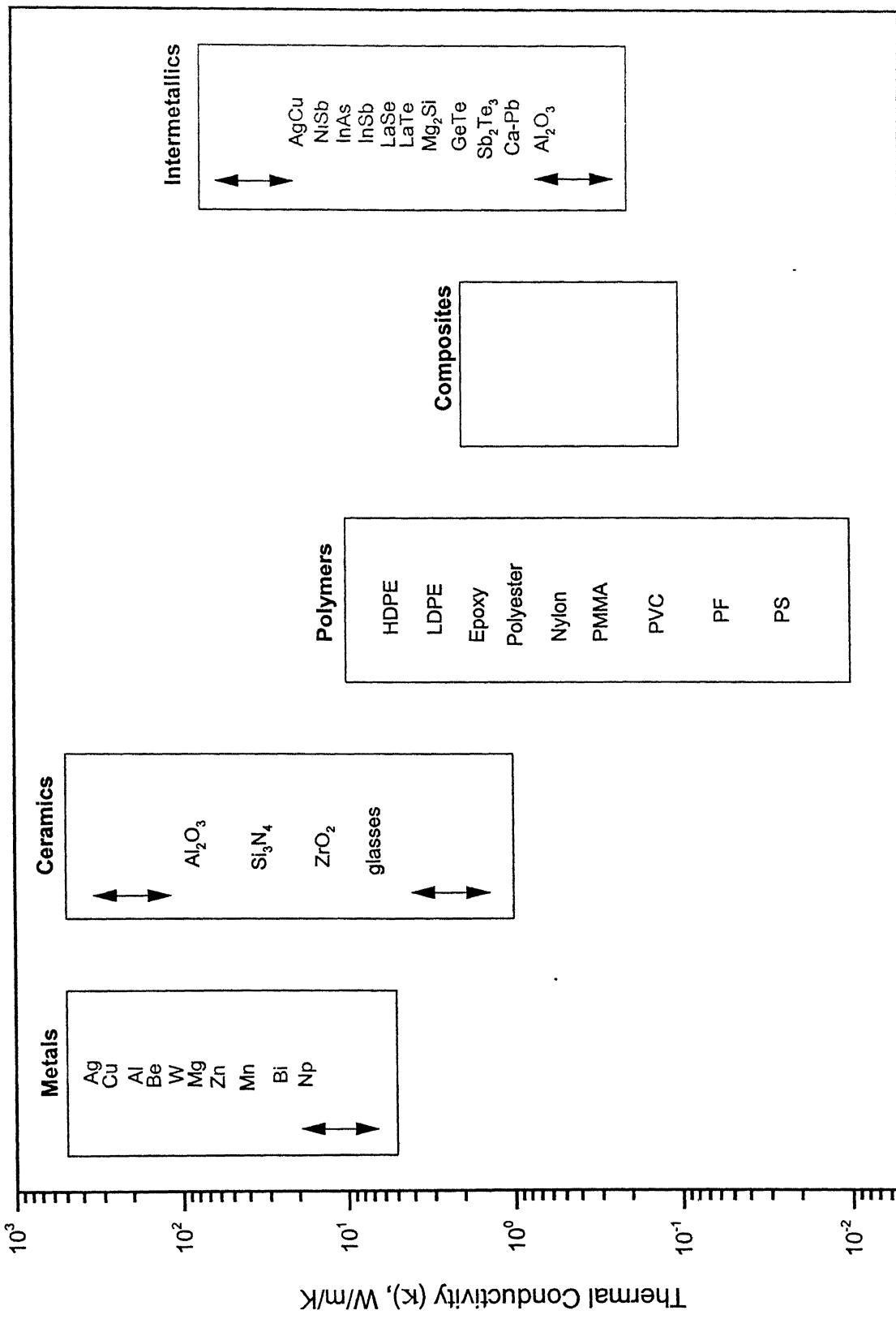
Fig. 2.5: Propety ranges for Thermal Conductivity (κ) for various category of materials
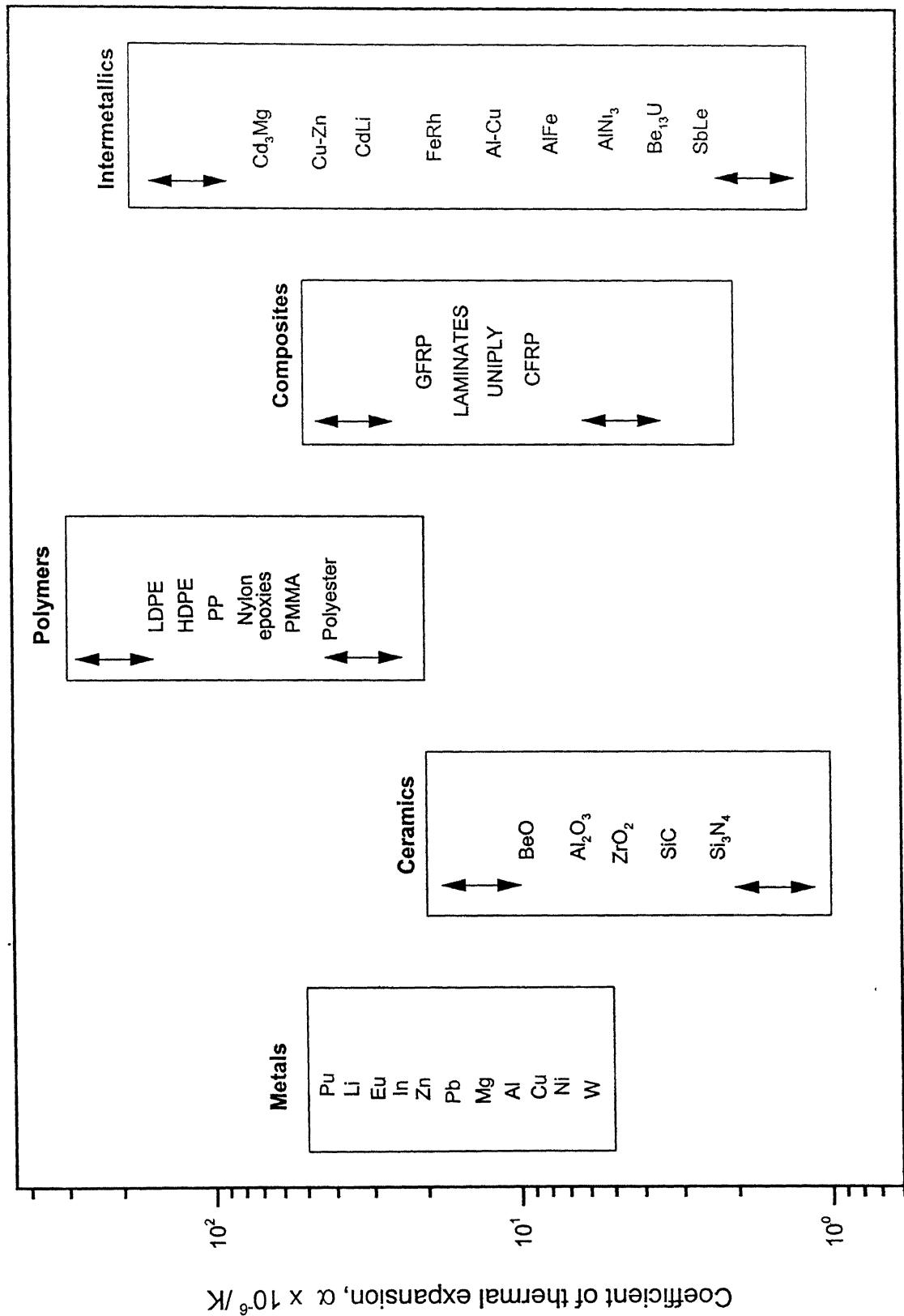
Fig. 2.6: Property ranges for Coefficient of thermal expansion (α) for various category of materials

Metals

Osmium
Tungsten
Chromium
Nickel
Iron+Steel
Copper
Titanium

Zinc
Tin
Magnesium

Lead

Ceramics

Diamond
WC,SiC
Al_2O_3, Si_3N_4
MgO
ZrO_2
Mullite
Cement
Graphite

Ice

Polymers

Alkyds

Melamines
Polymides
PMMA
Polystyrene
Nylon
Epoxy
(High density)
Polyethylene
(Low density)

Polypropylene

Rubbers

PVC

Foamed

Polymers

Composites

Cermets

CFRP's

Fibreglass

GFRP's

Woods‖grain

Woods,⊥grain

Intermetallics

CdTe
Cr_2Nb
WSi_2

10^4

10^2

10^0

10^{-2}

Young's Modulus E, GPa

Fig. 2.7: Propety ranges for elastic modulus (E) for various category of materials

31
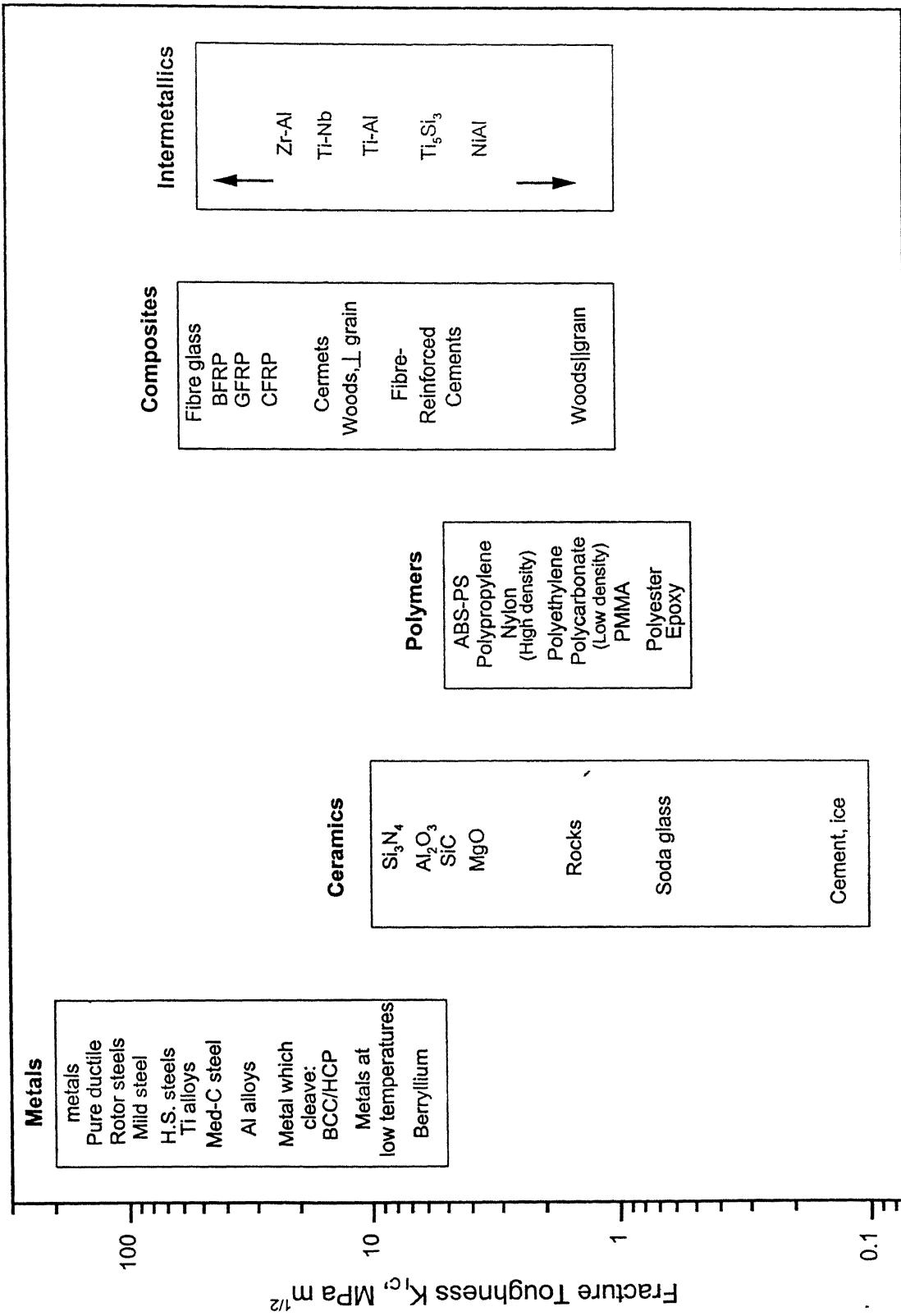
Fig. 2.8: Propety ranges for Fracture toughness (K_{Ic}) for various category of materials
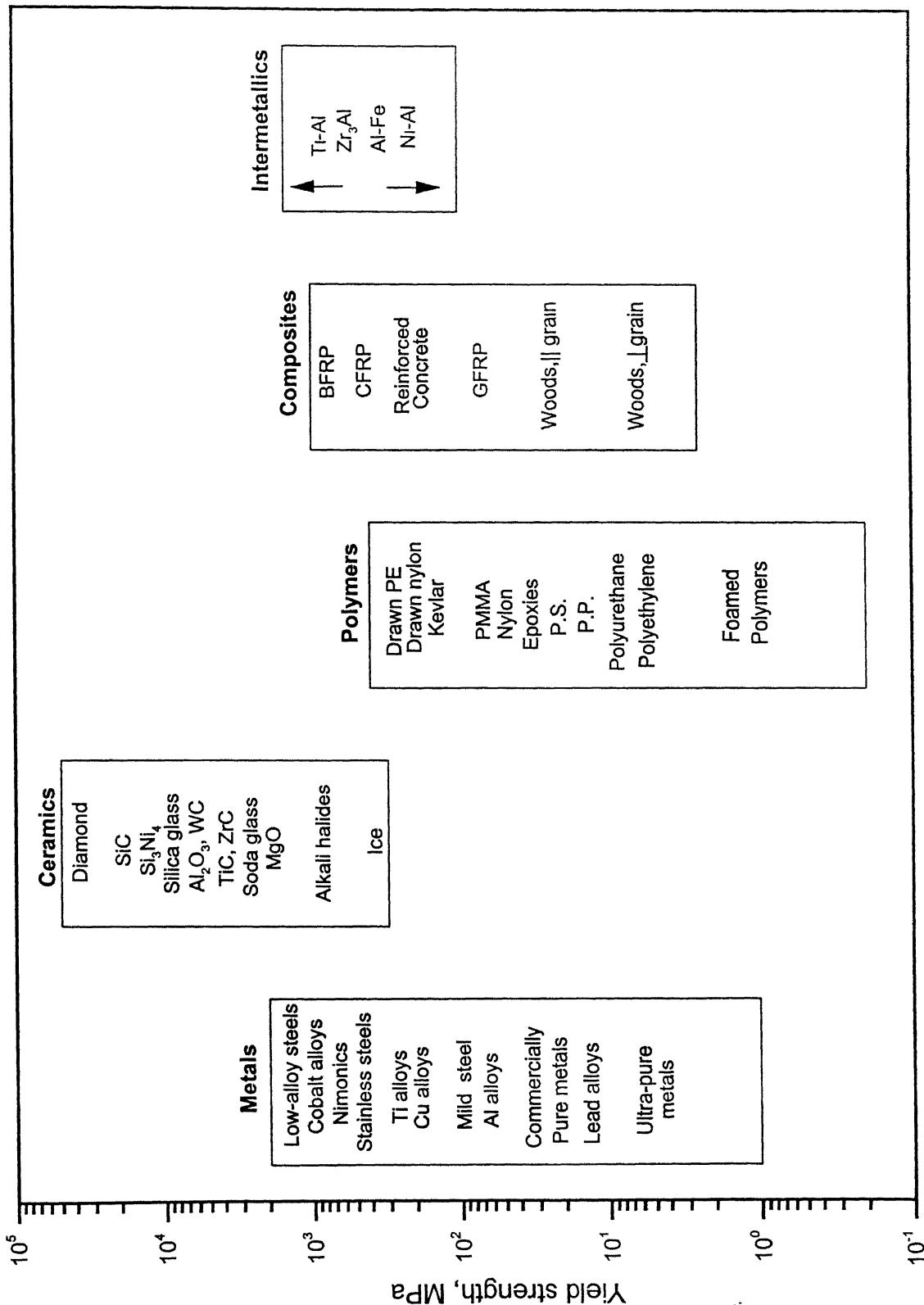
Fig. 2.9: Propety ranges for Yield Stress (σ_y) for various category of materials
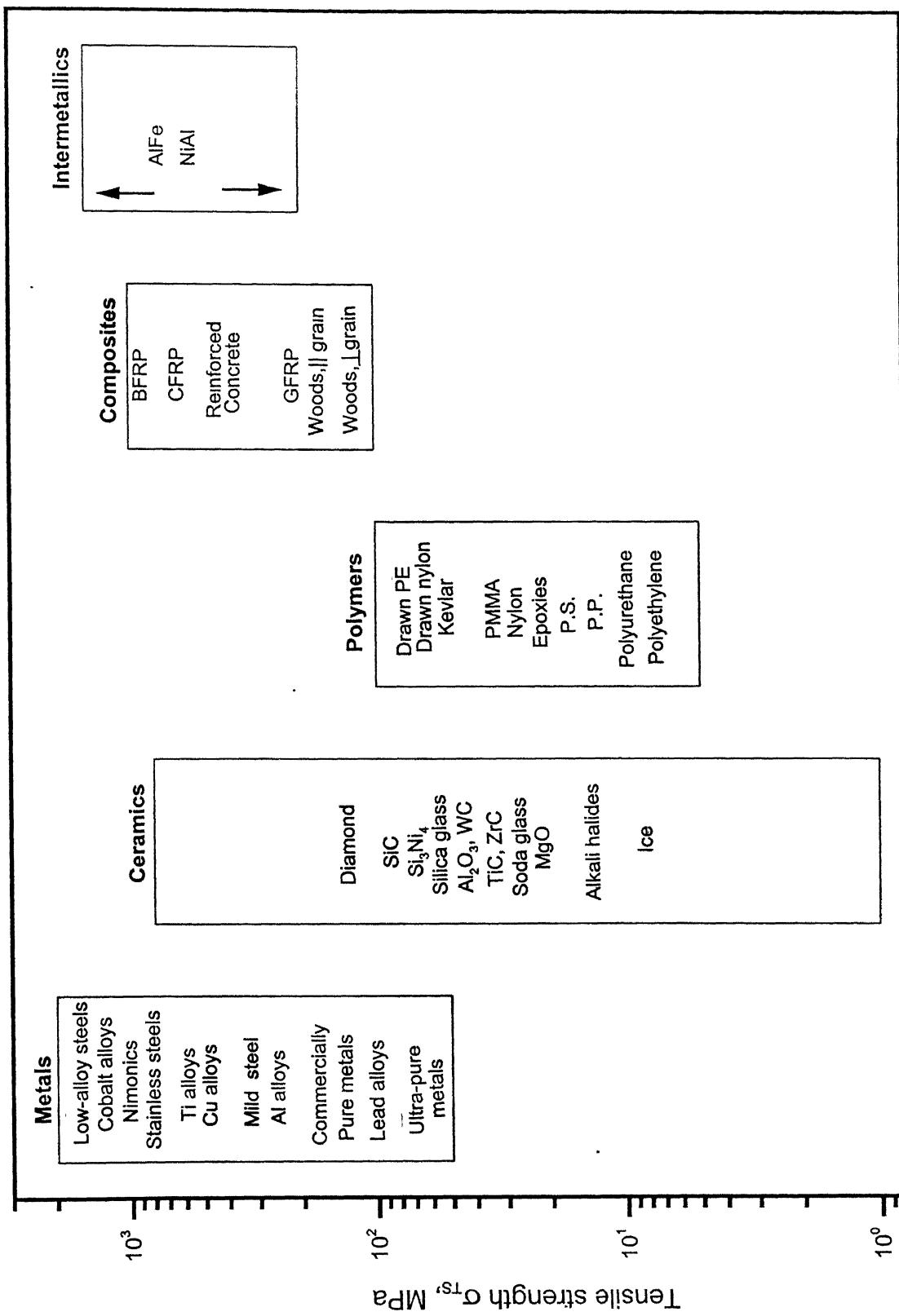
Fig. 2.10: Propety ranges for Tensile Strength (σ_{TS}) for various category of materials
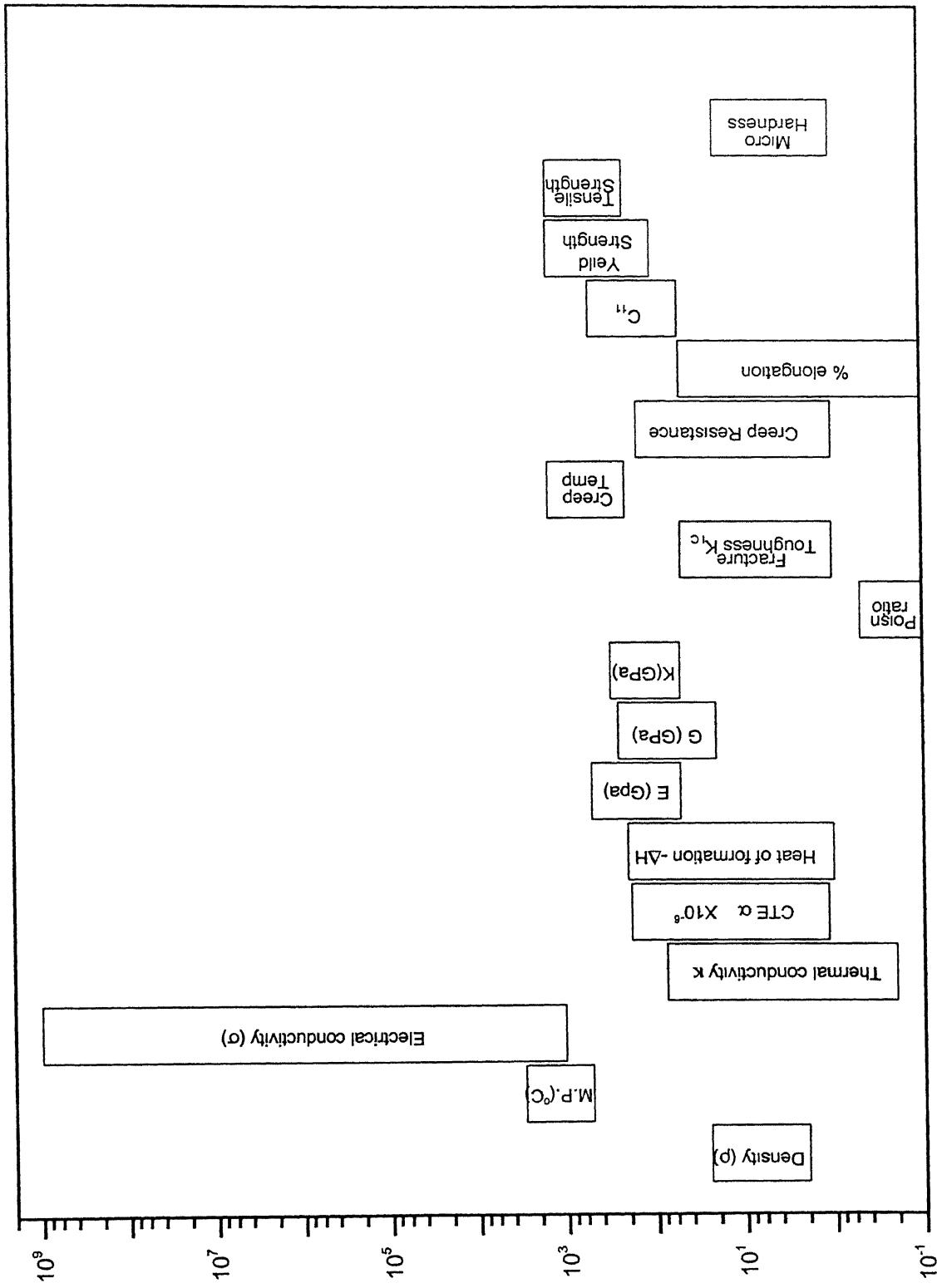
Fig. 2.11: Propety ranges for various properties of inermetallic compounds

Chapter 3

Correlations in Intermetallic Compounds

3.1 Literature Survey

A number of correlations between various physical properties have been investigated over the years for various classes of materials [7, 32]. Some correlations have a physical basis whereas others are empirical. In this chapter we will investigate the applicability of some of these correlations to intermetallic compounds. We first review some of the important correlations.

(a) Atomic volume V_m (m^3/k.mole)

The atomic volume denoted by V_m is given as

$$V_m = \frac{\overline{A}}{\rho} \qquad (3.1)$$

Where $\overline{A}$ is average atomic weight of the compound in (kg/k.mole) and ρ is the density in kg/m^3. The average atomic weight of the compound is given by

$$\overline{A} = \frac{mA_x + nA_y}{m + n}$$

Where A$_x$ and A$_y$ are the atomic weights of X and Y respectively.

(b) Relations between Elastic modulus E, Shear modulus G, Bulk modulus K and Poisson's ratio ν

We know for isotropic materials

$$G = \frac{E}{2(1+\upsilon)} \qquad (3.2)$$

$$K = \frac{E}{3(1-2\upsilon)} \qquad (3.3)$$

Theoretically ν may range between –1 and 0.5. However, for most materials ν varies between 0.2 and 0.4we can write above two relations as

$$C_L < \frac{G}{E} < C_H \qquad (3.4)$$

$$C_L < \frac{K}{E} < C_H \qquad (3.5)$$

Where C$_L$ and C$_H$ are lower and upper limits of the correlation.

(c) Relation between Elastic modulus E (GPa), Melting temperature T$_m$ (K)

(i) Relation between Elastic modulus E (GPa), Melting temperature T$_m$ (K), Atomic volume V$_m$ (m^3/k.mole) and Gas constant R (kJ/k.mole. K)

If the bonding between the atoms are stretched too far, they break. Similarly heat can break the bonds results in melting or sublimation. This is the basic relationship between elastic modulus E and melting temperature T$_m$. Bond stretching is characterized by bulk modulus K. The thermal energy per atom or molecule at melting point T$_m$ is RT$_m$/k.mole.

$$\frac{KV_m}{RT_m} = \text{constant}$$

Where R is the gas constant (8.314 kJ/k.mole.K). Expressing the above correlation with upper and lower limits,

$$C_L < \frac{KV_m}{RT_m} < C_H$$

or

$$C_L < \frac{EV_m}{RT_m} < C_H \qquad (3.6)$$

Similar relation can be obtained for E, V_m, T_m and C_p (KJ/Kmole.K) is given by

$$C_L < \frac{EV_m}{C_p T_m} < C_H \qquad (3.7)$$

(ii) Relation between Elastic modulus E (GPa), Melting temperature T_m (K), Density ρ (Kg/m³) and Specific heat C_p (kJ/kg.K)

The heat capacity is the heat required to raise the temperature of a solid by 1K. The molar heat capacity C_v^m (J/k.mole.K) is given by

$$C_v^m \approx 3R$$

$$C_V (kJ/kg.K) = \frac{3R}{\rho V_m}$$

In solid state heat capacity at constant pressure C_p is equal to that at constant volume, giving the correlation

$$C_L < \frac{C_p \rho V_m}{R} < C_H \qquad (3.8)$$

From eq. 3.6 and eq. 3.8, eliminating $\frac{V_m}{R}$, then eq. 3.8 becomes,

$$C_L < \frac{C_p \rho T_m}{E} < C_H \qquad (3.9)$$

(d) Relation between Microhardness H (GPa), Melting temperature T_m (K), Atomic volume V_m (m^3/k.mole), Boltzmann constant k (J/K) and Avagadro number (N)

The plot between microhardness and melting point shows that microhardness increases with melting temperature in Fig 3 1. This shows that hardness and melting temperature are not independent variables. Low melting materials tend to soft and high melting materials are hard. So we can say that microhardness varies linearly with melting temperature [3].

$$H \propto T_m$$

$$H V_m \propto N k T_m$$

Where

$$k = 1.38 \times 10^{-23} \text{ J/K}$$
$$N = 6.023 \times 10^{26} / \text{kmole}$$

$$\frac{H V_m}{N k T_m} = \text{constant}$$

Therefore

$$C_L < \frac{H V_m}{N k T_m} < C_H \qquad (3.10)$$

Similar relation can be obtained by replacing Nk with C_p (kJ/k.mole.K) as

$$C_L < \frac{H V_m}{C_p T_m} < C_H \qquad (3.11)$$

(e) Relation between Specific heat C_p (kJ/kg.K), Density ρ (Kg/m^3), Melting temperature T_m (K) and Hardness H (GPa)

From eq. 3.9, materials with higher elastic modulus will be having higher melting point and so hardness also. So we can write eq.3.9 as

$$C_L < \frac{C_p \rho T_m}{H} < C_H \qquad (3.12)$$

or from eq. 3.10, using Nk = R (Gas constant)
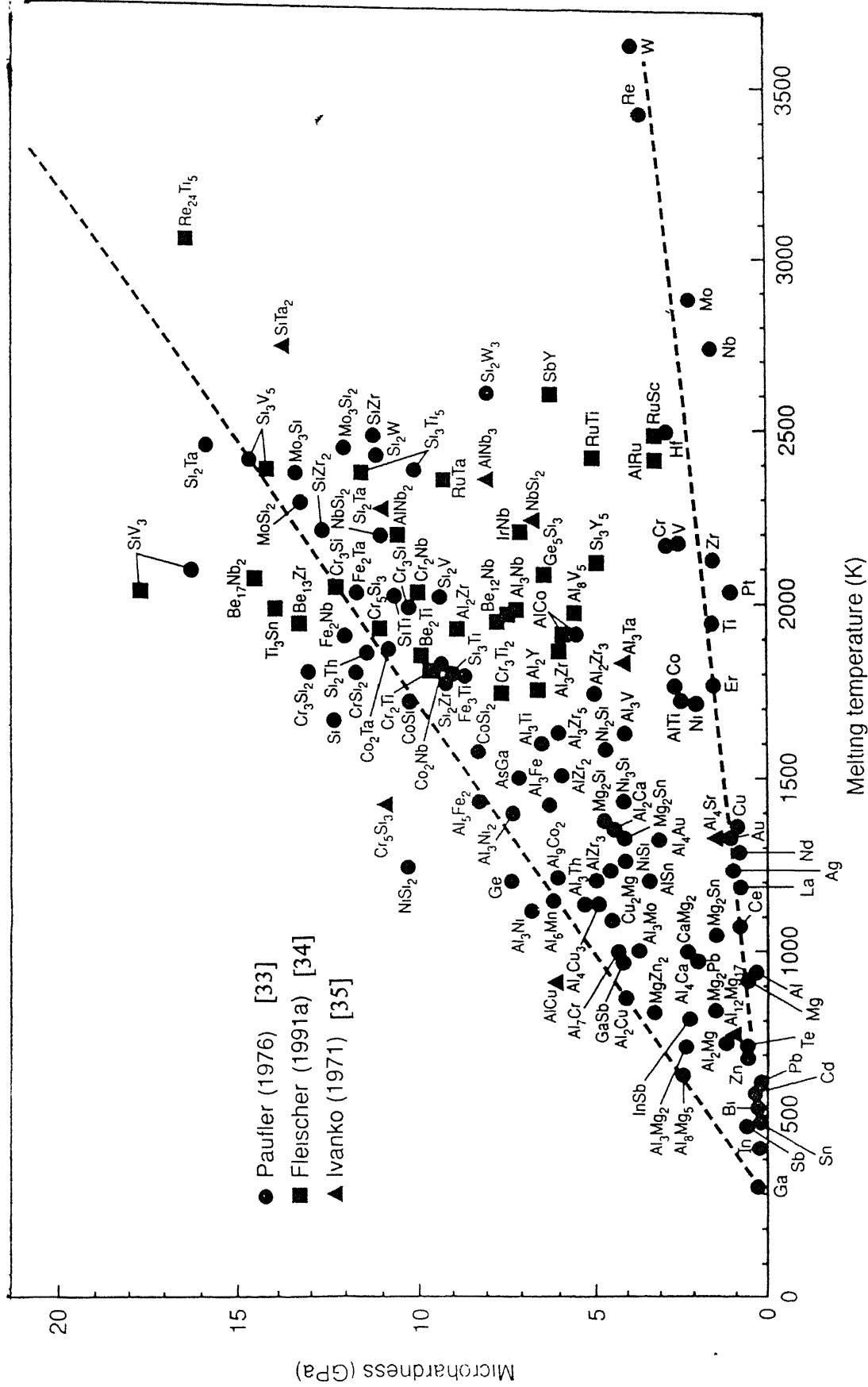
Fig 3 1 Plot between microhardness and melting temperature of metals and intermetallic compounds

$$C_L < \frac{H V_m}{T_m R} < C_H \qquad (3.13)$$

Eliminating $\dfrac{V_m}{R}$ from eq. 3.8 and eq. 3.13, we get

$$C_L < \frac{C_p \rho\, T_m}{H} < C_H \qquad (3.14)$$

Some examples of values for limits of correlations for metals and alloys, ceramics, polymers and elastomers are shown in table 3.1

Table 3.1: Examples of values for limits for correlations [7]

Material Class	Metals and Alloys		Ceramics		Polymers		Elastomers	
Property Group	C_L	C_H	C_L	C_H	C_L	C_H	C_L	C_H
G/E	0.3	0.4	0.33	0.5	0.29	0.41	0.3	0.5
K/E	0.5	2.0	0.55	2.2	1.0	3	20	1000
KV_m/RT_m	60	150	48	120	1.9	16	5.6	10
EV_m/RT_m	80	180	70	120	0.5	16	0.005	0.3
$C_p\rho V_m/R$	1.4	4.9	2.5	5.2	1	2.4	1.4	3.5
$C_p\rho T_m/K$	0.02	0.05	0.022	0.05	0.08	0.6	0.2	0.4
$K\alpha/C_p\rho$	0.3	0.84	0.25	0.9	0.05	0.24	0.14	0.25
$\alpha T_m (\times 10^{-3})$	14	27	4	28	18	60	19	180
$\lambda/bC_p(E\rho)^{1/2}$	1.5×10^6	2.4×10^7	4×10^5	5×10^6	2.5×10^4	8×10^5	1.5×10^6	1.5×10^7
$L_m\rho V_m/RT_m$	0.9	1.2	0.8	1.3	NA	NA	NA	NA
$L_m/C_p T_m$	0.24	0.47	0.5	0.9	NA	NA	NA	NA
$L_m\rho/K$	0.008	0.022	0.015	0.38	NA	NA	NA	NA
T_g/T_m	0.5	0.6	0.5	0.6	0.6	0.75	NA	NA
σ_y/E	0.2	8	10	40	6	60	1000	8000
σ_{ts}/σ_y	1.1	2.5	1.0	1.2	1.1	2.0	1	1.1
σ_{ts}/E	1.2	7.0	0.1	36	8	95	1000	8000
σ_{MOR}/σ_y	1.05	1.2	1.05	1.4	1.1	1.6	1	1.2
σ_c/σ_y	1	1.2	8	18	1.2	1.5	1	4
H/σ_y	2.2	7.5	3	200	2.8	4	3	10
σ_e/σ_{ts}	0.23	1.3	0.8	1	0.35	0.9	0.3	1
$K_{IC}/\sigma_y\sqrt{b}$	2000	36000	6	170	150	6500	0.1	150
$K_{IC}/E\sqrt{b}$	4	50	0.2	2	3	18	0.3	450
G_c/Eb	16	2500	0.05	4	25	3×10^5	0.1	$2\times10{+}5$

$N_o = 6.023 \times 10^{26}$/kmole; R is Gas constant, 8.314 kJ/kmole.K and $b = (V_m/N_o)^{1/3}$

(f) Correlation between Elastic modulus E, Density ρ, Coefficient of thermal expansion α and Specific heat C_p

The correlation between elastic modulus E, density ρ, coefficient of thermal expansion α and specific heat C_p is given by [7],

$$C_L < \frac{E\alpha}{C_P\rho} < C_H \qquad (3.15)$$

3.2 Results and Discussions

In this section, we present results for correlations described in section 3.1. Section 3.2.1 discuss the relations between E, G, and K for some of the intermetallic compounds and section 3.2.2 is a case study for silicides.

3.2.1 Correlations between Elastic modulus E, Shear modulus G and Bulk modulus K for intermetallic compounds

(a) Elasticity data derived from ultrasonic measurement

Elastic wave velocities measured using ultrasonic technique for a series of Ti compounds has been presented by [36]. Echo times for longitudinal and transverse waves are used to calculate two corresponding longitudinal and transverse velocities V_p and V_s respectively. From V_p, V_s and the density ρ, the Elastic modulus E, Bulk modulus K, shear modulus G and Poisson's ratio ν are calculated using the following relations. We assume that intermetallic compounds are elastically isotropic in the following equations hold.

$$G = \rho V_s^2$$

$$K = \rho \left[V_p^2 - \frac{4V_s^2}{3} \right]$$

$$(3.16)$$

$$E = \frac{9KG}{3K+G}$$

$$\upsilon = \frac{1}{2} \left[\frac{1 - 2\left(\frac{V_s}{V_p}\right)^2}{1 - \left(\frac{V_s}{V_p}\right)^2} \right]$$

It is observed that the average ratio of V_p and V_s, for about twenty polycrystalline intermetallic compounds of titanium, is 1.9. This is shown as

$$\frac{V_p}{V_s} \approx 1.9 \text{ and } \left[\frac{V_p}{V_s}\right]^2 \approx 3.62 \qquad (3.17)$$

$$\nu = 0.31$$

Using the relation $E = 2G(1+\nu)$, $E = 3K(1-2\nu)$ and eq. 3.17, we get the following relations

$$\frac{E}{G} \approx 2.62 \qquad (3.18)$$

$$\frac{E}{K} \approx 1.14 \qquad (3.19)$$

Fig. 3.2 shows the plot for Elastic modulus E versus Shear Modulus G. The slope of this plot is similar to that given by eq. 3.18 and the correlations with the limiting values can be expressed as,

$$2.2 < \frac{E}{G} < 2.7$$

$$\qquad (3.20)$$

$$0.8 < \frac{E}{K} < 2.5$$

(b) Binary Intermetallic compounds (melting temperature > 1500 °C)

Elasticity data for a number of binary intermetallic compounds having melting temperature greater than 1500°C have been presented by [37]. We find that the average ratio of V_p and V_s in this case is equal to 1.75. This can be expressed as,

$$\frac{V_p}{V_s} \approx 1.75, \upsilon \approx 0.26 \qquad (3.21)$$

and using eq. 3.21, we get

$$\frac{E}{G} \approx 2.51 \qquad (3.22)$$

$$\frac{E}{K} \approx 1.45 \qquad (3.23)$$

Fig. 3.3 shows the relation between Elastic modulus E versus Shear modulus G. The slope of this plot is in agreement with eq. 3.22 and the correlations with the limiting values can be expressed as

$$2.5 < \frac{E}{G} < 2.7$$

$$(3.24)$$

$$0.9 < \frac{E}{K} < 1.5$$

Various class of intermetallic compounds differ in respect to crystal structure, nature of bonding etc. Therefore we expect narrower limits on C_L and C_H for the above mentioned correlations.

3.2.2 Correlations for Intermetallic compounds of Silicides

As seen in the preceding section, better correlations and estimates are expected based on individual classes of materials. Therefore, correlations have been developed for various classes instead of the entire range of intermetallic compounds. Typical results for silicides are presented in Table 3.2.

(a) Coefficient of linear thermal expansion versus melting temperature

Fig. 3.4 shows the variation of coefficient of linear thermal expansion versus melting temperature. It can be shown from figure that the distribution follows the relation

$$\alpha T_m = constant$$

where c is constant and approximately equal to 20.12×10^{-3} from fig. 3.4. This relationship is useful in estimating the unknown properties of either α or T_m is known. This can be expressed as follows.

$$C_L < \alpha\, T_m < C_H \qquad\qquad (3.25)$$

where $C_L = 14.66 \times 10^{-3}$ and $C_H = 20.12 \times 10^{-3}$. Some estimates based on this correlation are shown in Table 3.3.
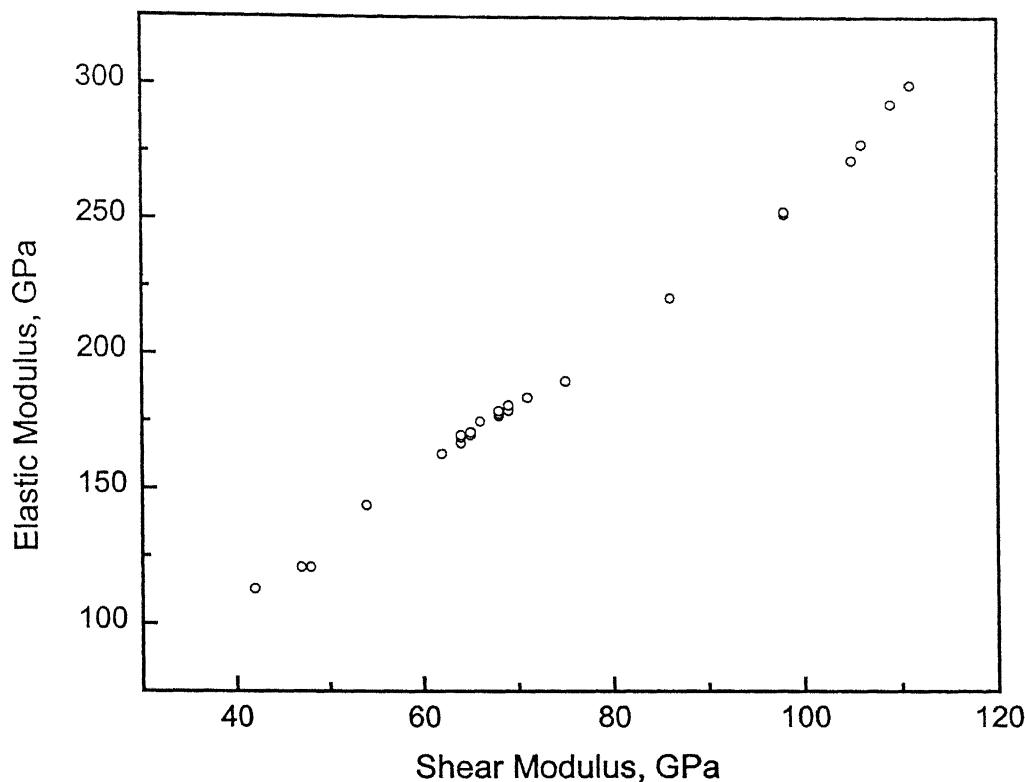
Fig.3.2: Plot of Elastic Modulus versus Shear Modulus for Ti intermetallic compounds
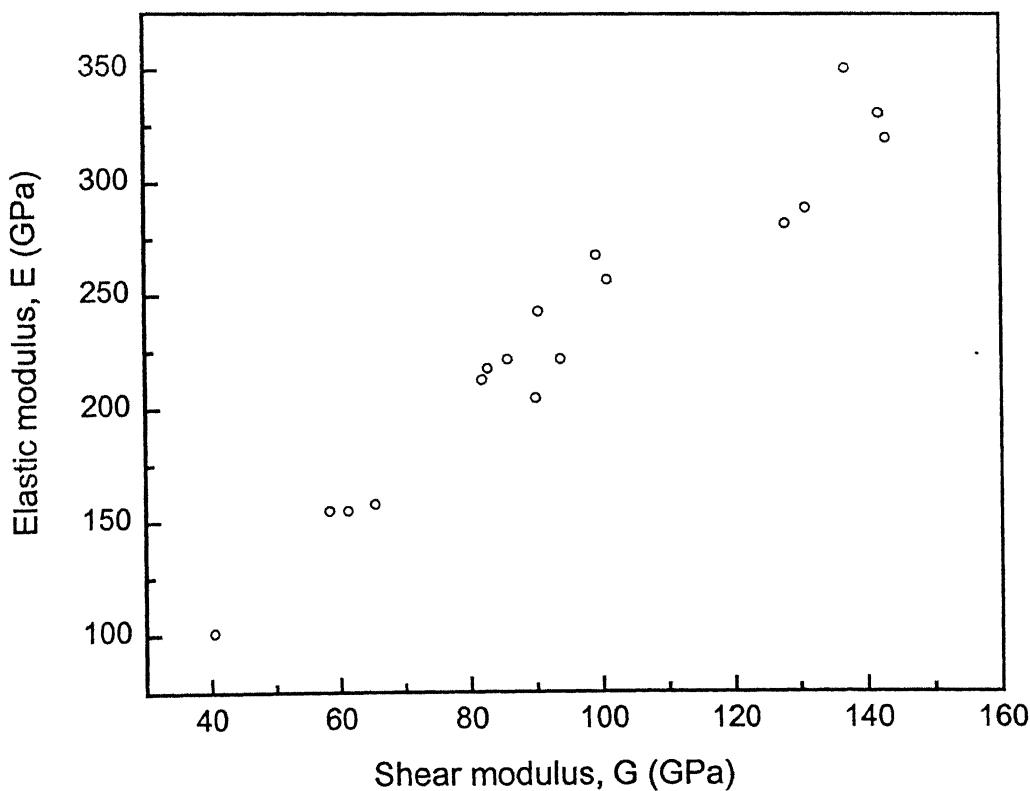
Fig. 3.3: Plot of Elastic Modulus versus Shear Modulus for intermetallic compounds with T_m > 1000°C

Table 3 2: values for limits of correlations for silicides

Property Relation (equation number)	Units	C_L	C_H
$\dfrac{E V_m}{R T_m}$ (3.6)	E in Gpa V_m in m^3/ k.mole R in kJ/ k.mole.K	81	240
$\dfrac{E V_m}{C_p T_m}$ (3 7)	C_p in kJ/ k.mole.K	5	54
$\dfrac{C_p \rho V_m}{R}$ (3.8)	C_p in kJ/ kg.K	2.9	25
$\dfrac{C_p \rho T_m}{E}$ (3.9)	C_p in kJ/ kg.K ρ in kg/m^3	0.03	0.2
$\dfrac{H V_m}{Nk T_m}$ (3.10)	H in GPa k is 1.380×10^{-23} J/K N is 6.023×10^{-23} /k.mole	3.8	12.5
$\dfrac{H V_m}{C_p T_m}$ (3.11)	C_p in kJ/ k.mole.K	0.2	3
$\dfrac{C_p \rho T_m}{H}$ (3.12)	C_p in kJ/ k.mole.K	0.4	4.5
$\dfrac{E \alpha}{C_p \rho}$ (3.15)	C_p in kJ/ kg.K	10^5	8×10^5
αT_m (3.25)	α in $\times 10^{-6}$ / K T_m in K	14.66×10^{-3}	20.12×10^{-3}
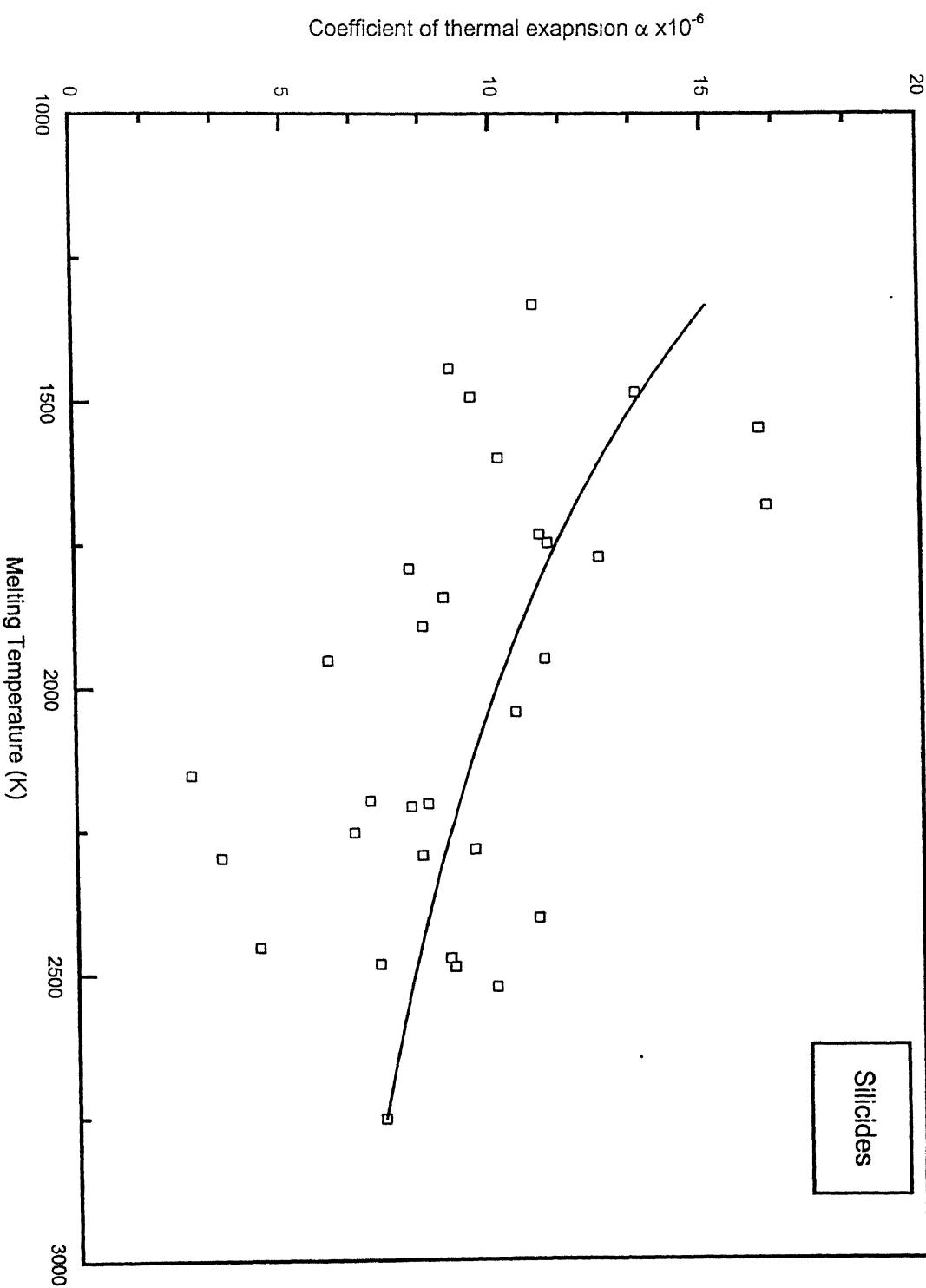
Fig. 3 4 plot showing Coefficient of thermal expansion α with melting temperature T_m for silicides showing the relation αT_m = constant

Table 3.3: Estimation of T_m for silicides using the correlation given by eq. 3.25

Name of the compound	$\alpha \times 10^{-6}$/K [38]	Correlation $\dfrac{1466 \times 10^{-3}}{\alpha} < T_m < \dfrac{2012 \times 10^{-3}}{\alpha}$	Calculated $\overline{T_m}$ (°C)	Actual T_m (°C) [38]	% error
Co$_3$Si	13.4	$1094 < T_m < 1501.5$	1297.75	1214	6
CrSi	11.3	$1297.3 < T_m < 1780.5$	1538.9	1475	4.33
MoSi$_2$	8.25	$1777 < T_m < 2438.9$	2107.95	2020 ± 20	4.33
TaSi$_2$	8.9	$1647.2 < T_m < 2260.6$	1953.9	2040	4.2

3.3 Degree of Metallicity in Intermetallic compounds

3.3.1 Introduction

Availability of property data and its description in terms of property ranges and correlations allow us to examine various aspects of intermetallic compounds. For example, from application point of view it is useful to study the degree of metallicity of intermetallic compounds. As mentioned earlier, the mechanical response of intermetallic compounds lies between that of metals and ceramic materials. One would therefore expect this to be reflected in systematic variations of coefficients associated with particular correlations for metallic, intermetallic and ceramic materials. Particularly, these variations must relate to the nature of bonding. In this section we explore these ideas through correlations between various properties.

3.3.2 Correlations involving Degree of Metallicity

In terms of mechanical properties, intermetallic compounds can be considered intermediate between metals and ceramics. For example, Fig. 3.5 shows the variation of yield stress and ductility for Ni, NiAl, Si and Al$_2$O$_3$ as a function of homologous temperature T/T$_m$ (T$_m$ = melting temperature) and reflect the effect of the nature of bonding on the mechanical properties [3]. NiAl also softens with increasing temperature at about 0.5 T$_m$ which is same as that for Si but higher that that forAl$_2$O$_3$. The brittle-to-ductile transition temperature of NiAl is about 0.4 T$_m$, same as that of Ni but lower than that of Si and Al$_2$O$_3$ (0.8 T$_m$). Thus NiAl bridges the gap between metals and ceramics. A similar effect of nature of bonding is observed on the correlation between hardness and

elastic modulus, which is shown in Fig. 3.6. For intermetallic compounds, there is a range in the nature of bonding, we expect a spread in the data and since the properties relate to the bonding characteristics, it is possible to develop correlations for estimating the gaps in the data for a group of isostructural compounds.

Another approach, based on mechanical properties, is through the temperature dependence of hardness. Hardness versus temperature plots for various materials (metals, ceramics, intermetallics) show an inflexion point at some characteristic temperature T_b, shown in Fig. 3.7 and can be described by the following equation:

$$H = A \, e^{-BT}$$

Where H is hardness, A and B are constants and T is temperature. Table 3.4 shows the data for a few materials. It is observed that the parameter B does not show any systematic variation. The parameter A reflects the intrinsic hardness of the material and increases with decreasing metallic character. The ratio T_b/T_m shows a decrease with decreasing metallic character, which reflects that for materials with more directional bonding, relaxation processes become dominant for plastic strain accumulation at lower homologous temperature.

Table 3.4: Data for some materials

Material	A (kg/mm^2)	B (x 10^3 /C)	T_b/T_m	T_m (^{o}C)
NiAl	410	0.863	0.38	1640
CoAl	580	1.209	0.44	1625
FeAl	600	0.663	0.46	1270
Metal I	140	0.6	0.55	1630
Metal II	100	1.1	0.55	1270

3.3.3 Trends in Elastic Coefficient Data

One of the earlier attempts at structural mapping of compounds in terms of nature of bonding was made by Pearson [39]. He found that separation between fourfold and sixfold coordinated structures was obtained on a map between electronegativity difference (Δx) and average principal quantum number ($\bar{n}$). His result is reproduced in Fig. 3.8. The figure shows a plot between electronegativity difference (Δx) and average principal quantum number ($\bar{n}$) for octahedrally coordinated compounds (NaCl type, B1) of ionic nature and tetrahedrally coordinated compound of covalent nature (Zincblende type, B3 and Wurtzite type, B4).
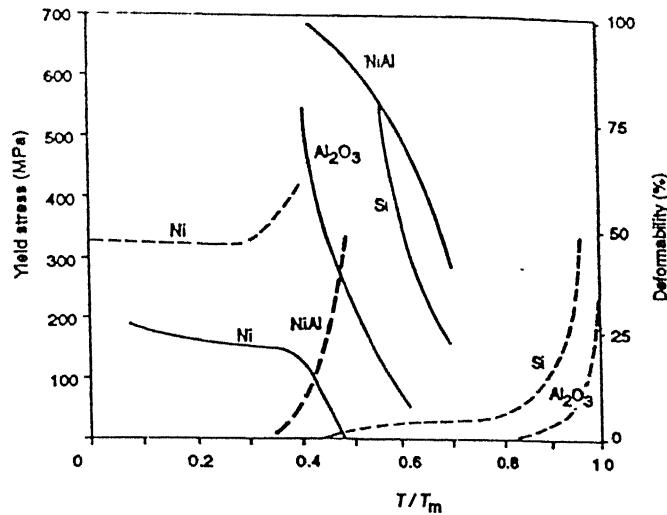
Fig. 3.5· Yield stress and deformability for various materials as a function of homologous temperature (T/T$_m$)
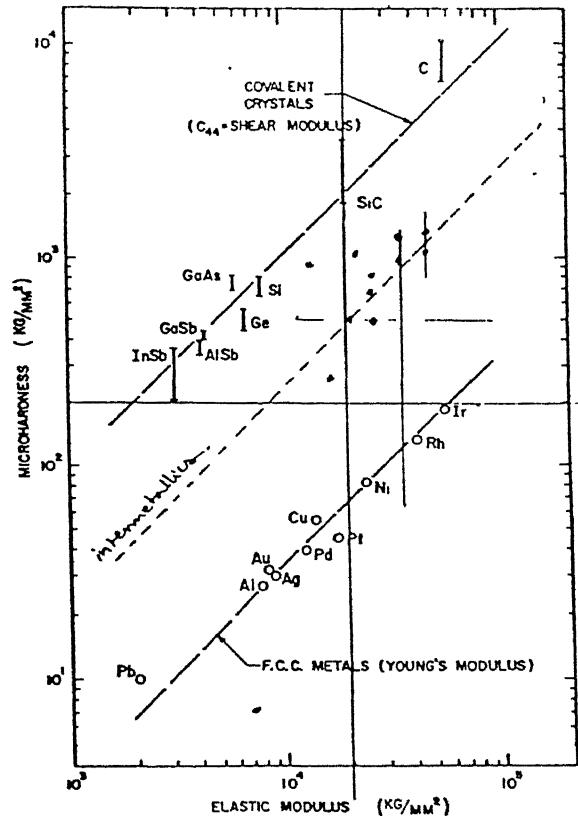
Fig. 3.6: Plot between elastic modulus E and microhardness for intermetallic compounds
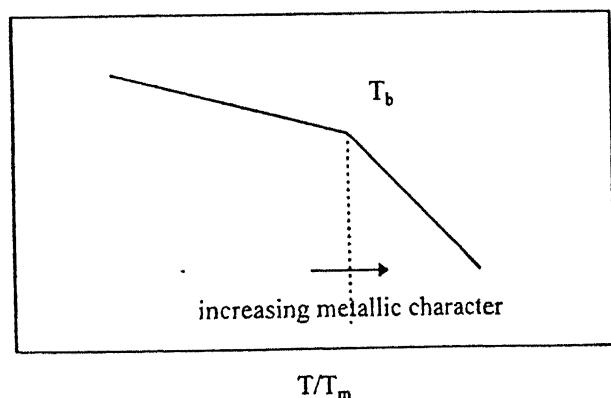
Fig 3 7 Plot between ln(Hardness) and homologous temperature (T/T$_m$)

We now propose that trend in elastic coefficient of compounds may appear in the above mentioned plots for the following reasons/assertions:

(a) Tetrahedral coordinated compounds lead to highly directional bonding and therefore higher stiffness.

(b) The distance of a compound from the boundary (b-b′) in Fig. 3.8 is in proportion to the degree of covalent bonding (assertion). Therefore E should vary as per trend I marked in figure.

(c) According to Dehlinger [39], the principal quantum number n of the valence shell of an atom is a directional character of the bonds formed by an atom with atoms of the same kind. As n increases, the atomic orbitals involved in the bond formation and hence the bonds themselves gradually lose their directional properties. $\bar{n}$ is introduced to extend this relationship to study the bond formed between unlike atoms [39]. So, the directional character of the bonds depends on $\bar{n}$ (trend II marked in Fig.3.8).

Therefore, the degree of directional bonding (and therefore the degree of metallicity) of an intermetallic compound can be viewed by its location on this plot. Accordingly, the scaling of C_{11} with distances along directions I and II from the boundary (b-b′) in Fig. 3.8 for a series of compounds was examined.

In Fig. 3.9(a) the materials A-F having varying degree of metallicity due to different values of Δx and $\bar{n}$ have elastic moduli which scale with relative distances from the boundary b-b`. For example, the moduli C_{11} of materials A, B and C are proportional to distances OA, OB and OC respectively (straight line passing through points A, B and C in Fig. 3.9(a)). Similarly the elastic moduli C_{11} of materials D, E and F are proportional to the distances O′D, O′E and O′F, respectively (straight line passing through points D, E and F in Fig. 3.9(a)). As we move up along b-b′, C_{11} decreases. This trend is captured by the line CF, BE and AD in C_{11}-δ map shown in Fig. 3.9(b) where δ represents distances in the b-b` (and the corresponding transverse direction) reference frame. Thus, the positions of octahedrally bonded compounds in the AB type Pearson map appear to have a correspondence with their positions on a C_{11}-δ map. If such a correlation is found to be general enough it would enable estimate of C_{11} for a compound for which $\bar{n}$ and Δx is known.

The above hypothesis was tested for a number of compounds. Consistent results were obtained (Fig.3.10), though more detailed study of this correlation must be carried out.
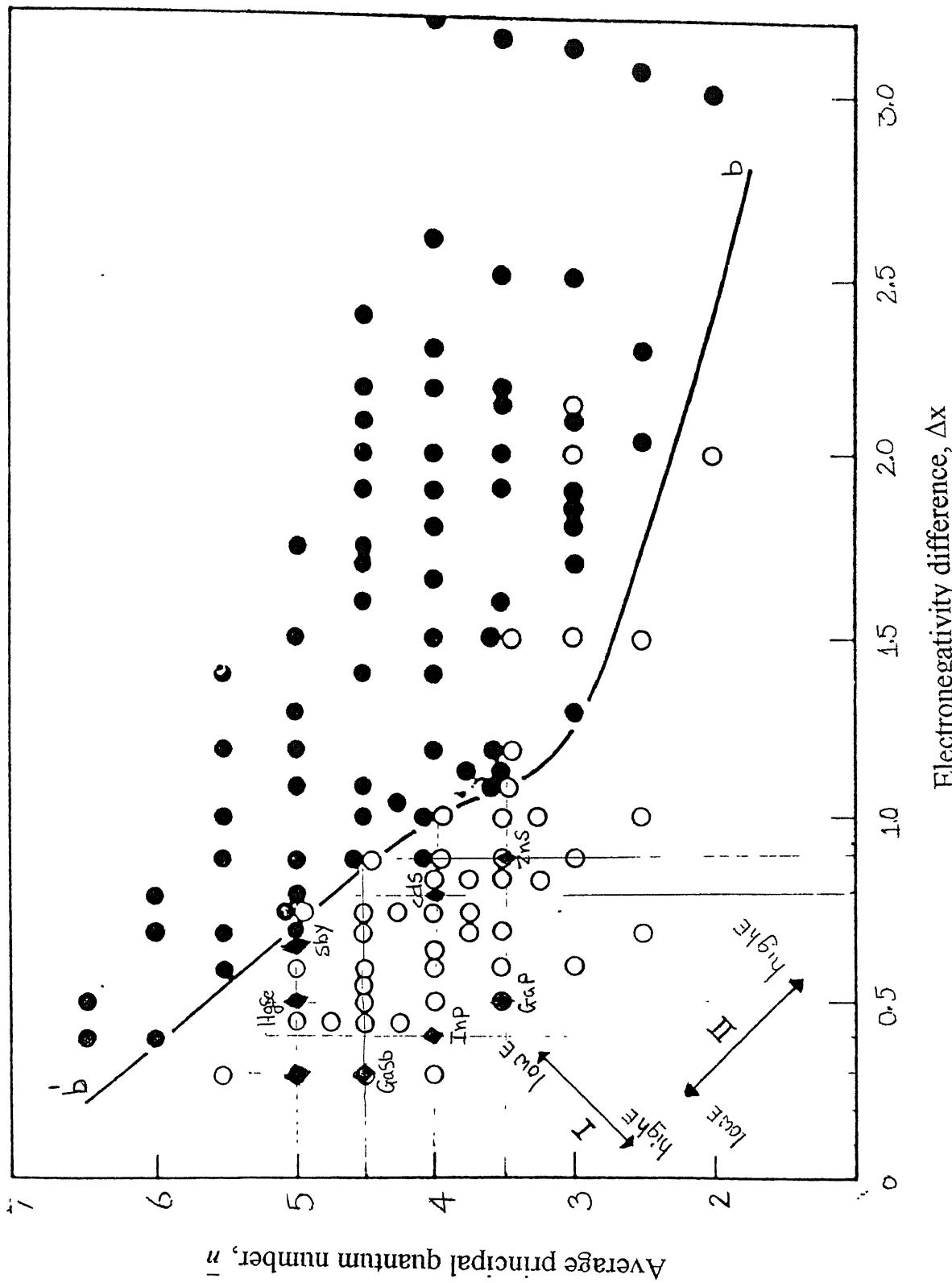
Fig 3·8: Plot between average quantum number $\bar{n}$ and electronegativity difference Δx for AB type compounds with tetrahedral and octahedral coordination

53
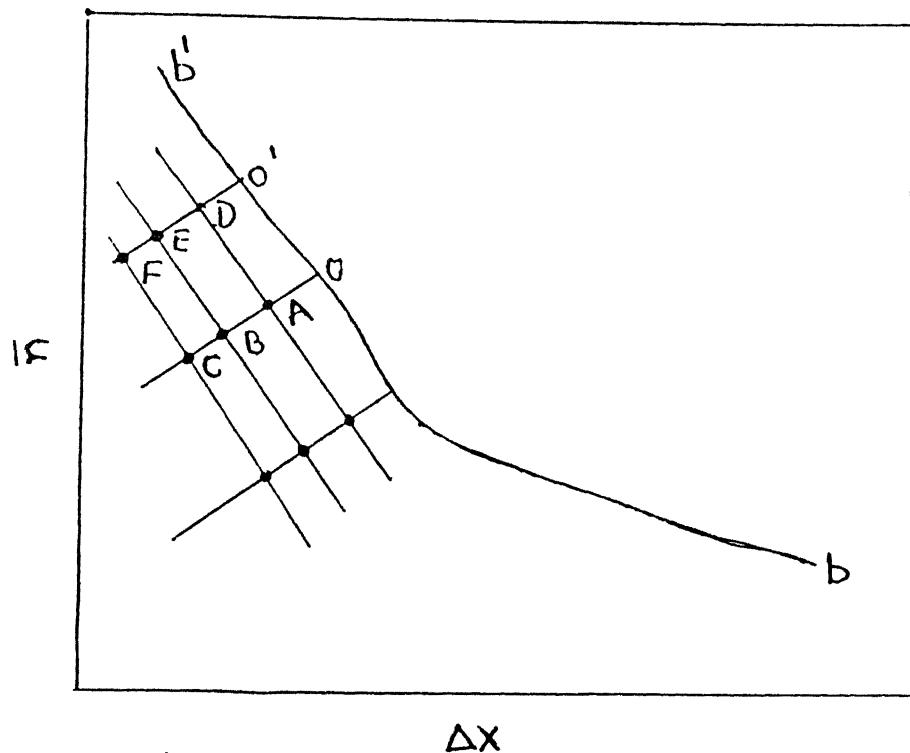
Fig. 3.9(a) Schematic variation of $\bar{n}$ versus Δx, showing
elastic modulus scaling with distance from the boundary bb'
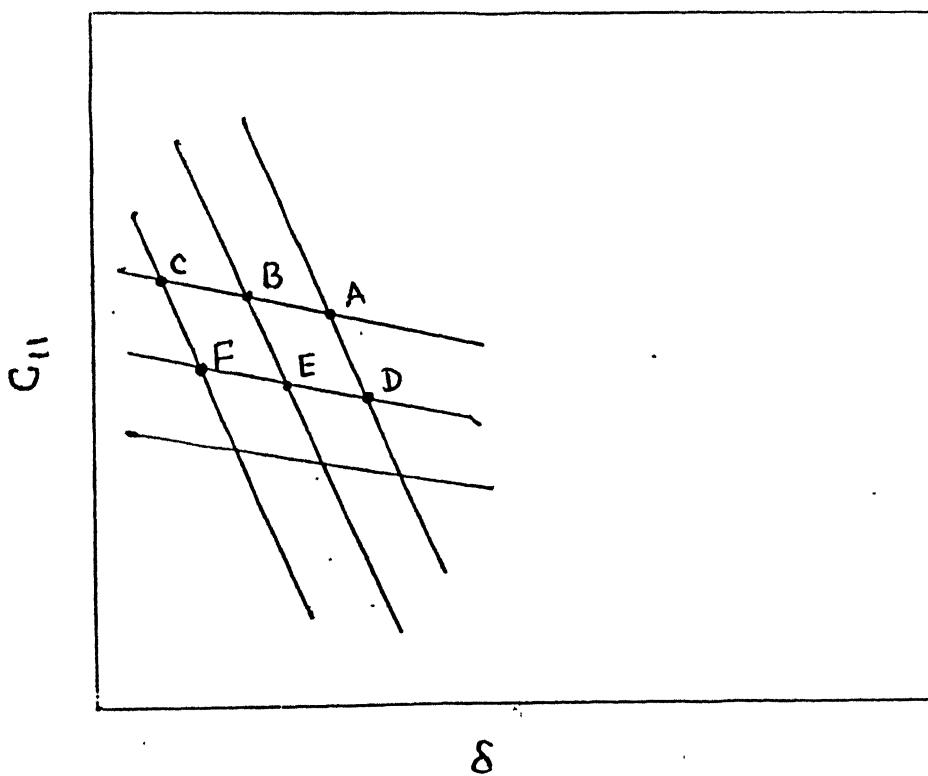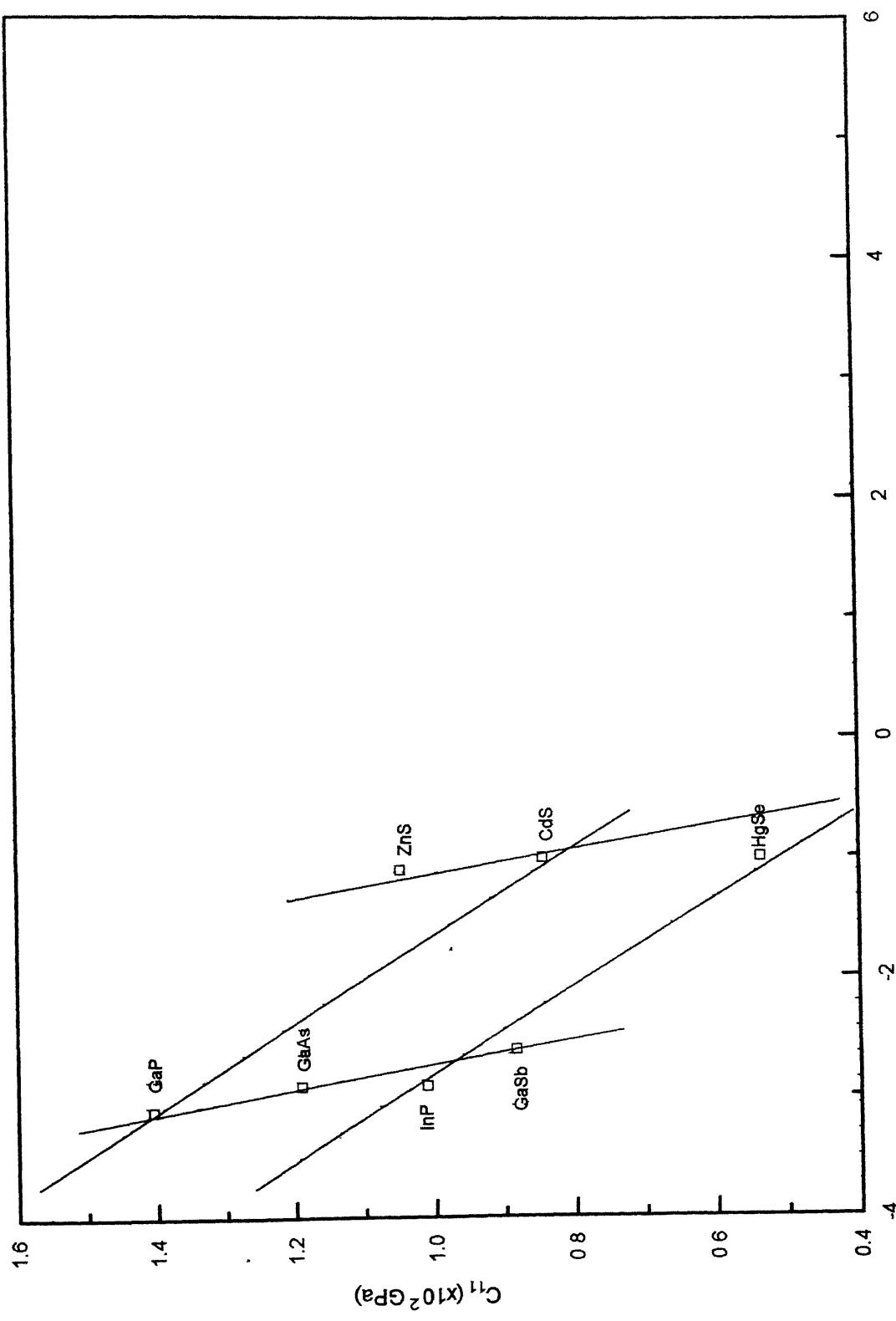
Fig. 3.10: Elastic constant C_{11} versus distance δ for tetrahedrally coordinated compounds

Chapter 4

Correlations based on Mendeleev Number

4.1 Introduction

The description of Mendeleev number is given in chapter 1. The success of Mendeleev number in achieving the structural separation for various intermetallic compounds suggests that Mendeleev number may correlate also with formation and properties of these compounds. For example, the ease of joining two materials(elements) by friction welding varies from "good weld formation" to "no joining". When such information for various materials is described on a chart where the corresponding Mendeleev number of the two materials are plotted on x and y axis, as shown in Fig. 4.1, clear separation of material pairs which weld with varying degree of success is obtained [17]. Therefore in this chapter we explore the existence of such correlations between Mendeleev number and some physical properties like density, melting temperature, heat of formation etc. Some correlations between two physical properties have already been
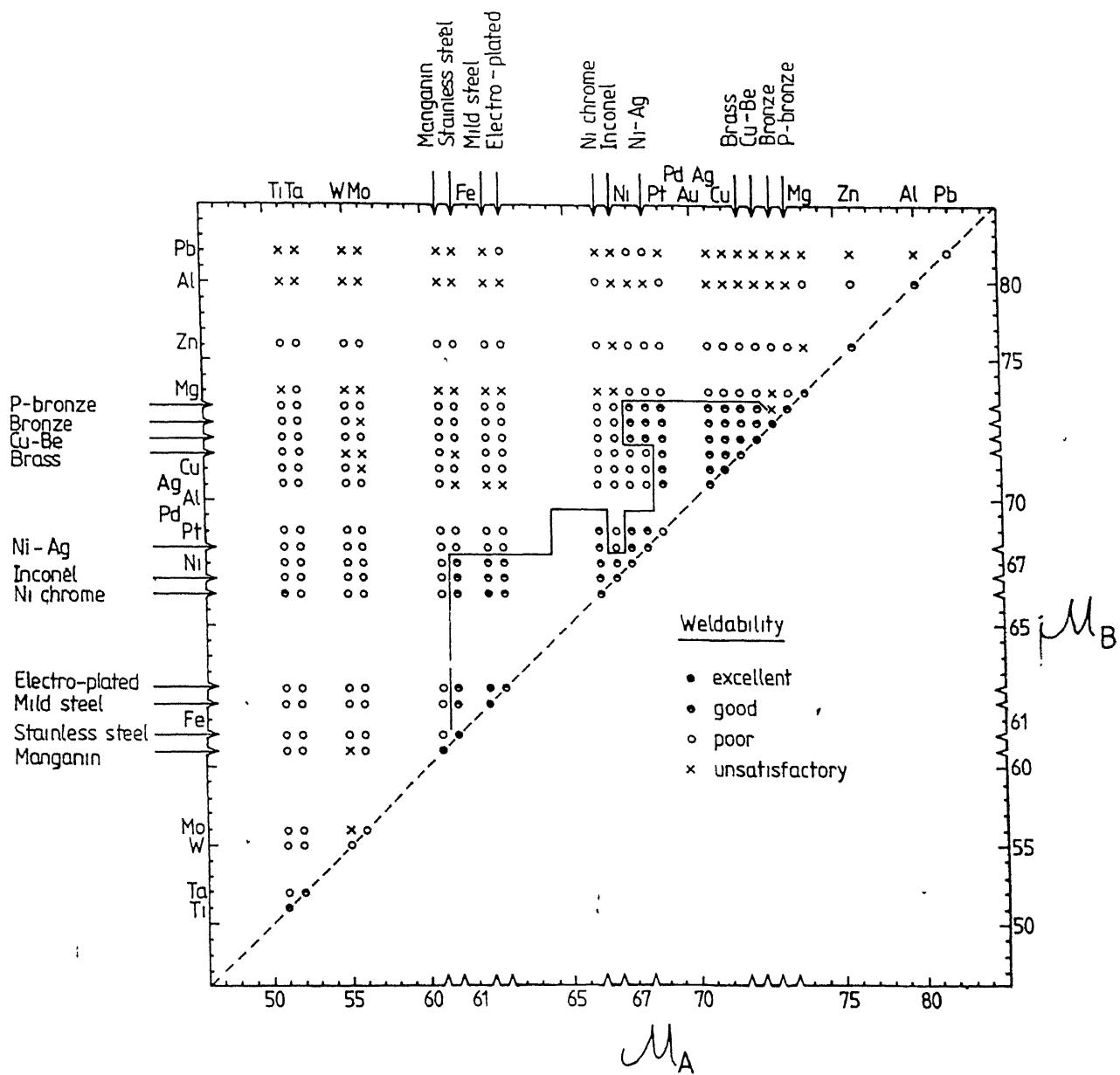
Fig. 4.1: Weldability property chart

presented in chapter 3. The approach is adhoc at this stage, but the results may guide us in conducting more systematic studies.

In section 4.2, we present some data on thermal study of binary intermetallic compounds and phase diagram study of intermetallic compounds, which are interpreted in terms of Mendeleev number Sections 4.2 and 4 3 discuss some methods in the estimation of unknown density and melting point of silicides. Finally section 4.4 is about the study of heat of formation of intermetallic compounds with Mendeleev number.

4.2 Some Applications of Mendeleev number

For a compound, we define an effective M as weighted average of individual Mendeleev numbers of the constituent elements. Similar definition has been used for design of ternary alloys [17]. Some of the important applications of Mendeleev number are

- Study of binary intermetallic compounds thermally
- Phase diagram study of intermetallic compounds

Now we will see these applications in detail.

(a) Thermal study of binary Intermetallic compounds

Using the information given in [40], on thermal study of binary intermetallic compounds, we analyzed that data in terms of variation with Mendeleev number M. This is shown in Fig. 4.2 and we can observe the three most significant regions of absence of chemical combination, chemical combination and no thermal study. From Fig. 4.2, we can observe that similar types of symbols are grouping together and as the thermal study continues we could see clear separation of these regions well.

(b) Phase diagram study of intermetallic compounds

Attempts for the existence or non–existence of binary intermetallic compounds by phase diagram studies have been made over the years and the data has been compiled in various ways shown in [41]. The data is plotted in terms of Mendeleev number in Fig. 4.3. The plot shows a part of chemical element versus chemical element where Mendeleev number is considered for each element. The plot shows clear separation of different regions with same identification. The various types of regions and their corresponding symbols are explained in Fig. 4.3.
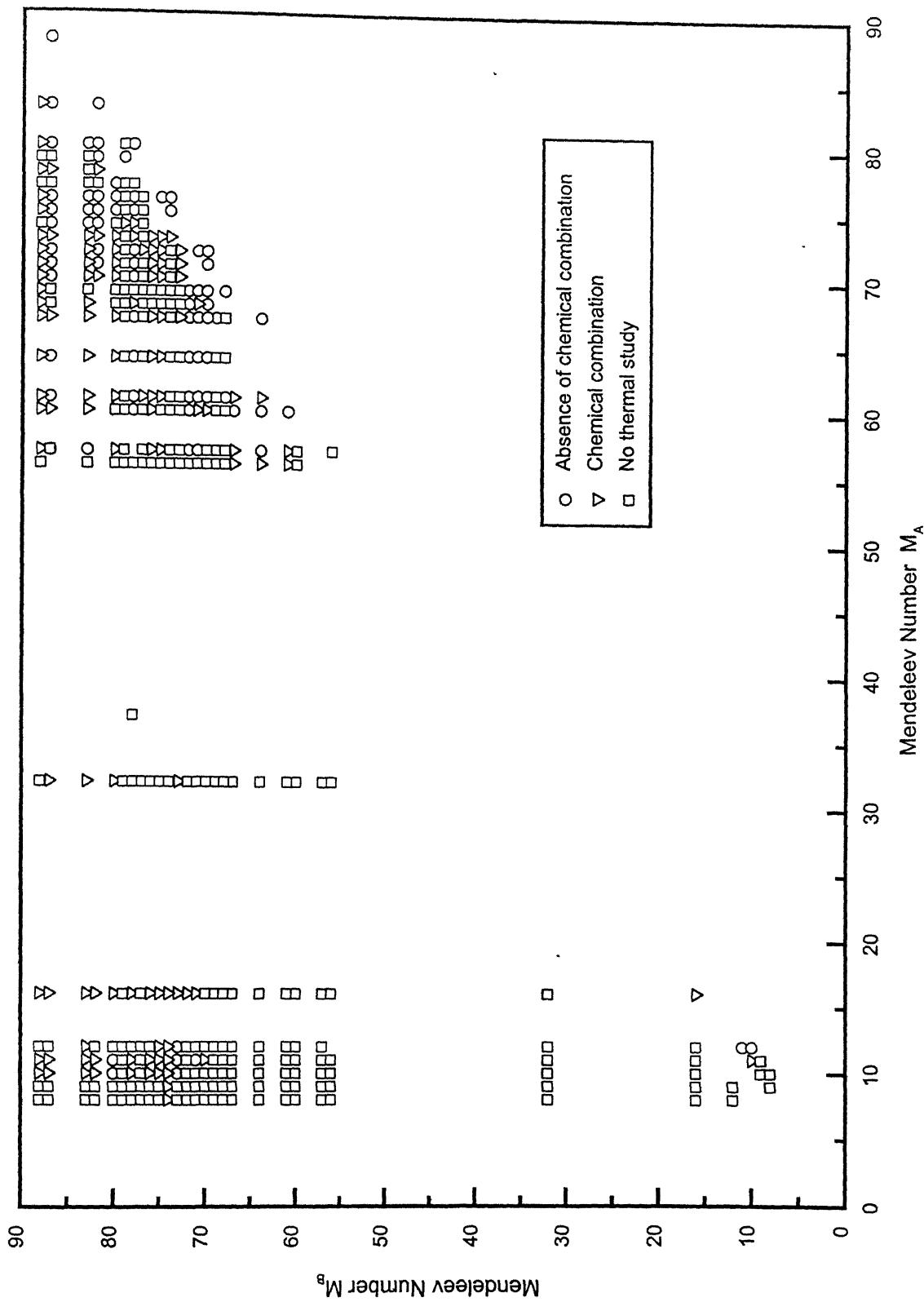
Fig. 4.2: Thermal study of binary intermetallic compounds

59
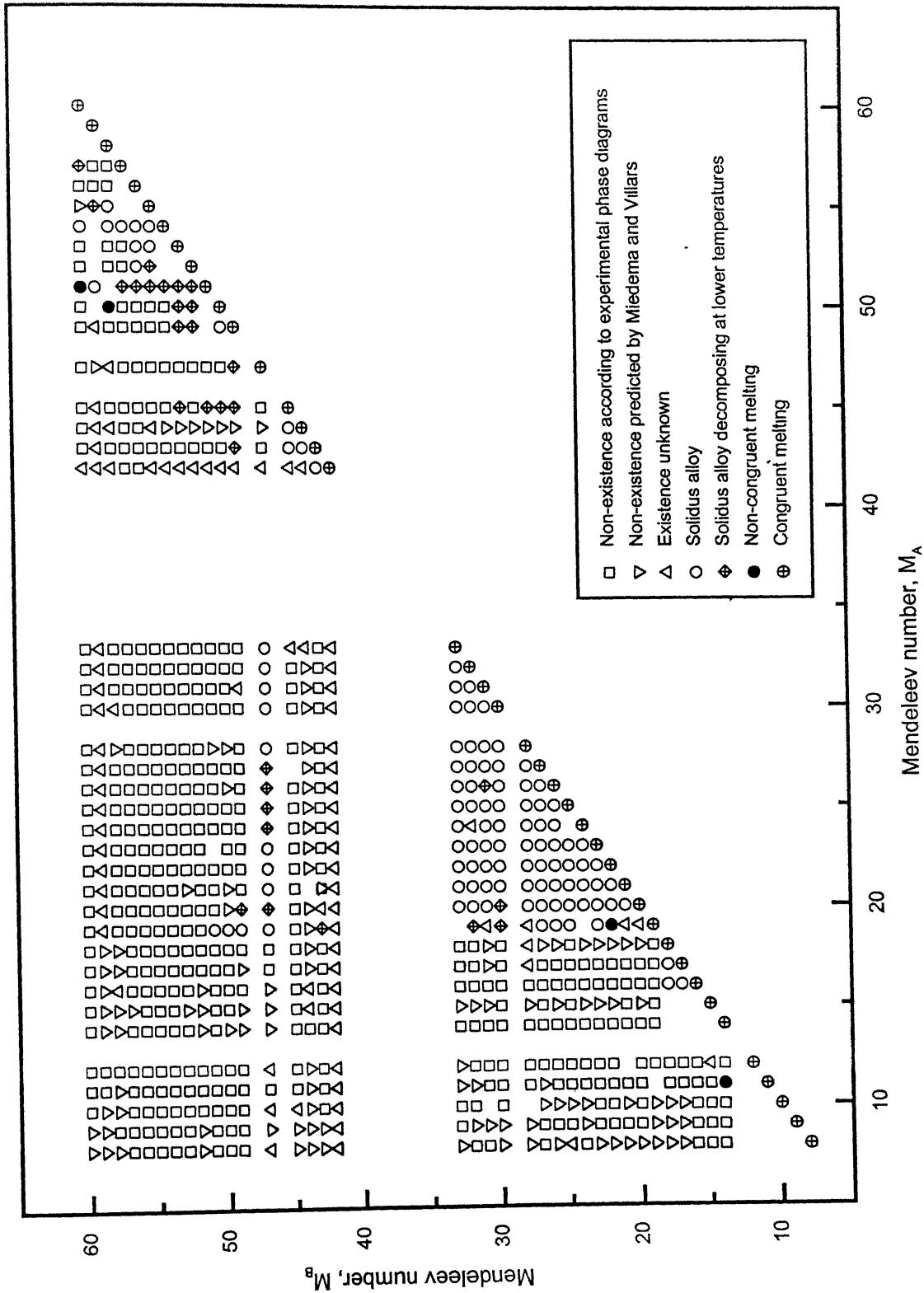
Fig. 4.3: Phase diagram study of intermetallic compounds

4.3 Estimation of unknown Density and Melting Temperature of Intermetallic Compounds of Silicides

In this section we will study some methods to estimate the unknown values of density and melting temperatures of some silicides by studying the variation of Mendeleev number with density as well as melting temperature.

4.3.1 Density versus Mendeleev number of Silicides

Fig. 4.4(a, b) shows the distribution of density of silicides as a function of their average Mendeleev number M_A. Now we will see some correlations between average Mendeleev number M_A and density ρ of silicides to know the unknown density values of some of silicides. The data for the densities of the silicides has been taken from [38]. In Fig. 4.4(b) we see some systematic (triangular) patterns appearing in terms of position of groups of compounds: (Ti, Zr, Hf)Si_2, (Ti, Zr, Hf)Si, (*, Zr, Hf)$_3Si_2$, (Ti, *, Hf)$_5Si_3$ and (*, Zr, Hf)$_2$Si. Each triangle represents silicides of particular type. These missing compounds, which are denoted by '*' are Ti_3Si_2, Zr_5Si_3 and Ti_2Si. We can also observe that all of these are similar triangles. The densities of unknown compounds can be found by making use of geometrical similarity of these patterns. This requires first the calculation of the average Mendeleev numbers of unknown compounds. Using this approach, the density values for the missing compounds are shown in table 4.1.

Table 4.1: calculated density values of silicides

Name of the compound	Measured density (kg/m^3)	Literature value (kg/m^3)
Zr_5Si_3	5946	*
TiSi	4292	4240
Ti_2Si	4324	*
Ti_3Si_2	4302	*
Nb_2Si	7351	*
Nb_5Si_3	7135	7110
V_2Si	6054	*

* Non availability of literature

Other correlations can be obtained from fig. 4.4(c). The silicides of Cr, Mo, W fall on straight lines with equal slopes. Each straight line represents a silicide of particular type. These compounds are (Cr, Mo, W)$_5Si_3$ and (Cr, Mo, W)Si_2. Using the slope, we can find unknown density values for similar type of silicides.
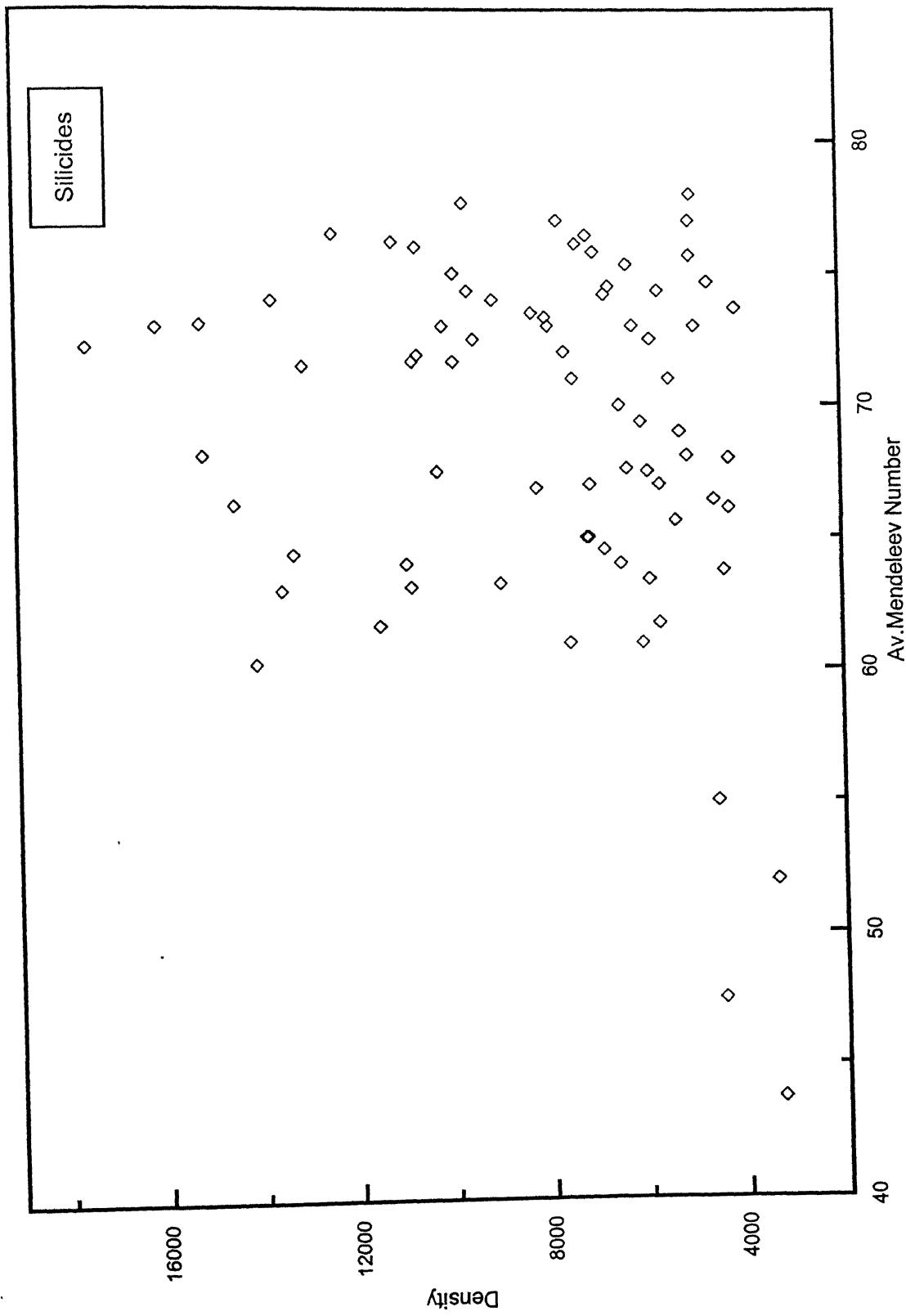
Fig. 4.4(a): Distribution of Density of silicides as a function of average Mendeleev number

63
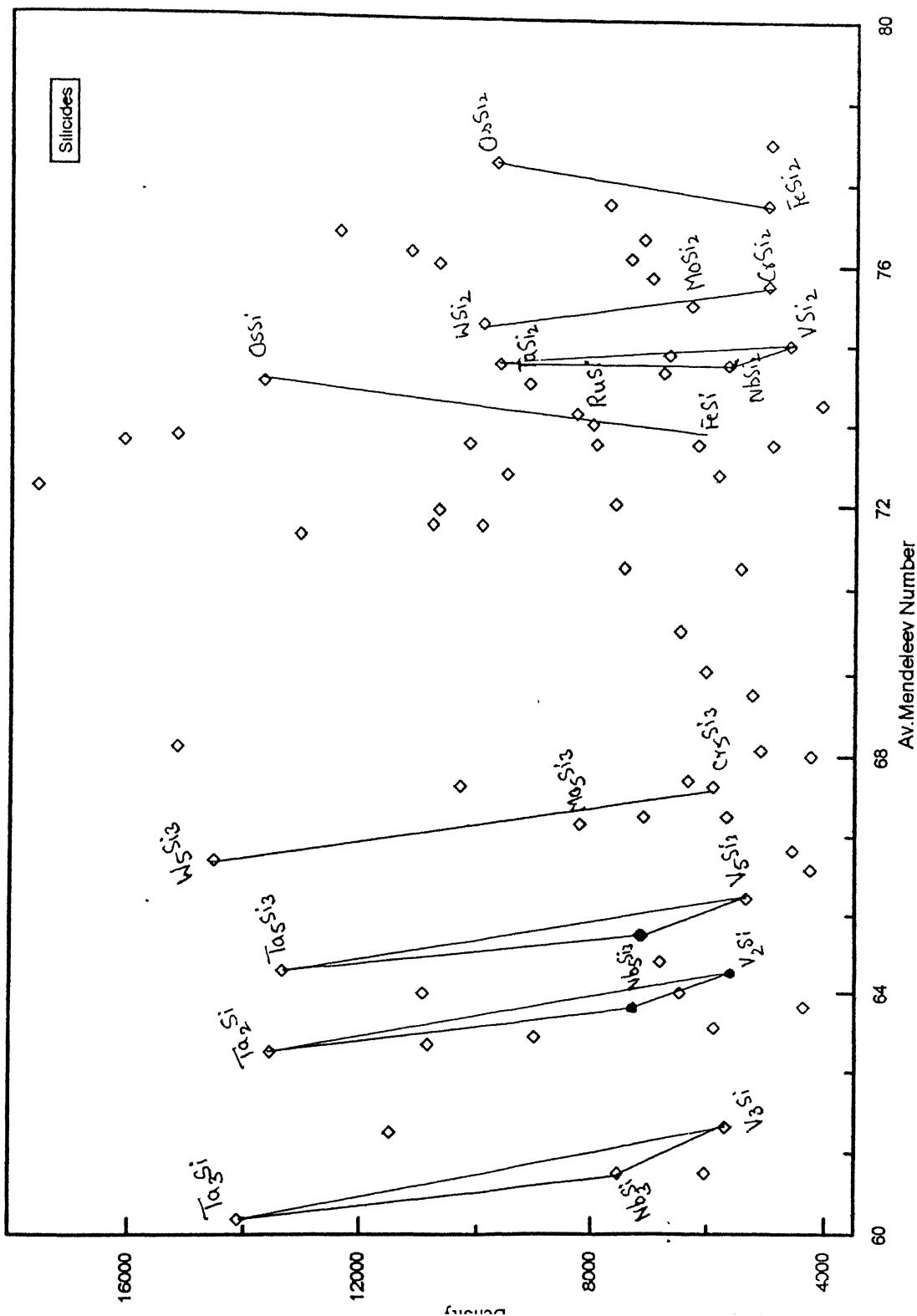
Fig. 4 4(c)· Distribution of density of silicides as a function of average mendeleev number

4.3.2 Melting temperature versus Mendeleev number of Silicides

Data for melting temperature of number of silicides was taken from [38]. Fig. 4 5(a) shows the distribution of melting point as a function of average Mendeleev number. No correlation or trend is evident in this figure. However, when we start looking at specific groups of compounds, geometrically similar patterns (similar to those in Fig. 4 4(b)) start appearing (Fig. 4.5(b)).

In fig. 4.5(b), we can observe some triangular patterns formed by compounds (Ni, Pd, Pt)$_3$Si, (Ni, Pd, Pt)$_2$Si and (Ni, Pd, Pt)Si. We also observe the compounds NiSi$_2$, Ni$_4$Si and Ni$_5$Si$_2$, which gives the idea of triangles formed by (Ni, Pd, Pt)Si$_2$, (Ni, Pd, Pt)$_4$Si and (Ni, Pd, Pt)$_5$Si$_2$. Again, by using the geometrical similarity observed in the average Mendeleev number of a compound, we can estimate its melting temperature if we know melting temperature of related compounds. For example, the calculated melting points of Ti$_2$Si and Ti$_3$Si$_2$ (from Fig. 4.5(b) are shown in Table 4.2.

Table 4.2: calculated Melting temperature values of silicides

Name of the compound	Melting temperature °C	Literature Value °C
Hf$_3$Si$_2$	2625	2650 ± 50
Hf$_5$Si$_3$	2614	2600 ± 50
Ti$_2$Si	2028.5	*
Ti$_3$Si$_2$	2142.8	*
W$_3$Si	2531.5	*

* Non availability of literature

Other correlations can be observed in Fig. 4.5(c). The silicides of VIA group elements also form similar triangles. These are (Cr, Mo, W)$_5$Si$_3$, (Cr, Mo, W)Si$_2$ and (Cr, Mo, *)$_3$Si.

4.4 Heat of Formation of Intermetallic Compounds as a function of Mendeleev Number

In the preceding section we looked at correlations between Melting temperature T_m and Mendeleev number M. Since T_m relates to the nature of bonding, we therefore expect similar correlations to exist between Mendeleev number and nature of bonding and various other physical properties. In this section we therefore explore such correlations between Mendeleev number M and heat of formation of intermetallic compounds.
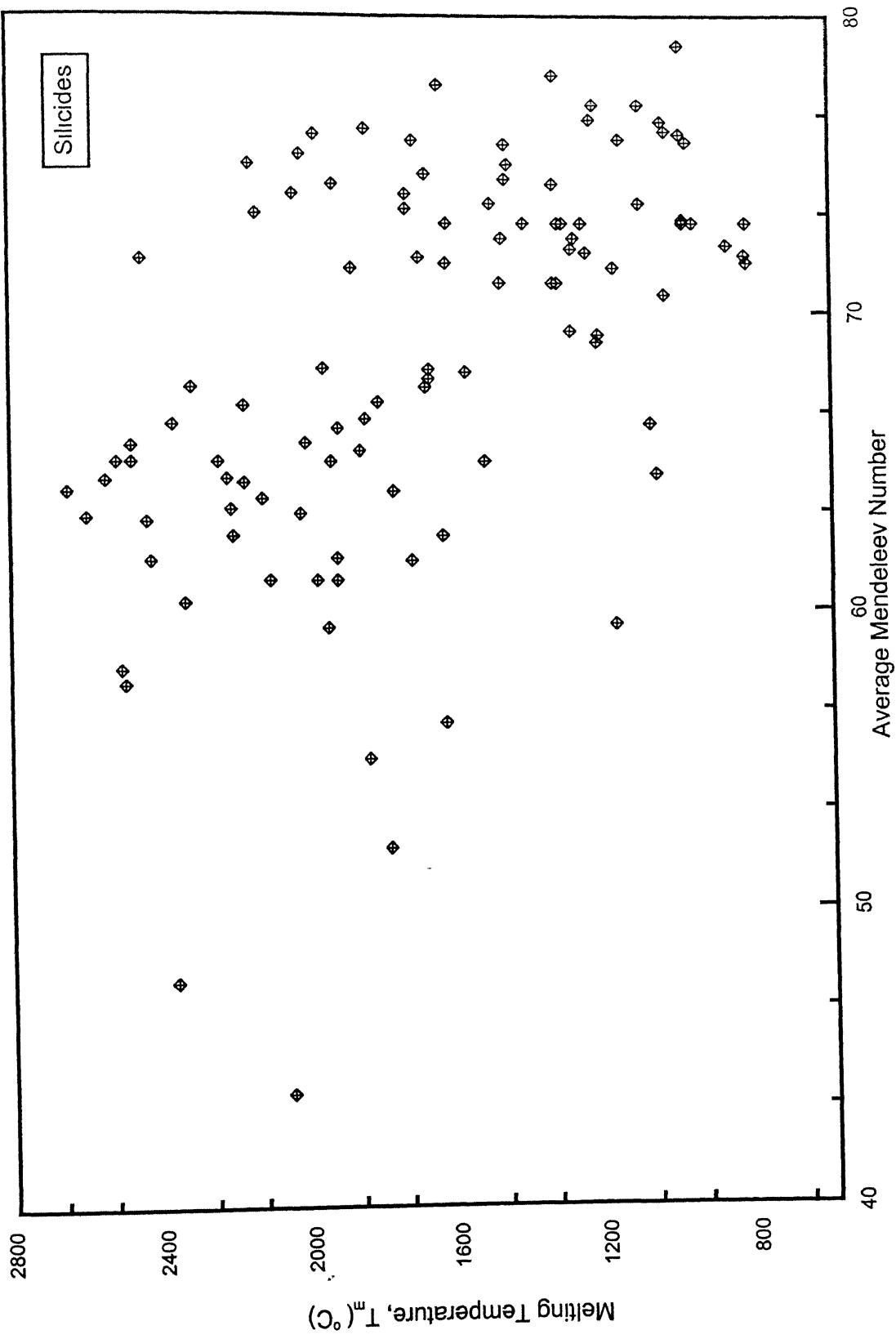
Fig. 4.5(a): Distribution of melting temperatures of silicides as a function of average Mendeleev number
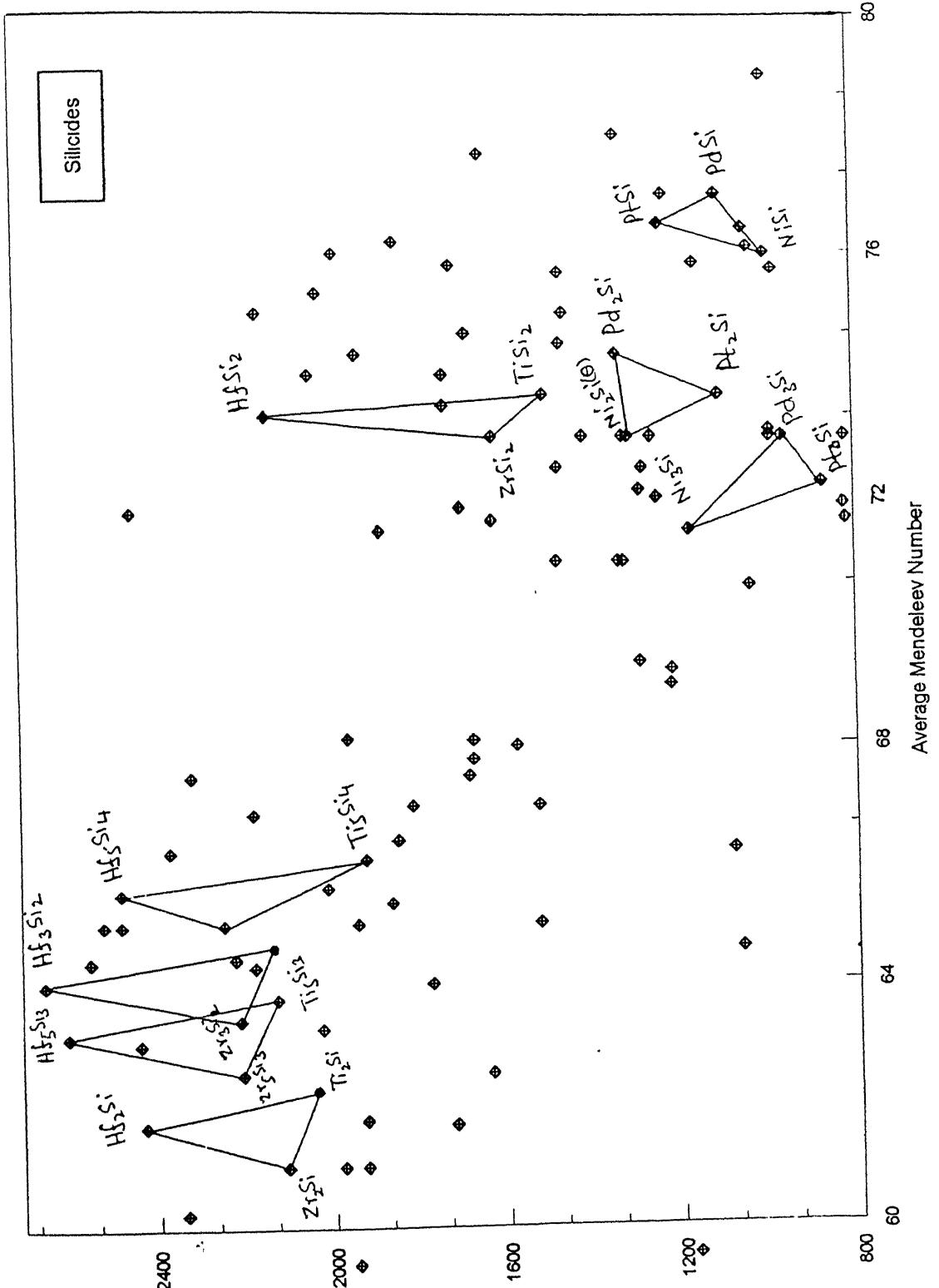
Fig. 4.5(b): Distribution of melting temperatures of silicides as a function of average Mendeleev number
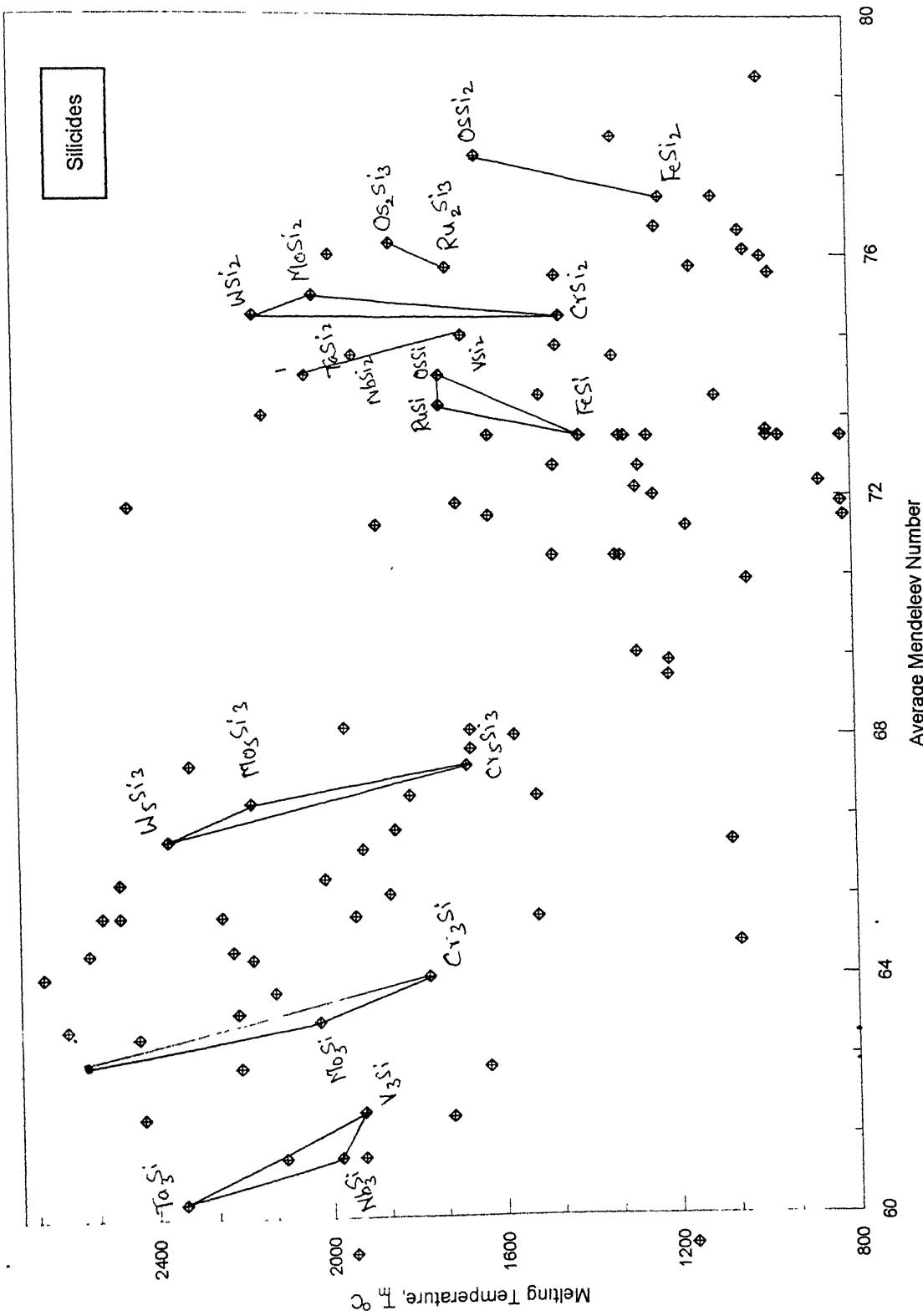
Fig 4.5(c): Distribution of melting temperatures of silicides as a function of average Mendeleev number

4.4.1. Heat of Formation (-ΔH) and Types of Bonding in Intermetallic Compounds

Heat of formation of Intermetallic compounds

The heat of formation of intermetallic compounds is the difference between the enthalpies of the compound and the component elements.

$$\Delta H = \Delta F + T\Delta S$$

Where ΔF is the free energy of formation and ΔS is the change in entropy. A decrease in the free energy accompanies the formation of an intermetallic compound from its component elements. A compound is stable with respect to competing neighbouring phases in a multicomponent system if its free energy is lower than that of a mixture of these phases. So the free energy of formation of intermetallic compounds is always negative. The temperature entropy product is small [42], so the heat of formation of intermetallic compounds is usually negative. In principle, the heat of formation of a stable phase may be positive if the free energy of formation is small and entropy-temperature product is positive and sufficiently large.

If the heat of formation is negative, it is called exothermic heat of formation and if it is positive, then endothermic heat of formation. Generally, intermetallic compound forms negative heat of formation, so we always talk of exothermic heat of formation.

Types of bonding in Intermetallic Compounds

The bonding in intermetallic compounds are considered as mainly ionic, covalent, metallic and intermediate between these types. Intermetallic compounds have large exothermic heat of formation when the nature of bonding is different from the bonding in the components.

Ionic bonding

The predominant ionic bonding of intermetallic compounds is found in the binary systems for which the electronegativity difference is large. The example of this type of compounds and their crystal structures are shown below [43].

$$
\begin{array}{lll}
AB: & \text{Sodium Chloride (NaCl)} & B1 \\
 & \text{Zinc Blende (ZnS)} & B3 \\
 & \text{Wurzite (ZnS)} & B4 \\
A_2B_3: & La_2O_3 & D5 \\
AB_3: & BiF_3 & DO_3 \\
\end{array}
$$

Pauling [44] suggested the following equation for the heat of formation of ionic compound as

$$\Delta H \text{ (k.cal/mole)} = -23.07 (X_A - X_B)^2 - 55.4\, n_N - 26\, n_O$$

where n_N, n_O are the number of nitrogen atoms and oxygen atoms, respectively. When the number density of nitrogen and oxygen atoms become zero i.e., $n_N = n_O = 0$, then

$$\Delta H \text{ (k.cal/g-atom)} = -23.07\ Z\ (X_A - X_B)^2$$

where Z is the number of valence links, X_A, X_B are the electronegativities of the constituent elements.

Covalent bonding

Covalent bonding is found in compounds of elements of group III B with the elements of V B group and each atom tends to form four covalent bonds. The phases have zinc blende (B3) structure. Intermetallic compounds in which bonding is largely covalent form only if the difference in electronegativities of the components is small. As this difference increases, the atom in the covalent bond becomes polarized and this contributes to the ionicity of the bond. As the ionicity increases the contribution to the heat of formation is also increases [43].

Metallic bonding

There are two types of compounds in metallic compounds. These are electron compounds (β- Brass, γ- Brass and ε - Brass type) and Laves phases (C14 and C15 type). Compounds with metallic bonding are formed by metallic elements which have same atomic size and similar electronegativities. Electron compounds are formed if their components belong to different groups in the periodic table and their atomic sizes do not differ by more than approximately 15 %. The main characteristic nature of electron compounds is valence electron to atom ratio (valence electron concentration, VEC) [43]. The ranges for VEC of intermetallic compounds according to their nature of bonding are given in Table A.3 in Appendix. So the main effect of substituting solute for a solvent atom is a change of valence electron to atom ratio. The main structural types of laves phases are Cubic (MgCu$_2$, C15), Hexagonal (MgNi$_2$, C14), Hexagonal (MgZn$_2$, C36).

Mixed bonding

Intermetallic compounds possess mainly two types of mixed bonding. One is ionic-metallic bonding and the other is ionic – metallic – covalent bonding. Intermetallic compounds in which bonding is intermediate between ionic and metallic possess antimorphous fluorite, CaF$_2$ (C1) structure. Intermetallic compounds with ionic-metallic-covalent bonding are found in Nickel Arsenide (B8) structure. This type of bonding is found in compounds of AB type in which A is usually a transition metal and B belongs to III B – VI B groups [43].

4.4.2 Comparison of Heats of Formation (-ΔH) of Intermetallic Compounds according to their Nature of Bonding

This section deals with the ranges of heat of formation of binary intermetallic compounds according to their nature of bonding. The information is given in [43] and we analyzed in terms of Mendeleev number to give ranges for heat of formation and Fig. 4.6 is plotted between Average Mendeleev Number and heat of formation of intermetallic compounds. The compounds with similar bonding and similar structure types are grouped together indicating the application of average Mendeleev number.

The ionic contribution is the main factor for high heats of formation and is observed in the compounds with ionic bonding of type (B1 & $D5_2$), ionic-metallic (C1), partial ionic compounds of type (B3 & B4) and ionic-metallic- covalent compounds (B8). The numerical values of heats of formation increase as the degree of ionicity increases in the bond. That's the reason compounds with ionic nature are having high heats of formation compared to the compounds with covalent and metallic bonds.

Covalent compounds (B3 & B4) possess less heats of formation values when compared to the compounds with ionic nature because the sharing of atoms in the covalent bond involves a small change than the electron transfer in the ionic bond. The compounds with ionic - metallic are partial ionic compounds having C1 structure. The ionicity of these compounds is responsible for having high heats of formation values, but it is less than that of ionic compounds. From Fig.4.6, the heat of formation of intermetallic compounds with ionic bonding range from −10 to −60 k.cal/g-atom and for compounds with covalent bonding range from −3 to −8 k.cal/g-atom.

The compounds with ionic-metallic-covalent bonding are having NiAs (B8) structure and are having intermediate values of heats of formation between ionic and metallic bonding compounds. From Fig. 4.6, the range of heat of formation of these compounds exist from −2 to − 12 k.cal/g-atom.

Compounds with metallic bonding have low heats of formation values compared with ionic and covalent compounds. In these compounds, minor ionic contributions to the bonding of electron compounds come from the difference between the electronegativity of the components increases. The heats of formation metallic compounds are less than −8 k.cal/g-atom, but a fewer are having higher heats of formation values. This comes from the compounds with one of the component is transition metal, the increase in the heats formation comes from the electron transfer from the other component to the partly filled inner shells of transition metal. The ranges of heat of formation for all those compounds, observed from Fig. 4.6, are summarized in Table 4.3.

The electronegativity difference (ΔX), which is the measure of ionic character and is responsible for giving rise to comparatively high heats of formation in intermetallic compounds, is plotted against heat of formation (-ΔH, k.cal/g-atom) for various binary intermetallic compounds in Fig 4.7. As it is known that the electronegativity difference is proportional to the heat of formation and also indicates that ionic compounds have high electronegativity differences and so having high heat of formation values. As ΔX is decreasing from ionic compounds of type B1 to metallic compounds of type A3, the heat of formation also decreases from ionic to metallic compounds.

71
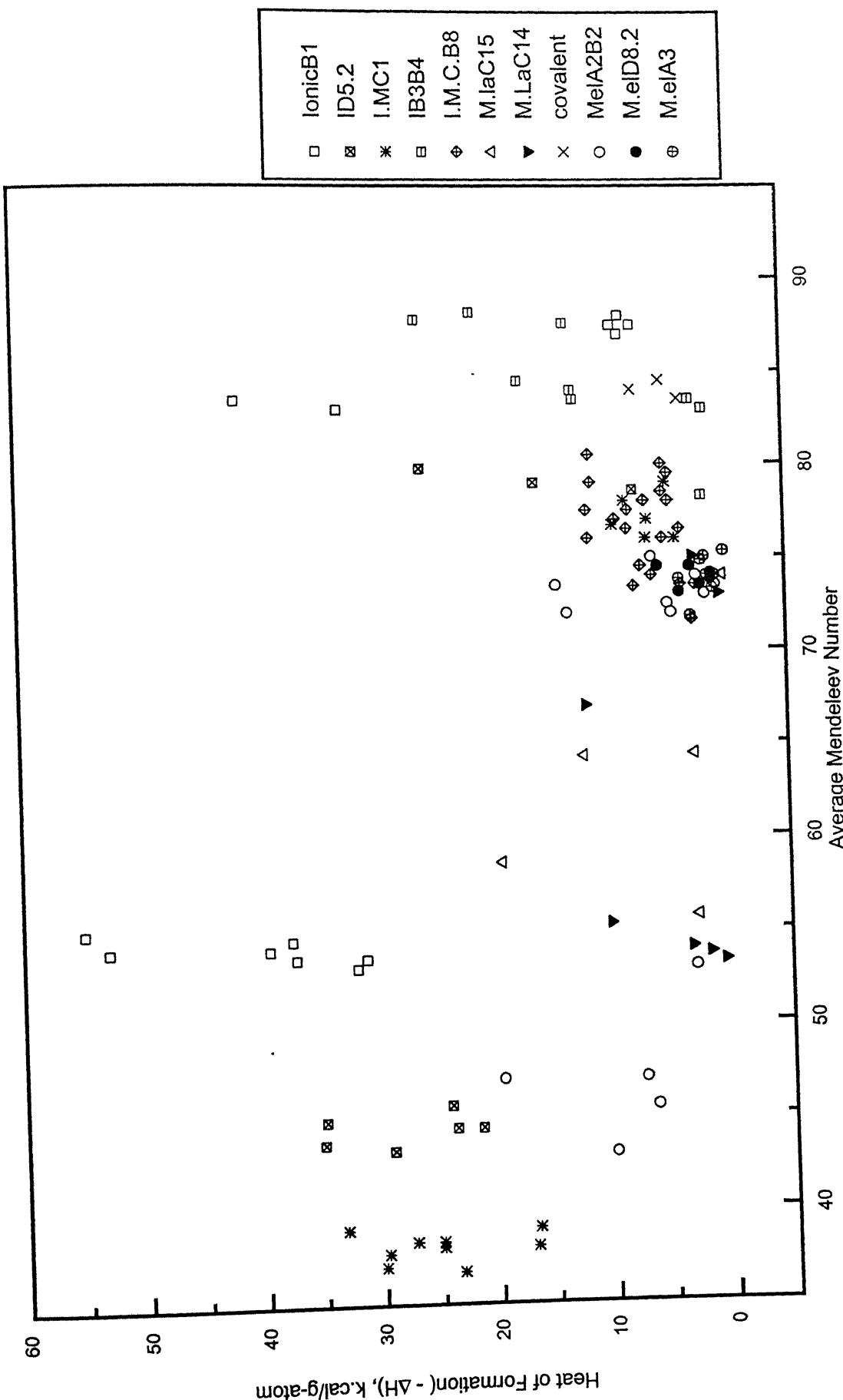
Fig. 4.6: Heat of formation of intermetallic compounds plotted against average Mendeleev number, according to their nature of bonding

72
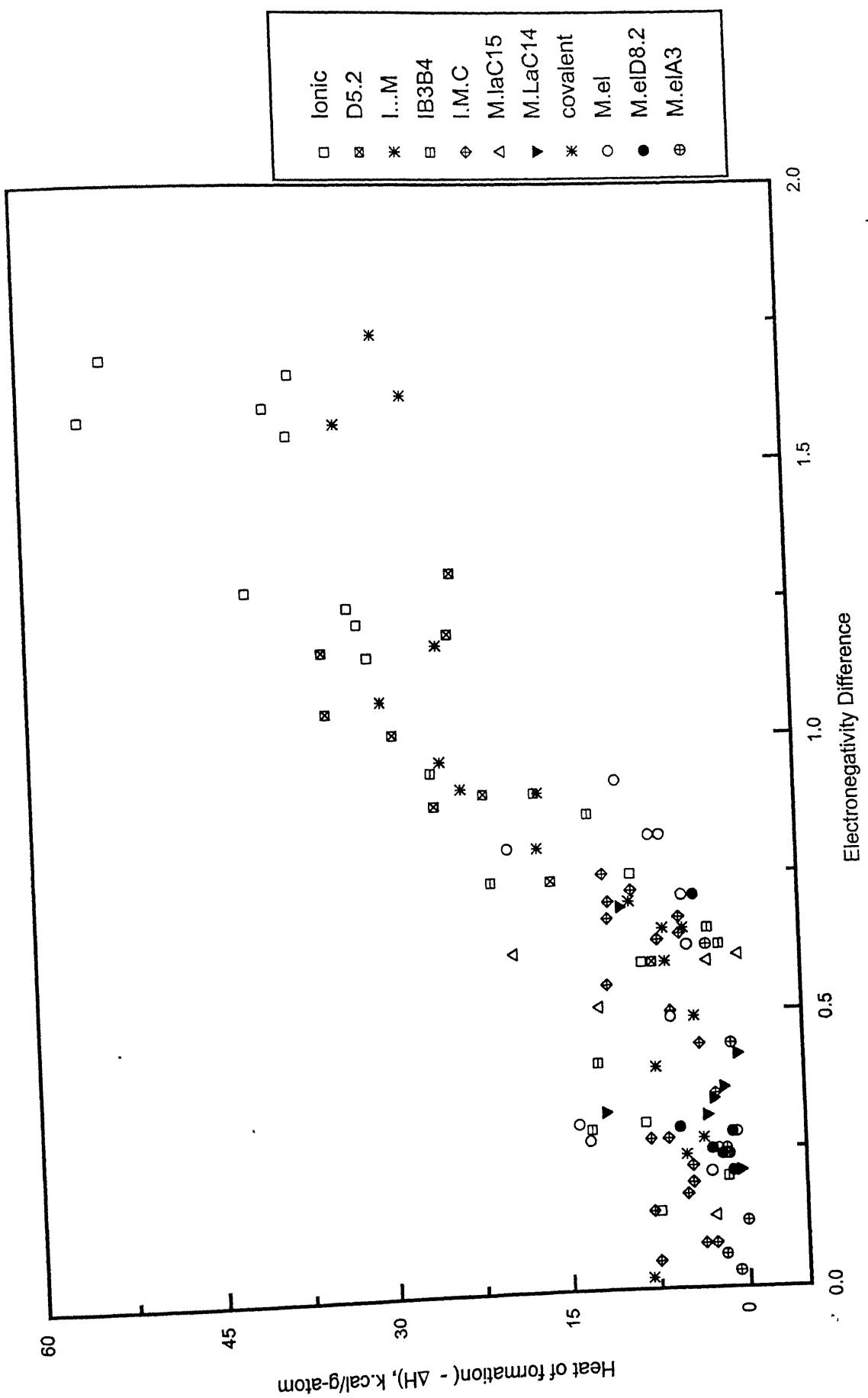
Fig. 4.7: Heat of formation as a function of electronegativity difference for intermetallic compounds

Table 4.3: Ranges of heat of formation of binary intermetallic compounds according to their bonding.

Nature of bonding	$-\Delta H$ in k.cal/g-atom
Ionic bonding Ionic B1 (NaCl type) Ionic D5$_2$ (La$_2$O$_3$ type)	 30 – 60 10 – 40
Mixed bonding Ionic – Metallic C1 (CaF$_2$ type) Partial ionic B3 & B4 (Zinc Blende and Wurzite) Ionic – Metallic – Covalent B8 (NiAs type)	 5 – 35 2 – 25 2 – 12
Covalent bonding Covalent B3 & B4 (Zinc blende & Wurzite)	 3 – 8
Metallic bonding Electron compounds A2 & B2, D8$_2$ and A3 (β-, γ-, and ε - Brass type) Laves phases C14, C15 (MgZn$_2$, MgCu$_2$ type)	 < 8 < 5

4.4.3 Heat of formation (- ΔH) of Intermetallic compounds formed by various combination of groups in the periodic table

The heat of formation of binary intermetallic compounds as a function of average Mendeleev number can be studied in association with the compounds formed by various combination of elements in different groups of the periodic table as shown in Fig. 4.8. This will provide information about the type of bonding to be expected when different elements of the periodic system combine to form binary intermetallic compounds. This also gives the range of heats of formation for various intermetallic compounds formed from the different elements of groups in the periodic table, which inturn comes from the nature of bonding and structure type. The source of information is given in [43] and we used Mendeleev number in predicting the type of bonding and their heat of formation for some intermetallic compounds. This is shown as follows.

Compounds formed from the combination of elements of group I

From Fig. 4.8, the heat of formation of binary intermetallic compounds formed by combination of elements of group I with the elements of group II toV are numerically

smaller than 15 k.cal/g-atom and increases from I-II to I–V compounds. All of these come under the structure types A2, B2, $D8_2$, A3, C14 and C15 and are metallic bonding compounds. These also include the partial ionic compounds of the type DO_3 and $L1_0$.

The compounds formed by the element of group I and VI are considered to be of two types. One with compounds of low heats of formation (Cu_2Se, C1 and Ag_2Se, B3 or B4 type) indicate their metallic nature and the other is compounds of high heats of formation indicates ionic nature. These are CaF_2 (C1) type, Ionic-Metallic bonding compounds with heat of formation in the range 20–35 k.cal/g-atom.

Compounds formed from the combination elements of group II

From Fig. 4.8, the compounds of the elements of group II with the elements of II and III have heats of formation in the range 0–20 k.cal/g-atom and are metallic compounds of A2, B2, C15 and C14 type. These include MgTl (A2 or B2), CaTl (A2 or B2) and $CaAl_2$ (C15). The heats of formation of compounds of group II with group IV have range from 5–25 k.cal/g-atom and are considered of ionic–metallic bonding (C1 type). The compounds of the elements of group II and V are ionic compounds of type $D5_2$ (La_2O_3) and have range 5–30 k.cal/g-atom. The compounds of the elements of group II with VI are (NaCl, B1 type) having highest heats of formation among all the group combinations and have range 30-60 k.cal/g-atom.

Compounds formed from the combination of elements of group III

The compounds formed by the combination of group III and V are covalent compounds of B3 (ZnS) type, include InSb, GaSb and and have range 3–8 k.cal/g-atom. The compounds of group III and VI are ionic-metallic, have range 13–26 k.cal/g-atom and are of B3 and B4 structure.

Compounds formed from the combination of elements of group IV and VI

The compounds formed from the elements of groups IV and VI are NaCl (B1) type but their heat of formation is less than 10 k.cal/g-atom, indicates the metallic nature of these compounds. So these compounds are considered as ionic – metallic bonding compounds.

Compounds formed from the combination of elements of the group VII and VIII

The compounds formed in this category have NiAs (B8) structure and the heat of formation of these compounds range 2–12 k.cal/g-atom. The higher values of heats of formation of these compounds indicate their ionic nature and lower values indicates their metallic nature. The intermediate values indicates their covalent nature and all together these compounds are considered as ionic – metallic – covalent type.

The ranges for heats of formation several intermetallic compounds formed from the different elements of various groups, observed from Fig. 4.8, are summarized in the Table 4.4.

Fig. 4.8 gives the useful information in predicting the nature of bonding, heat of formation and their crystal structures of binary intermetallic compounds. From Fig.4.8,
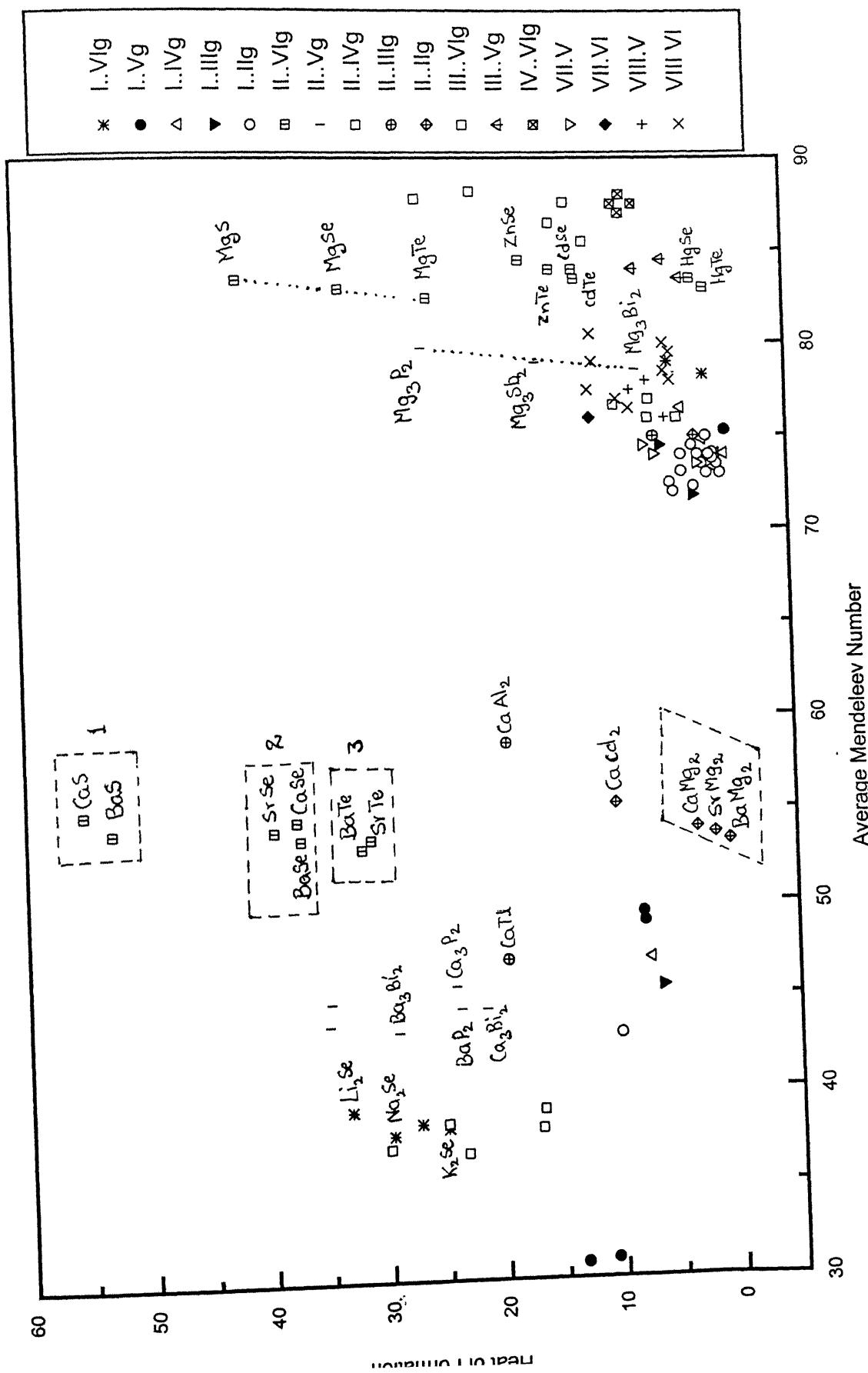
Fig. 4.8: Heat of formation of intermetallic compounds plotted against average Mendeleev number according to variuos combinations of elements belong to different groups in the periodic table

Table 4.4 Ranges of heat formation for binary intermetallic compounds formed by different combinations of various groups.

Group combination	Crystal structure	Nature of bonding	$-\Delta H$, k.cal/gatom
I – II I – III I – IV	A2, B2, A3, C14, C15, D8$_2$	Metallic	< 10
I – V	Ll$_0$, DO$_3$, A3	Partial Ionic	< 15
I - VI	C1	Ionic – Metallic	20 – 35
II – II II – III	A2, B2, C14, C15	Metallic	< 20
II – IV	C1	Ionic – Metallic	5 – 25
II – V	D5$_2$	Ionic	5 – 30
II – VI	B1	Ionic	30 – 60
III – V	B3	Covalent	3 – 8
III – VI	B3, B4	Partial Ionic or Ionic – Metallic	13 – 26
IV – VI	B1	Ionic – Metallic	< 10
VII – V VII – VI VIII – V VIII – VI	B8	Ionic – Metallic – covalent	2 – 12

the compounds formed by the elements of group II with the elements of group VI are grouped into three domains. These are sulphide, sellenide and telluride domains. The sulphide domain contain sulphides of calcium and barium, the sellenide domain contain sellenides of calcium, strontium and barium and the telluride domain contain the tellurides of barium and strontium. The compounds in these domains are ionic compounds of B1 (NaCl type). These domains are arranged in the decreasing order of electronegativities of S, Se and Te. So the corresponding electronegativity difference of the compounds within the domain as well as among the domains vary in the same manner as for S, Se and Te. And so the heats of formation of these compounds, which are proportional to electronegativity difference shown in Fig. 4.7, also vary in that manner. In domain 2, the sellenides of calcium, strontium and barium are located nearer to each other so we can predict the existence of SrS in domain 1 and CaTe in domain 3. It is also worth to mention that the compounds SrS and CaTe are also ionic compounds of B1 (NaCl type). Moreover we can say that CaS > CaSe > CaTe, SrS > SrSe > SrTe and BaS > BaSe > BaTe. So Fig. 4.8 is also useful in comparing the magnitudes of heats of formation of unknown compounds with the heats of formation of known compounds and indicates their existence in the corresponding domains.

The similar trends can be observed for MgS, MgSe, MgTe compounds. However it is observed that the slopes of the lines joining the compounds Ca(S, Se, (Te)), Sr((S), Se, Te), Ba(S, Se, Te) and Mg(S, Se, Te) (by assuming the existence of the compounds SrS and CaTe) are equal. This makes the process much simpler in identifying the unknown heats of formation of SrS and CaTe compounds. This type of trend is observed mostly for AB type ionic compounds of B1 (NaCl type). Similar observation can be found in IIB and VIB compounds of Zn(Se, Te), Cd(Se, Te), and Hg(Se, Te). The compounds formed from the elements of group IIA with the elements of group IIB are (Ca, Sr, Ba)Mg_2 and $CaCd_2$. It is observed from the Fig. 4.8 that the compounds (Ca, Sr, Ba)Mg_2 forming magnesium domain. So it precludes that compounds (Ca, (Sr), (Ba))Cd_2 also form cadmium domain and indicates the existence of $SrCd_2$ and $BaCd_2$ compounds. These are metallic bonding compounds of C14 ($MgZn_2$ type).

More trends can be found for the other compounds by careful observation, which gives the existence various binary intermetallic compounds.

4.4.4 Heat of formation and Stability of Intemetallic phases in various intermetallic systems

If several intermetallic phases with single compositions occur in a particular binary system, their heats of formation lie at the corners of the polygon when plotted against atomic fraction of the one of the components in the system [45]. This is observed in Ti-Al, Fe-Al and Ni-Al systems [3]. In this section we studied for Al-Cr, Li-Sn, and Ni-Si systems and also interpreted in terms of their average Mendeleev number. Similar results are obtained for these systems, in both cases, except to the scales along x-axis and are shown in Figs. 4.9(a-e). These plots are useful in comparing the stability of various phases in each system. For example, Al_4Cr, Li_7Sn_2 and Ni_3Si_2 phases have high negative heats of formation and hence more stable (strongest bonding) phases compared to the other phases in Al-Cr, Li-Sn and Ni-Si systems respectively.

78
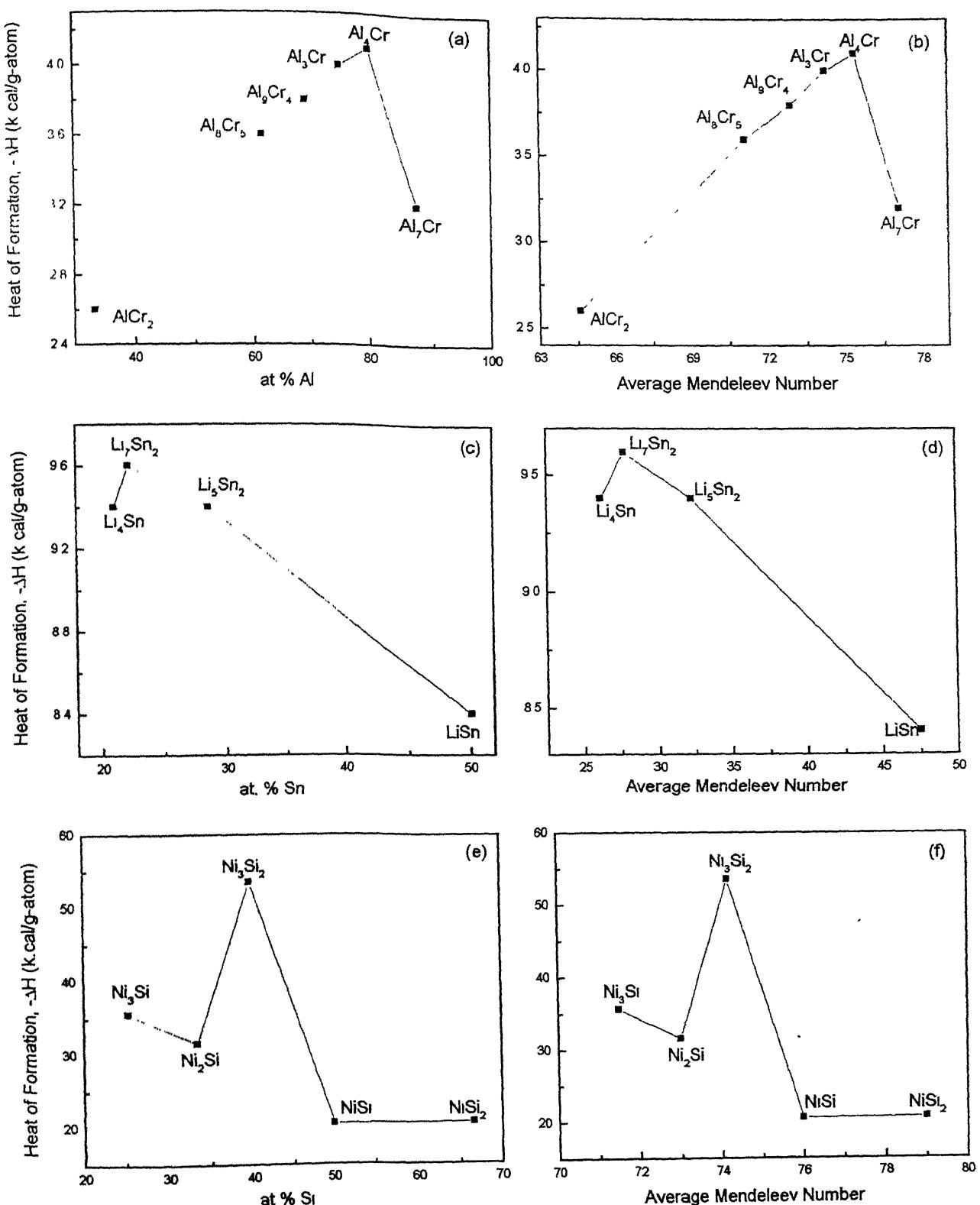
Fig.4.9: Heat of formation of intermetallic compounds plotted against atomic
fraction and average Mendeleev number for Al - Cr in (a) and (b), Li - Sn in
(c) and (d), Ni - Si in (e) and (f) respectively

Chapter 5

Conclusions and Future work

5.1 Conclusions

This work has dealt with trends in materials data for intermetallic compounds. The major aspects can be summed up as follows:

1. A data comprising of property data for more than 100 intermetallic compounds has been developed. This should be helpful for design activities.

2. The compiled data has subsequently been used to determine property ranges and to explore various correlations.

3. Property ranges for various categories of materials including intermetallic compounds are compared which are useful for materials selection in mechanical design.

4 Correlations between various physical properties are discussed and the limits of correlations are described for intermetallic compounds as well as silicides as a special case In case of silicides, melting temperature for the compounds Co_3Si, $CrSi$, $MoSi_2$ and $TaSi_2$ are estimated and compared with literature values Good comparison is obtained.

5. Preliminary results on correlation involving degree of metallicity of intermetallic compounds are explored and systematic variations are observed in C_{11}-δ map

6. Correlations between various properties and Mendeleev number are explored. The values of density and melting point for some silicides are predicted and ranges for heats of formation of intermetallic compounds are given according to their nature of bonding and various combination of elements belong to different groups in the periodic table.

Preliminary results support the hypothesis that since Mendeleev number allows good structural separation of compounds in Pettifor maps, it should also be useful index in developing correlations with various properties of intermetallic compounds.

5.2 Suggestions for Future work

1 Systematic studies in materials selection in mechanical design is given for metals, ceramics, polymers and composites by Ashby[22]. This analysis can be applied to intermetallic compounds based on the property ranges developed in this work [section 2.5].

2 Correlations with limiting values between various physical properties for metals, ceramics, polymers and elastomers are given in [7], which are shown in Table 3.1 in this work. We studied these correlations for silicides and this can be extended to aluminides, beryllides and some other miscellaneous intermetallic compounds.

3 We gave preliminary results in correlations involving degree of metallicity and this can be extended to observe more trends in this area.

4 Correlation based on Mendeleev number can be viewed in a detailed manner.

References

1 K. Karsten, *Pogg. Ann.*, Series 2, **46**, 1839, 160

2 Alan J. Ardell, *Intermetallic Compounds: Principles and Practice*, **v2**, "*Intermetallic as precipitates and despersoids in high strength alloys*", chapter 12, John Wiley & Sons, 1995

3 *Intermetallic compounds, Principles and Practice*, edited by J.H. Westbrook and R.L. Fleischer, **v2**, John Wiley & Sons, 1995

4 V.K. Sikka, J.T. Mauity and K. Anderson, *Mat. Sc. Engg. A*, **A153**, 1992, 712

5 *Engineering Properties of Selected Ceramic Materials*, edited by J.F. Lynch, C.G. Ruderer and W.H. Duckworth, Battle Memorial Instt., The American Ceramic Society Inc., 1966

6 J.R. Rodgers and P. Villars, *M.R.S. Bulletin*, **vXVIII**, 1993, 27

7 *Checks and Estimates for Material Properties*, M.F. Ashby, Cambridge Engg. Design Centre, 1996

8 P. Villars, *J. less-Comma Met.*, **92**, 1983, 215

9 P. Villars, *J. less-Comma Met.*, **99**, 1984, 33

10 P. Villars, *J. less-Comma Met.*, **102**, 1985, 199

11 W.B. Pearson, *The Crystal Chemistry and Physics of Metals and Alloys*, John Wiley and Sons, New York, 1972

12 D.G. Pettifer, *First supplement to the Pergamon Encyclopedia of Materials Science and Engineering*, edited by R.W. Cahn, Pergamon, Oxford, 1988, p. 51

13 D.G. Pettifer, *New Sci.*, **110**, (1510), 1986

14 D.G. Pettifer, *Physical Metallurgy*, edited by R.W. Cahn and P. Haasen, chapter 3, 73-152, 1983, Amsterdam, North-Holland, 1983

15 D.G. Pettifer, *J. Phys. C*, Solid State Phys.,19, 1986, 285

16 D.G. Pettifer and R. Podloucky, *Phys. Rev. Lett.*, **55**, 1985, 261

17 D.G. Pettifer, *Mat. Sc. and Tech.*,4, 1988, 675

18 M.F. Ashby and David R.H. Jones, *Engineering Materials: An Introduction to their properties and applications,*v34, Pergamon Press, 1980

19 U.D Saibaba and Om Prakash, *Data on Intermetallic Compounds,* Department of Mechanical Engineering, Indian Institute of Technology, Kanpur, 2000

20 D.R. Askeland, *The Science and Engineering of Materials,* Chapman and Hall, 1990

21 *CRC handbook of Chemistry & Physics,* 79th ed, edited by David R. Lide, CSC Press LLC, 1998

22 M.F. Ashby, *Material Selection in Mechanical Design,* 2nd edn, Butterworth-Heinemann, 1992

23 Touloukian, *Thermo physical properties of matter: Thermal conductivity of metallic elements and alloys,* The TPRC data series, v1, 1970

24 Touloukian, *Thermo physical properties of matter: Thermal expansion of metals and alloys,* The TPRC data series, v12, 1975

25 Smith, *Metals Reference Book,* 6th edn., edited by Eric A. Brandes, R669, Sm6m6

26 *Intermetallic compounds: Principles & Practice,* edited by J.H. Westbrook and R.L. Fleischer, v1, John Wiley & Sons, 1995

27 M.F. Ashby, *Engineering Material: An Introduction to microstructures, Processing and Design,* v39, Pergamon Press, 1986

28 B. Chalmers, *Physical metallurgy,* John Wiley & sons, 1962

29 W.B. Pearson, *Handbook of lattice spacings, structure of metals and alloys,* Pergamon Press, 1967

30 W.F. Pearson, *Handbook of lattice spacings, structure of metals and alloys,* Pergamon Press, 1958

31 *Encyclopedia of Material Science & Engineeringg,* v1, edited by R. Cahn, Pergamon Press, 1988

32 *Rules of thumb for physical scientists,* compiled by D.J. Fisher, Trans Tech publications Ltd., Switzerland, 1988.

33 P. Paufler, *intermetallic Phasen,* VEB Deutscher Verlag für Grundstoffindustrie, Leipzig, 1976, 165

34 R.L. Fleischer, *Proc. Int. Symp. Intermetallic Compounds*, edited by O. Izumi, The Japan Institute of Metals, Sendai, 1991a, 157

35 A.A. Ivanko, *Handbook of Hardness Data*, edited by G.V. Samsonov, Akad. Sci. Ukranian SSSR, 1971

36 R.L. Fleischer, R.S. Gilmore and R.J. Zabala, *J. Appl. Phys.*, **64**, 1988, 2964

37 R.L. Fleischer, R.S. Gilmore and R.J. Zabala, *Acta. Meta..*, **37**, 1989, 2801

38 K. Maex and M.V. Rossum, *Properties of Metal Silicides*, INSPEC publication, 1995

39 E. Mooser and W.B. Pearson, *Acta. Cryst*, **12**, 1959, 1015

40 *Intermetallic compounds, Principles and Practice*, edited by J.H. Westbrook and R.L. Fleischer, **v2**, John Wiley & Sons, 1995, p 12

41 *Intermetallic compounds, Principles and Practice*, edited by J.H. Westbrook and R.L. Fleischer, **v2**, John Wiley & Sons, 1995, p. 269

42 R. Hultgren, R.L. Orr, P.D. Anderson, and K.K. Kelly, *Selected values of thermodynamic properties of metals and alloys*, John Wiley & Sons, New York, 1963

43 J.H. Westbrook, *Intermetallic compounds*, John Wiley & Sons, 1967

44 L. Pauling, *The nature of chemical bond*, 3rd edn, Cornell Univ. Press, Ithaca, New York, 1960

45 C. Wagner, *Thermodynamics of Alloys*, Addison-Wesley Reading, Mass., 1952

Appendix A

Crystal Structure of Intermetallic Compounds

The crystal structures of tens of thousands of binary, ternary and quaternary phases have been developed since the advent of x-ray crystallography in 1910. These crystal structures are having importance in alloy formation. In this section, we will see various nomenclatures, which describe the crystal structures of various materials. In the following section we will see in brief about crystal structure of intermetallic compounds.

A.1 Crystal structure nomenclature

In general crystals structures are preliminarily classified according to the fourteen Bravais lattices and then the number of atoms in the conventional crystallographic unit cell for standard space group. Secondary classification within these groups follows the numerical order of 230 space groups and finally within any space group structures follow an alphabetical order of their names. The important nomenclatures that generally come across are given below

- ASTM nomenclature
- Pearson nomenclature
- Strukturbericht type

ASTM nomenclature

ASTM uses a single arbitrary capital letter to characterize each of fourteen Bravais lattices as shown in Table A.1.

Pearson nomenclature

Pearson chosen two characters, which are widely used to identify crystal types. The nomenclature involves a small letter to identify the space lattice. He retained the crystallographic letters for this purpose. To these is added a number equal to the number of atoms in the unit cell conventionally selected for a particular crystal type. When determining number of atoms in the unit cell, it should be remembered that each atom that is shared with an adjacent cell (or cells) must be counted as only a fraction of an atom. The Pearson symbols for the fourteen space lattices are shown in Table A.1.

Strukturbericht type

The above classification symbols are, of course, not possible names for structure types, since there may be indefinite number of structural types falling under a given class.

Table A.1: Representative nomenclatures for fourteen Bravais lattices

Crystal System	Lattice Parameters & Angles	Space lattice	Lattice symbol	Small letter designation by Pearson	Pearson Symbol	ASTM symbol
Triclinic (anorthic)	$a \neq b \neq c$ $\alpha \neq \beta \neq \gamma$	Primitive	P	a	aP	Z
Monoclinic	$a \neq b \neq c$ $\alpha = \gamma = 90° \neq \beta$ or $a \neq b \neq c$ $\alpha = \beta = 90° \neq \gamma$	Primitive Base – centered	P C	m	mP mC	M N
Orthorhombic	$a \neq b \neq c$ $\alpha = \beta = \gamma = 90°$	Primitive Base – centered Face – centered Body – centered	P C F I	o	oP oC oF oI	O Q S P
Tetragonal	$a = b \neq c$ $\alpha = \beta = \gamma = 90°$	Primitive Body – centered	P I	t	tP tI	T U
Hexagonal	$a = b \neq c$ $\alpha = \beta = 90°$ $\gamma = 120°$	Primitive	P	h	hP	H
Rhombohedral (or trigonal)	$a = b = c$ $\alpha = \beta = \gamma \neq 90°$ $<120°$	Primitive	R	h	hR	R
Cubic	$a = b = c$ $\alpha = \beta = \gamma = 90°$	Primitive Face – centered Body – centered	P F I	c	cP cF cI	C F B

The best that can be done is to name each structure type after a representative substance, for example, Cu_3Au which has that structure. This nomenclature is known as Strukturbericht type symbols which are fairly used and recognized for simple structures. This is an arbitrary system of structure type names, and also somewhat arbitrary method of allotting the names. The representation of Strukturbericht type symbols is explained below.

Strukturbericht Symbol	Structure Name	Pearson Symbol
A1	Cu	cF24
A2	W	cI2
.	.	.
.	.	.
.	.	.
B1	NaCl	cF8
B2	CsCl	cP2
.	.	.
.	.	.
C1	CF_2	cF12

In this representation, crystal structures were classified by a designation consisting of a capital letter.

- A for elements
- B for AB type phases
- C for AB_2 type phases
- D for other binary phases
- E for ternary phases
- L for superlattices

followed by a number consecutively assigned at the time the type was reported. To further distinguish among crystal types, inferior letters and numbers, as well as, prime marks were added to some designations. For example,

B_e	CdSb	oP16
C_{11b}	$MoSi_2$	tI6

A.2 Space group nomenclature

Space group notation is a symbolic description of the space lattice and symmetry of a crystal. It consists of the symbol for space lattice followed by letters and numbers that designate the symmetry of the crystal. The relations among common Pearson

symbols, space groups, structure prototypes and Strukturbericht designations for crystal structures are shown in Table A.2.

A.3 Crystal structure of Intermetallic compounds

Intermetallic compounds have different crystal structures than the crystal structure of its constituent chemical elements in the binary case or of its binary boundary intermetallic compounds in the ternary case. A crystal structure is completely determined by the following data.

- Chemical formula
- Crystal system and unit cell dimensions
- Space group
- Occupation number and coordinates of the occupied point sets

The first crystal studies of intermetallic compounds showed relatively simple structures like those of common metals. Now that hundreds of crystallographic analysis have been completed. It is apparent that this group of compounds embraces many exceeding complex structural arrangements. The most common structures are among the most simple, certain of these belonging to the AB, AB_2 and AB_3 types. For example

AB: NaCl, CsCl, ZnS, NiAs etc.
AB_2: $MgCu_2$, CaF_2 etc.
AB_3: Cu_3Au etc.

Some examples of these structures are shown in Fig. A.1.

AB
TYPES

Na Cl

Cs Cl

ZnS

Ni As

AB₂
TYPE

LAVES
Mg Cu₂ TYPE

AB₃
TYPE

Cu₃ Au
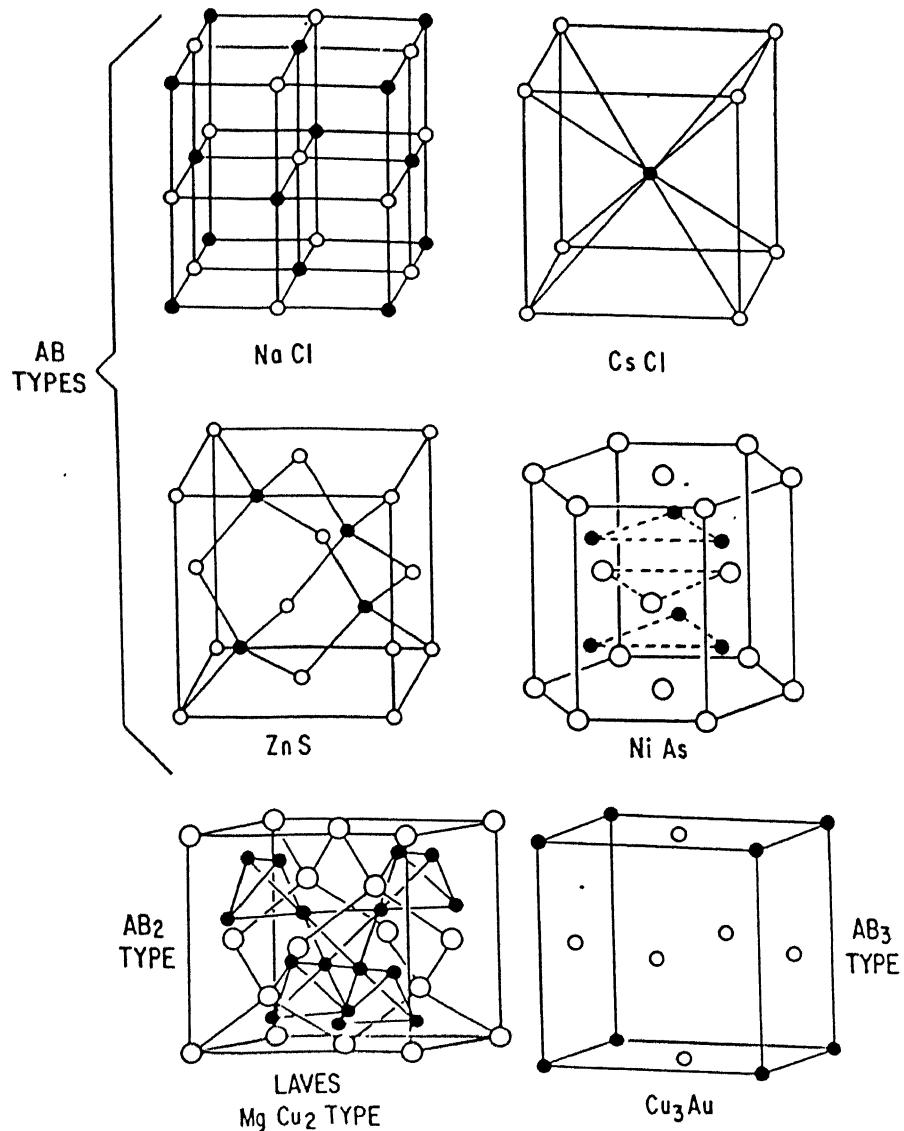
Fig A.1: Some examples of crystal structure of intermetallic compounds

Crystal Structure Nomenclature*

Arranged Alphabetically by Pearson-Symbol Designation

Pearson symbol	Prototype	Strukturbericht designation	Space group	Pearson symbol	Prototype	Strukturbericht designation	Space group
cF4	Cu	A1	Fm$\bar{3}$m	cP6	Ag$_2$O	C3	Pn$\bar{3}$m
cF8	C (diamond)	A4	Fd$\bar{3}$m	cP7	CaB$_6$	D2$_1$	Pm$\bar{3}$m
	NaCl (rock salt)	B1	Fm$\bar{3}$m	cP8	Cr$_3$Si (βW)	A15	Pm$\bar{3}$n
	ZnS (sphalerite)	B3	F$\bar{4}$3m		FeSi	B20	P2$_1$3
cF12	CaF$_2$ (fluorite)	C1	Fm$\bar{3}$m	cP12	Cu$_3$VS$_4$ (sulvanite)	H2$_4$	P$\bar{4}$3m
	MgAgAs	C1$_b$	F$\bar{4}$3m		FeS$_2$ (pyrite)	C2	Pa3
cF16	AlCu$_2$Mn (Heusler)	L2$_1$	Fm$\bar{3}$m		NiSbS (ullmanite)	FO$_1$	P2$_1$3
	BiF$_3$ (AlFe$_3$)	DO$_3$	Fm$\bar{3}$m	cP20	βMn	A13	P4$_1$32
	NaTl	B32	Fd$\bar{3}$m	cP36	BaHg$_{11}$	D2$_e$	Pm$\bar{3}$m
cF24	AuBe$_5$	C15$_b$	F$\bar{4}$3m	cP39	Mg$_2$Zn$_{11}$	D8$_c$	Pm$\bar{3}$
	SiO$_2$ (β cristobalite)	C9	Fd$\bar{3}$m	cP52	Cu$_9$Al$_4$ (γ brass)	D8$_3$	P$\bar{4}$3m
	Cu$_2$Mg (Laves)	C15	Fd$\bar{3}$m	hP1	HgSn$_{6-10}$	A$_f$	P6/mmm
cF32	CuPt$_3$	L1$_4$	Fm$\bar{3}$c	hP2	Mg	A3	P6$_3$/mmc
cF52	UB$_{12}$	D2$_f$	Fm$\bar{3}$m		WC	B$_h$	P$\bar{6}$m2
cF56	Al$_2$MgO$_4$ (spinel)	H1$_1$	Fd$\bar{3}$m	hP3	AlB$_2$	C32	P6/mmm
	Co$_3$S$_4$	D7$_2$	Fd$\bar{3}$m		CdI$_2$	C6	P$\bar{3}$m1
cF68	Co$_9$S$_8$	D8$_9$	Fm$\bar{3}$m		Fe$_2$N	L'3	P6$_3$/mmc
cF80	Sb$_2$O$_3$ (senarmontite)	D5$_4$	Fd$\bar{3}$m		LiZn$_2$	C$_k$	P6$_3$/mmc
cF112	Fe$_3$W$_3$C (η carbide)	E9$_3$	Fd$\bar{3}$m		γSe	A8	P3$_1$21
	NaZn$_{13}$	D2$_3$	Fm$\bar{3}$c	hP4	αLa	A3'	P6$_3$/mmc
cF116	Cr$_{23}$C$_6$	D8$_4$	Fm$\bar{3}$m		BN ·	B$_k$	P6$_3$/mmc
	Mn$_{23}$Th$_6$, Cu$_{16}$Mg$_6$Si$_7$ (G-phase)	D8$_a$	Fm$\bar{3}$m		C (graphite)	A9	P6$_3$/mmc
cI2	W	A2	Im$\bar{3}$m		NiAs	B8$_1$	P6$_3$/mmc
cI16	CoU	B$_e$	I2$_1$3		ZnS (wurtzite)	B4	P6$_3$mc
cI28	Th$_3$P$_4$	D7$_3$	I$\bar{4}$3d	hP5	La$_2$O$_3$	D5$_2$	P$\bar{3}$m1
cI32	CoAs$_3$ (skutterudite)	DO$_2$	Im$\bar{3}$		Ni$_2$Al$_3$	D5$_{13}$	P$\bar{3}$m1
cI40	Ge$_7$Ir$_3$	D8$_f$	Im$\bar{3}$m	hP6	CaCu$_5$	D2$_d$	P6/mmm
	Pu$_2$C$_3$	D5$_c$	I$\bar{4}$3d		CoSn	B35	P6/mmm
cI52	Cu$_5$Zn$_8$ (γ brass)	D8$_2$	I$\bar{4}$3m		Cu$_2$Te	C$_h$	P6/mmm
	Fe$_3$Zn$_{10}$ (γ brass)	D8$_1$	Im$\bar{3}$m		HgS	B9	P3$_1$21
cI54	Sb$_2$Tl$_7$	L2$_2$	Im$\bar{3}$m		MoS$_2$	C7	P6$_3$/mmc
cI58	αMn (χ-phase)	A12	I$\bar{4}$3m		Ni$_2$In	B8$_2$	P6$_3$mmc
cI76	Cu$_{15}$Si$_4$	D8$_6$	I$\bar{4}$3d	hP8	Na$_3$As	DO$_{18}$	P6$_3$/mmc
cI80	Mn$_2$O$_3$	D5$_3$	Ia$\bar{3}$		Ni$_3$Sn	DO$_{19}$	P6$_3$/mmc
cI96	AlLi$_3$N$_2$	E9$_d$	Ia$\bar{3}$		TiAs	B$_i$	P6$_3$/mmc
cI162	Mg$_{32}$(Al,Zn)$_{49}$	D8$_c$	Im$\bar{3}$	hP9	CrSi$_2$	C40	P6$_2$22
cP1	αPo	A$_h$	Pm$\bar{3}$m		Fe$_2$P	C22	P$\bar{6}$2m
cP2	CsCl	B2	Pm$\bar{3}$m		γAgZn	B$_b$	P$\bar{3}$
cP4	AuCu$_3$	L1$_2$	Pm$\bar{3}$m		SiO$_2$ (high quartz)	C8	P6$_2$22
	ReO$_3$	DO$_9$	Pm$\bar{3}$m	hP10	Pt$_2$Sn$_3$	D5$_b$	P6$_3$/mmc
cP5	AlFe$_3$C (perovskite)	L'1$_2$	Pm$\bar{3}$m	hP12	CuS	B18	P6$_3$/mmc
	CaTiO$_3$ (perovskite)	E2$_1$	Pm$\bar{3}$m		MgZn$_2$ (Laves)	C14	P6$_3$/mmc
	Fe$_4$N	L'1	P$\bar{4}$3m		SiO$_2$ (β tridymite)	C10	P6$_3$/mmc

Table A.2: Crystal structure nomenclatures are arranged alphabetically by Pearson symbol designation and Strukturbericht designation [3]

Arranged Alphabetically by Pearson-Symbol Designation (*continued*)

Pearson symbol	Prototype	Strukturbericht designation	Space group
hP14	W₂B₅	$D8_h$	$P6_3/mmc$
hP16	Mn₅Si₃	$D8_8$	$P6_3/mcm$
	Ni₃Ti	$D0_{24}$	$P6_3/mmc$
hP18	Al₄C₄Si	$E9_4$	$P6_3mc$
	Al₈FeMg₃Si₆	$E9_b$	$P\bar{6}2m$
	Mg₂Ni	C_e	$P6_222$
hP20	Fe₅Th₇	$D10_2$	$P6_3mc$
	Th₇S₁₂	$D8_k$	$P6_3/m$
hP24	Cu₃P	$D0_{21}$	$P6_3cm$
	MgNi₂ (Laves)	$C36$	$P6_3/mmc$
hP28	Co₂Al₅	$D8_{11}$	$P6_3/mmc$
hR1	αHg	$A10$	$R\bar{3}m$
	βPo	A_i	$R\bar{3}m$
hR2	αAs	$A7$	$R\bar{3}m$
hR3	αSm	$C19$	$R\bar{3}m$
hR4	NaCrS₂	$F5_1$	$R\bar{3}m$
hR5	Bi₂Te₃	$C33$	$R\bar{3}m$
	Ni₃S₂	$D5_e$	$R32$
hR6	CaSi₂	$C12$	$R\bar{3}m$
	NiS (millerite)	$B13$	$R\bar{3}m$
hR7	Al₄C₃	$D7_1$	$R\bar{3}m$
	Mo₂B₅	$D8_i$	$R\bar{3}m$
hR10	αAl₂O₃ (corundum)	$D5_1$	$R\bar{3}c$
hR13	Fe₇W₆ (μ-phase)	$D8_5$	$R\bar{3}m$
hR15	B₄C	$D1_g$	$R\bar{3}m$
hR26	Cr₅Al₈	$D8_{10}$	$R\bar{3}m$
hR32	CuPt	$L1_1$	$R\bar{3}m$
mC6	AuTe₂ (calaverite)	$C34$	$C2/m$
mC8	CuO (tenorite)	$B26$	$C2/c$
mC12	ThC₂	C_g	$C2/c$
mC14	δNi₃Sn₄	$D7_e$	$C2/m$
mC16	FeKS₂	$F5_4$	$C2/c$
mP12	AgAuTe₄ (sylvanite)	$E1_b$	$P2/c$
	ZrO₂	$C43$	$P2_1/c$
mP20	As₂S₃	$D5_f$	$P2_1/c$
mP22	Co₂Al₉	$D8_d$	$P2_1/c$
mP24	FeAsS	$E0_7$	$P2_1/c$
mP32	AsS (realgar)	B_l	$P2_1/c$
	βSe	A_i	$P2_1/c$
mP64	αSe	A_k	$P2_1/c$
oC4	αU	$A20$	$Cmcm$
oC8	CaSi	B_c	$Cmmc$
	αGa	$A11$	$Cmca$
	CrB	$B33$	$Cmcm$
	I₂	$A14$	$Cmca$
	P (black)	$A17$	$Cmca$
oC12	ZrSi₂	$C49$	$Cmcm$
oC16	BRe₃	$E1_a$	$Cmcm$
oC20	PdSn₄	$D1_c$	$Aba2$
oC24	PdSn₂	C_f	$Aba2$
oC28	Al₃Mn	$D2_h$	$Cmcm$
oF24	TiSi₂	$C54$	$Fddd$
oF40	Mn₄B	$D1_f$	$Fddd$
oF48	CuMg₂	C_b	$Fddd$
oF72	GeS₂	$C44$	$Fdd2$
oF128	αS	$A16$	$Fddd$
oI12	SiS₂	$C42$	$Ibam$
oI14	Ta₃B₄	$D7_b$	$Immm$
oI20	Al₃U	$D1_b$	$Imma$
oI28	Ga₂Mg₅	$D8_8$	$Ibam$
oI4	AuCd	$B19$	$Pmma$
oI6	FeS₂ (marcasite)	$C18$	$Pnnm$
	CaCl₂	$C35$	$Pnnm$
oP8	αNp	A_c	$Pnma$
	ηNiSi	B_d	$Pbnm$

Pearson symbol	Prototype	Strukturbericht designation	Space group
oP8	βCu₃Ti	$D0_a$	$Pmmn$
	FeB	$B27$	$Pnma$
	GeS	$B16$	$Pnma$
	SnS	$B29$	$Pmcn$
	MnP	$B31$	$Pnma$
	TiB	B_m	$Pnma$
oP12	Co₂Si, NiSiTi (E-phase)	$C23$	$Pnma$
	Co₂Si	$C37$	$Pbnm$
	HgCl₂	$C28$	$Pmnb$
oP16	Al₃Ni	$D0_{20}$	$Pnma$
	AsMn₃	$D0_d$	$Pmmn$
	BaS₃	$D0_{17}$	$P42_1m$
	CdSb	B_e	$Pbca$
	CuS₂Sb (wolfsbergite)	$F5_6$	$Pnma$
	Fe₃C (cementite)	$D0_{11}$	$Pnma$
oP20	Cr₃C₂	$D5_{10}$	$Pnma$
	Sb₂S₃	$D5_8$	$Pnma$
	Sb₂O₃ (valentinite)	$D5_{11}$	$Pccn$
oP24	AuTe₂ (krennerite)	$C46$	$Pma2$
	CuFe₂S₃ (cubanite)	$E9_c$	$Pnma$
	TiO₂ (brookite)	$C21$	$Pbca$
oP40	Cr₇C₃	$D10_1$	$Pnma$
tI2	αPa	A_a	$I4/mmm$
	In	$A6$	$I4/mmm$
tI4	βSn	$A5$	$I4_1/amd$
tI6	CaC₂	$C11_a$	$I4/mmm$
	MoSi₂	$C11_b$	$I4/mmm$
	ThI₂	$L'2_b$	$I4/mmm$
tI8	Al₃Ti	$D0_{22}$	$I4/mmm$
tI10	Al₄Ba	$D1_3$	$I4/mmm$
	MoNi₄	$D1_a$	$I4/m$
tI12	Al₂Cu	$C16$	$I4/mcm$
	ThSi₂	C_c	$I4_1/amd$
tI14	Al₂CdS₄	$E3$	$I\bar{4}$
tI16	Al₃Zr	$D0_{23}$	$I4/mmm$
	CuFeS₂ (chalcopyrite)	$E1_1$	$I\bar{4}2d$
	Cu₂FeSnS₄ (stannite)	$H2_6$	$I\bar{4}2m$
	Ir₃Si	$D0'$	$I4/mcm$
	MoB	B_g	$I4_1/amd$
	SiU₃	$D0_c$	$I4/mcm$
	TlSe	$B37$	$I4/mcm$
tI18	Fe₈N	$D2_e$	$I4/mmm$
tI26	Mn₁₂Th	$D2_b$	$I4/mmm$
tI28	MnU₆	$D2_c$	$I4/mcm$
tI32	Cr₅B₃	$D8_l$	$I4/mcm$
	Ni₃P	$D0_e$	$I\bar{4}$
	W₅Si₃	$D8_m$	$I4/mcm$
tP2	δCuTi	$L2_a$	$P4/mmm$
	βNp	A_d	$P42_12$
tP4	AuCu	$L1_0$	$P4/mmm$
	CuTi₃	$L6_0$	$P4/mmm$
	γCuTi	$B11$	$P4/nmm$
	PbO	$B10$	$P4/nmm$
	PtS	$B17$	$P4_2/mmc$
tP6	Cu₂Sb	$C38$	$P4/nmm$
	PbFCl	$E0_1$	$P4/nmm$
	TiO₂ (rutile)	$C4$	$P4_2/mnm$
tP10	Pb₄Pt	$D1_d$	$P4/nbm$
	Si₂U₃	$D5_a$	$P4/mbm$
tP16	PdS	$B34$	$P4_2/m$
tP20	B₄Th	$D1_e$	$P4/mbm$
tP30	βU	A_b	$P4_2/mnm$
	σCrFe	$D8_b$	$P4_2/mnm$
tP40	Al₇Cu₂Fe	$E9_a$	$P4/mnc$
	Zn₃P₂	$D5_y$	$P4_2/nmc$
tP50	γB	A_g	$P4_2/nnm$

Arranged Alphabetically by Strukturbericht Designation

Strukturbericht designation	Prototype	Pearson symbol	Space group	Strukturbericht designation	Prototype	Pearson symbol	Space group
A_a	αPa	tI2	I4/mmm	B20	FeSi	cP8	P2_13
A_b	βU	tP30	P4_2/mnm	B26	CuO (tenorite)	mC8	C2/c
A_c	αNp	oP8	Pnma	B27	FeB	oP8	Pnma
A_d	βNp	tP4	P4_2 1 2	B29	SnS	oP8	Pmcn
A_f	HgSn_{6-10}	hP1	P6/mmm	B31	MnP	oP8	Pnma
A_g	γB	tP50	P4_2/nnm	B32	NaTl	cF16	Fd3m
A_h	αPo	cP1	Pm3m	B33(=B_f)	CrB	oC8	Cmcm
A_i	βPo	hR1	R3m	B34	PdS	tP16	P4_2/m
A_k	αSe	mP64	P2_1/c	B35	CoSn	hP6	P6/mmn
A_l	βSe	mP32	P2_1/c	B37	TlSe	tI16	I4/mcm
A1	Cu	cF4	Fm3m	C_a	Mg_2Ni	hP18	P6_22
A2	W	cI2	Im3m	C_b	CuMg_2	oF48	Fddd
A3	Mg	hP2	P6_3/mmc	C_c	ThSi_2	tI12	I4_1/amd
A3'	αLa	hP4	P6_3/mmc	C_e	PdSn_2	oC24	Aba2
A4	C (diamond)	cF8	Fd3m	C_g	ThC_2	mC12	C2/c
A5	βSn	tI4	I4_1/amd	C_h	Cu_2Te	hP6	P6/mmn
A6	In	tI2	I4/mmm	C_k	LiZn_2	hP3	P6_3/mm.
A7	αAs	hR2	R3m	C1	CaF_2 (fluorite)	cF12	Fm3m
A8	γSe	hP3	P3_121	C1_b	MgAgAs	cF12	F43m
A9	C (graphite)	hP4	P6_3/mmc	C2	FeS_2 (pyrite)	cP12	Pa3
A10	αHg	hR1	R3m	C3	Ag_2O	cP6	Pn3m
A11	αGa	oC8	Cmca	C4	TiO_2 (rutile)	tP6	P4_2/mnn
A12	αMn (χ-phase)	cI58	I43m	C6	CdI_2	hP3	P3m1
A13	βMn	cP20	P4_132	C7	MoS_2	hP6	P6_3/mm.
A14	I_2	oC8	Cmca	C8	SiO_2 (high quartz)	hP9	P6_22
A15	Cr_3Si (β-W)	cP8	Pm3n	C9	SiO_2 (β cristobalite)	cF24	Fd3m
A16	αS	oF128	Fddd	C10	SiO_2 (β tridymite)	hP12	P6_3/mm.
A17	P (black)	oC8	Cmca	C11_a	CaC_2	tI6	I4/mmm
A20	αU	oC4	Cmcm	C11_b	MoSi_2	tI6	I4/mmm
B_a	CoU	cI16	I2_13	C12	CaSi_2	hR6	R3m
B_b	ζAgZn	hP9	P3	C14	MgZn_2 ⎫ Laves	hP12	P6_3/mm.
B_c	CaSi	oC8	Cmmc	C15	Cu_2Mg ⎭	cF24	Fd3m
B_d	ηNiSi	oP8	Pbnm	C15_b	AuBe_5	cF24	F43m
B_e	CdSb	oP16	Pbca	C16	Al_2Cu	tI12	I4/mcm
B_f (= B33)	CrB	oC8	Cmcm	C18	FeS_2 (marcasite)	oP6	Pnnm
B_g	MoB	tI16	I4_1/amd	C19	αSm	hR3	R3m
B_h	WC	hP2	P6m2	C21	TiO_2 (brookite)	oP24	Pbca
B_i	TiAs	hP8	P6_3/mmc	C22	Fe_2P	hP9	P62m
B_k	BN	hP4	P6_3/mmc	C23	Co_2Si, NiSiTi (E-phase)	oP12	Pnma
B_l	AsS (realgar)	mP32	P2_1/c	C28	HgCl_2	oP12	Pmnb
B_m	TlB	oP8	Pnma	C32	AlB_2	hP3	P6/mmm
B1	NaCl (rock salt)	cF8	Fm3m	C33	Bi_2Te_3	hR5	R3m
B2	CsCl	cP2	Pm3m	C34	AuTe_2 (calaverite)	mC6	C2/m
B3	ZnS (sphalerite)	cF8	F43m	C35	CaCl_2	oP6	Pnnm
B4	ZnS (wurtzite)	hP4	P6_3mc	C36	MgNi_2 (Laves)	hP24	P6_3/mm.
B8_1	NiAs	hP4	P6_3/mmc	C37	Co_2Si	oP12	Pbnm
B8_2	Ni_2In	hP6	P6_3/mmc	C38	Cu_2Sb	tP6	P4/nmn
B9	HgS (cinnabar)	hP6	P3_121	C40	CrSi_2	hP9	P6_22
B10	PbO	tP4	P4/nmm	C42	SiS_2	oI12	Ibam
B11	γCuTi	tP4	P4/nmm	C43	ZrO_2	mP12	P2_1/c
B13	NiS (millerite)	hR6	R3m	C44	GeS_2	oF72	Fdd2
B16	GeS	oP8	Pnma	C46	AuTe_2 (krennerite)	oP24	Pma2
B17	PtS (cooperite)	tP4	P4_2/mmc	C49	ZrSi_2	oC12	Cmcm
B18	CuS (covellite)	hP12	P6_3/mmc	C54	TiSi_2	oF24	Fddd
B19	AuCd	oP4	Pmma	D0_a	βCu_3Ti	oP8	Pmmn
				D0_c	SiU_3	tI16	I4/mcm

Arranged Alphabetically by Strukturbericht Designation (*continued*)

Strukturbericht designation	Prototype	Pearson symbol	Space group	Strukturbericht designation	Prototype	Pearson symbol	Space group
DO_c'	Ir_3Si	$tI16$	$I4/mcm$	$D8_d$	Co_2Al_9	$mP22$	$P2_1/c$
DO_d	$AsMn_3$	$oP16$	$Pmmn$	$D8_e$	$Mg_{32}(Al,Zn)_{49}$	$cI162$	$Im\bar{3}$
DO_e	Ni_3P	$tI32$	$I\bar{4}$	$D8_f$	Ge_7Ir_3	$cI40$	$Im\bar{3}m$
DO_2	$CoAs_3$ (skutterudite)	$cI32$	$Im\bar{3}$	$D8_g'$	Ga_2Mg_5	$oI28$	$Ibam$
DO_3	$BiF_3, AlFe_3$	$cF16$	$Fm\bar{3}m$	$D8_h$	W_2B_5	$hP14$	$P6_3/mmc$
DO_9	ReO_3	$cP4$	$Pm\bar{3}m$	$D8_i$	Mo_2B_5	$hR7$	$R\bar{3}m$
DO_{11}	Fe_3C (cementite)	$oP16$	$Pnma$	$D8_k$	Th_7S_{12}	$hP20$	$P6_3/m$
DO_{17}	BaS_3	$oP16$	$P42_1m$	$D8_l$	Cr_5B_3	$tI32$	$I4/mcm$
DO_{18}	Na_3As	$hP8$	$P6_3/mmc$	$D8_m$	W_5Si_3	$tI32$	$I4/mcm$
DO_{19}	Ni_3Sn	$hP8$	$P6_3/mmc$	$D8_i$	Fe_3Zn_{10}	$cI52$	$Im\bar{3}m$
DO_{20}	Al_3Ni	$oP16$	$Pnma$	$D8_2$	Cu_5Zn_8 ⎫ γ brass	$cI52$	$I\bar{4}3m$
DO_{21}	Cu_3P	$hP24$	$P6_3cm$	$D8_3$	Cu_9Al_4 ⎬	$cP52$	$P\bar{4}3m$
DO_{22}	Al_3Ti	$tI8$	$I4/mmm$	$D8_4$	$Cr_{23}C_6$ ⎭	$cF116$	$Fm\bar{3}m$
DO_{23}	Al_3Zr	$tI16$	$I4/mmm$	$D8_5$	Fe_7W_6 (μ-phase)	$hR13$	$R\bar{3}m$
DO_{24}	Ni_3Ti	$hP16$	$P6_3/mmc$	$D8_6$	$Cu_{15}Si_4$	$cI76$	$I\bar{4}3d$
$D1_a$	$MoNi_4$	$tI10$	$I4/m$	$D8_8$	Mn_5Si_3	$hP16$	$P6_3/mcm$
$D1_b$	Al_4U	$oI20$	$Imma$	$D8_9$	Co_9S_8	$cF68$	$Fm\bar{3}m$
$D1_c$	$PdSn_4$	$oC20$	$Aba2$	$D8_{10}$	Cr_5Al_8	$hR26$	$R\bar{3}m$
$D1_d$	Pb_4Pt	$tP10$	$P4/nbm$	$D8_{11}$	Co_2Al_5	$hP28$	$P6_3/mmc$
$D1_e$	B_4Th	$tP20$	$P4/mbm$	$D10_1$	Cr_7C_3	$oP40$	$Pnma$
$D1_f$	Mn_4B	$oF40$	$Fddd$	$D10_2$	Fe_3Th_7	$hP20$	$P6_3mc$
$D1_g$	B_4C	$hR15$	$R\bar{3}m$	$D8_{11}$	Co_2Al_5	$hP28$	$P6_3/mmc$
$D1_3$	Al_4Ba	$tI10$	$I4/mmm$	$E0_1$	$PbFCl$	$tP6$	$P4/nmm$
$D2_b$	$Mn_{12}Th$	$tI26$	$I4/mmm$	$E0_7$	$FeAsS$	$mP24$	$P2_1/c$
$D2_c$	MnU_6	$tI28$	$I4/mcm$	$E1_a$	$MgCuAl_2$	$oC16$	$Cmcm$
$D2_d$	$CaCu_5$	$hP6$	$P6/mmm$	$E1_b$	$AgAuTe_4$ (sylvanite)	$mP12$	$P2/c$
$D2_e$	$BaHg_{11}$	$cP36$	$Pm\bar{3}m$	$E1_1$	$CuFeS_2$ (chalcopyrite)	$tI16$	$I\bar{4}2d$
$D2_f$	UB_{12}	$cF52$	$Fm\bar{3}m$	$E2_1$	$CaTiO_3$ (perovskite)	$cP5$	$Pm\bar{3}m$
$D2_g$	Fe_8N	$tI18$	$I4/mmm$	$E3$	Al_2CdS_4	$tI14$	$I\bar{4}$
$D2_h$	Al_6Mn	$oC28$	$Cmcm$	$E9_a$	Al_7Cu_2Fe	$tP40$	$P4/mnc$
$D2_1$	CaB_6	$cP7$	$Pm\bar{3}m$	$E9_b$	$Al_8FeMg_3Si_6$	$hP18$	$P\bar{6}2m$
$D2_3$	$NaZn_{13}$	$cF112$	$Fm\bar{3}c$	$E9_c$	Mn_3Al_9Si	$hP26$	$P6_3/mmc$
$D5_a$	Si_2U_3	$tP10$	$P4/mbm$	$E9_d$	$AlLi_3N_2$	$cI96$	$Ia\bar{3}$
$D5_b$	Pt_2Sn_3	$hP10$	$P6_3/mmc$	$E9_e$	$CuFe_2S_3$ (cubanite)	$oP24$	$Pnma$
$D5_c$	Pu_2C_3	$cI40$	$I\bar{4}3d$	$E9_3$	Fe_3W_3C (η carbide)	$cF112$	$Fd\bar{3}m$
$D5_d$	Ni_3S_2	$hR5$	$R32$	$E9_4$	Al_4C_4Si	$hP18$	$P6_3mc$
$D5_f$	As_2S_3	$mP20$	$P2_1/c$	$F0_1$	$NiSbS$ (ullmanite)	$cP12$	$P2_13$
$D5_1$	$αAl_2O_3$ (corundum)	$hR10$	$R\bar{3}c$	$F5_a$	$FeKS_2$	$mC16$	$C2/c$
$D5_2$	La_2O_3	$hP5$	$P\bar{3}m1$	$F5_1$	$NaCrS_2$	$hR4$	$R\bar{3}m$
$D5_3$	Mn_2O_3	$cI80$	$Ia\bar{3}$	$F5_6$	CuS_2Sb (wolfsbergite)	$oP16$	$Pnma$
$D5_4$	Sb_2O_3 (senarmontite)	$cF80$	$Fd\bar{3}m$	$H1_1$	Al_2MgO_4 (spinel)	$cF56$	$Fd\bar{3}m$
$D5_8$	Sb_2S_3	$oP20$	$Pnma$	$H2_4$	Cu_3VS_4 (sulvanite)	$cP8$	$P\bar{4}3m$
$D5_9$	Zn_3P_2	$tP40$	$P4_2/nmc$	$H2_6$	Cu_2FeSnS_4	$tI16$	$I\bar{4}2m$
$D5_{10}$	Cr_3C_2	$oP20$	$Pnma$	$L'1$	Fe_4N	$cP5$	$Pm\bar{3}m$
$D5_{11}$	Sb_2O_3 (valentinite)	$oP20$	$Pccn$	$L'1_2$	$AlFe_3C$ (perovskite)	$cP5$	$Pm\bar{3}m$
$D5_{13}$	Ni_2Al_3	$hP5$	$P\bar{3}m1$	$L'2_b$	ThH_2	$tI6$	$I4/mmm$
$D7_a$	$δNi_3Sn_4$	$mC14$	$C2/m$	$L'3$	Fe_2N	$hP3$	$P6_3/mmc$
$D7_b$	Ta_3B_4	$oI14$	$Immm$	$L1_a$	$CuPt_3$	$cF32$	$Fm\bar{3}c$
$D7_1$	Al_4C_3	$hR7$	$R\bar{3}m$	$L1_0$	$AuCu$	$tP4$	$P4/mmm$
$D7_2$	Co_3S_4	$cF56$	$Fd\bar{3}m$	$L1_1$	$CuPt$	$hR32$	$R\bar{3}m$
$D7_3$	Th_3P_4	$cI28$	$I\bar{4}3d$	$L1_2$	$AuCu_3$	$cP4$	$Pm\bar{3}m$
$D8_a$	$Mn_{23}Th_6, Cu_{16}Mg_6Si_7$ (G-phase)	$cF116$	$Fm\bar{3}m$	$L2_a$	$δCuTi$	$tP2$	$P4/mmm$
$D8_b$	$σCrFe$	$tP30$	$P4_2/mnm$	$L2_1$	$AlCu_2Mn$ (Heusler)	$cF16$	$Fm\bar{3}m$
$D8_c$	Mg_2Zn_{11}	$cP39$	$Pm\bar{3}$	$L2_2$	Sb_2Tl_7	$cI54$	$Im\bar{3}m$
				$L6_0$	$CuTi_3$	$tP4$	$P4/mmm$

A.4 Valence electron concentration and heat of formation

The ranges for valence electron concentration of various compounds according to their nature of bonding is shown in Table A.3.

$$VEC = \frac{Total\ number\ of\ valence\ e^-\ of\ the\ components}{Total\ number\ of\ atoms}$$

Table A.3: Ranges for valence electron concentration (VEC) of intermetallic compounds according to their bonding nature.

Nature of bonding	VEC
Metallic	0-3
Electron compounds β- Brass	$\frac{3}{2}$
γ- Brass	$\frac{21}{13}$
ε - Brass	$\frac{7}{4}$
Laves phases C14 C15	0-3 1-3
Ionic / covalent compounds	4-5
Ionic B1	4-5
D5$_2$	$\frac{16}{5}$
Covalent B3 & B4	4-5
Ionic – Metallic C1	$\frac{16}{5}$
Ionic – Metallic – Covalent B8	1-4